The role of conserved residues in *Lactobacillus casei* Dihydrofolate reductase

A thesis submitted for the degree of Doctor of Philosophy
at the University of Leicester

Jaswir Basran
Department of Biochemistry, University of Leicester
October 1994

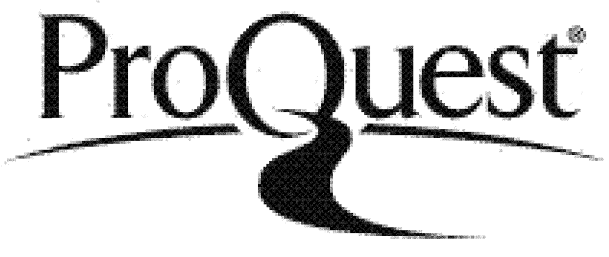

ProQuest LLC
789 East Eisenhower Parkway
P.O. Box 1346
Ann Arbor, MI 48106-1346

ABSTRACT

Mutants of three conserved residues in Dihydrofolate reductase (DHFR) from *Lactobacillus casei* have been studied to assess their roles in ligand binding and catalysis.

Aspartate26 has been widely postulated to be the source of the proton in the reaction catalysed by DHFR; this was probed by the Aspartate26→Asparagine (D26N) mutation. The rate of hydride ion transfer, which governs k_{cat} in the D26N mutant, is reduced by a factor of 10 (pH 7.5) when compared to the wild-type enzyme. The results argue against the role of Aspartate26 as the primary proton donor, but may be more consistent with a mechanism whereby it promotes enolisation of the substrate during the reaction.

The Tryptophan21→Histidine (W21H) mutant binds the coenzyme NADPH over 1000-fold more weakly than wild-type DHFR. The magnitude of the negative cooperative effect between NADPH and FH_4 (a crucial feature of the kinetic scheme of DHFR), has been greatly reduced in the W21H mutant, suggesting an important role for Tryptophan21 in the mechanism of negative cooperativity. The pH dependence of k_{cat} for W21H (which is equivalent to the rate of hydride ion transfer) has a form that reflects the cooperative ionisation of two groups. Kinetic and NMR results suggest that the new Histidine21 is one of the groups responsible for the unusual ionisation curve.

Substrate, inhibitor and coenzyme binding are unaffected by the Arginine57→Lysine (R57K) mutation. With the wild-type enzyme, loss of the ion-pair interaction between MTX and Arginine57 also leads to a loss of the interaction with Histidine28; this is not the case with the R57K mutant. The Arginine57→Lysine substitution has little effect on the rate of catalysis although the apparent pK_a of k_{cat} is reduced by 0.6 units, despite the site of catalysis being more than 15Å away from the site of the mutation. The origin of this effect may be due to electrostatic or structural factors.

ACKNOWLEDGEMENTS

There are numerous people whom I would like to thank for their advice and assistance during my postgraduate research work. Firstly I would like to thank my supervisor Professor Gordon C.K. Roberts for giving me the opportunity to work in his laboratory, his overall guidance and continued enthusiasm on the project that was a constant incentive during the course of this thesis. Special thanks go to Marco Casarotto and Amrik Basran for their advice, encouragement and support. I owe much to Marco, for his friendship, for the last four years on DHFR, for help with the NMR work and for proof-reading this thesis.

Sincere thanks go to Ronnie Frederick, Philip Dawson, Cathy Gibson, Rachel Bellingham, Kay Sorimachi, Vasudevan Ramesh, Peter Kilby, Andy Prescott, Jean Newby, Bart Ailey, LuYun Lian and Charnjit Seehra for their help and kindness. I would also like to thank all other members of the Biological NMR Centre (past and present) for making it such an enjoyable place to work.

I am grateful to John Arnold, Janette Thomas and Ramin Badii for familiarising me with DHFR, to Igor Barsukov for producing the colour prints in this thesis and to Jackie Ellis for help with the stopped-flow machine. I would also like to thank Drs Jim Feeney and Berry Birdsall at NIMR, Mill Hill, London and my committee members Professor W.V Shaw and Dr. C.R Bagshaw.

Last but not least I would like to thank my family for their constant support and encouragement.

ABBREVIATIONS

AMINO ACIDS

Ala (A)	Alanine
Arg (R)	Arginine
Asn (N)	Asparagine
Asp (D)	Aspartic acid
Cys (C)	Cysteine
Gln (Q)	Glutamine
Glu (E)	Glutamic acid
Gly (G)	Glycine
His (H)	Histidine
Ile (I)	Isoleucine
Leu (L)	Leucine
Lys (K)	Lysine
Met (M)	Methionine
Phe (F)	Phenylalanine
Pro (P)	Proline
Ser (S)	Serine
Thr (T)	Threonine
Trp (W)	Tryptophan
Tyr (Y)	Tyrosine
Val (V)	Valine

APS	Ammonium persulphate

BASES

A	Adenine
C	Cytosine
G	Guanine
T	Thymine

DEAE	Diethylaminoethyl
DHFR	Dihydrofolate reductase
DNA	Deoxyribonucleic acid
dNTP	deoxynucleoside triphosphate
ddNTP	dideoxynucleoside triphosphate
EDTA	Ethylenediamine tetraacetic acid
FH_2	Dihydrofolate
FH_4	Tetrahydrofolate
^2H	Deuterium
IPTG	Isopropyl β-D-thiogalactopyranoside
MTX	Methotrexate

MUTANTS

D26N	DHFR with the Aspartate 26→Asparagine mutation
R57K	DHFR with the Arginine 57→Lysine mutation
W21H	DHFR with the Tryptophan 21→Histidine mutation
W21H/D26N	DHFR with the Tryptophan 21→Histidine and Aspartate 26→Asparagine mutations

$NADP^+$	Nicotinamide adenine dinucleotide phosphate (oxidised form)
NADPH	Nicotinamide adenine dinucleotide phosphate (reduced form)
NMR	Nuclear magnetic resonance
PABG	*para*-aminobenzoyl glutamic acid
PAGE	Polyacrylamide gel electrophoresis
PEG	Polyethylene glycol
PYR	Pyrimethamine
SDS	Sodium dodecyl sulphate
TEMED	N,N,'N,'N-tetramethylethylenediamine
TMP	Trimethoprim
UV	Ultraviolet
X-gal	5-bromo-4-chloro-3-indolyl-β-D-galactopyranoside

CONTENTS

CHAPTER 3 D26N DHFR

CHAPTER 4 W21H and W21H/D26N DHFR

CHAPTER 5 R57K DHFR

CHAPTER 6 GENERAL DISCUSSION

APPENDIX A

APPENDIX B

CHAPTER 1 INTRODUCTION

1.1 INTRODUCTION

Dihydrofolate reductase (DHFR; E.C. 1.5.1.3) catalyses the NADPH-dependent reduction of 7,8 dihydrofolate (FH_2), and at a much slower rate folate, to 5,6,7,8 tetrahydrofolate (FH_4):

$$\text{folate} + H^+ + \text{NADPH} \rightleftharpoons FH_2 + \text{NADP}^+ \qquad (1)$$

$$FH_2 + H^+ + \text{NADPH} \rightleftharpoons FH_4 + \text{NADP}^+ \qquad (2)$$

The structure of folate is shown in Figure 1.1. The molecule consists of essentially three components; the pteridine ring, a *para*-aminobenzoyl group and a glutamic acid moiety.

Figure 1.1 The structure of folate

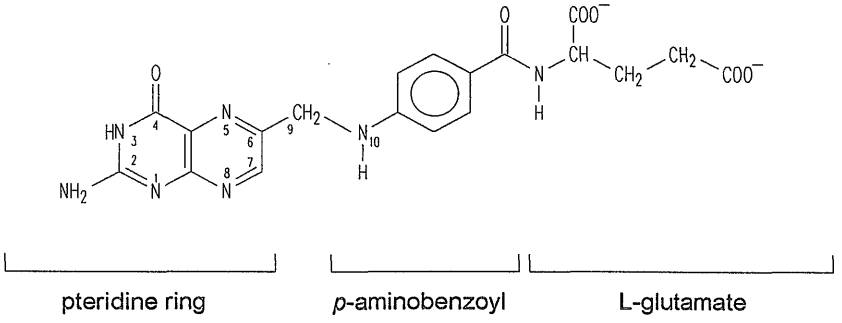

In organisms which can utilise folate as a substrate (equation 1 above), FH_2 is formed by reduction of the pteridine C7-N8 double bond; subsequent reduction of the N5-C6 double bond produces FH_4:

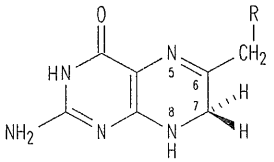

dihydrofolate (FH_2)

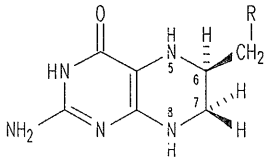

tetrahydrofolate (FH_4)

R= *p*-aminobenzoyl-L-glutamic acid

DHFR plays a crucial metabolic role in the cell by maintaining intracellular pools of FH_4 (Figure 1.2). FH_4 acts as a carrier of one carbon units in the biosynthesis of thymidylate, purines and some amino acids (Blakley, 1969). The single carbon units, which can be in the form of methyl (-CH_3), methylene (-CH_2-), methenyl (-CH=) or formyl (CHO) groups are carried either on N5, N10 or form a bridge between N5 and N10. An important feature of the scheme shown in Figure 1.2 is the relationship between DHFR and the enzyme thymidylate synthetase (TS). In the reaction catalysed by TS, a molecule of FH_2 is regenerated for each molecule of thymidylate produced. Interestingly DHFR isolated from protozoa exists as a bifunctional enzyme that has both DHFR and TS activities (Blakley, 1984, Freisheim and Matthews, 1984). From Figure 1.2 it can be seen that the FH_2 produced by the TS-catalysed reaction must be reduced by DHFR in order to replenish *in vivo* levels of FH_4; failure to do so would lead to a deficiency of thymidylate (and purines) with consequent disruption of DNA synthesis and eventual cell death.

Since the DHFR catalysed reaction is ultimately related to DNA synthesis it has become a potential target for chemotherapeutic agents. In fact this is the principal reason why it has been the subject of such intense study with the result that it is by far the best characterised enzyme of folate metabolism. DHFR is found in nearly every type of living cell (Kraut and Matthews, 1987). This diversity has meant that a major objective of the research has been to find improved species selective drugs i.e. those that will inhibit the infecting organism rather than mammalian DHFR. An example of such an inhibitor is

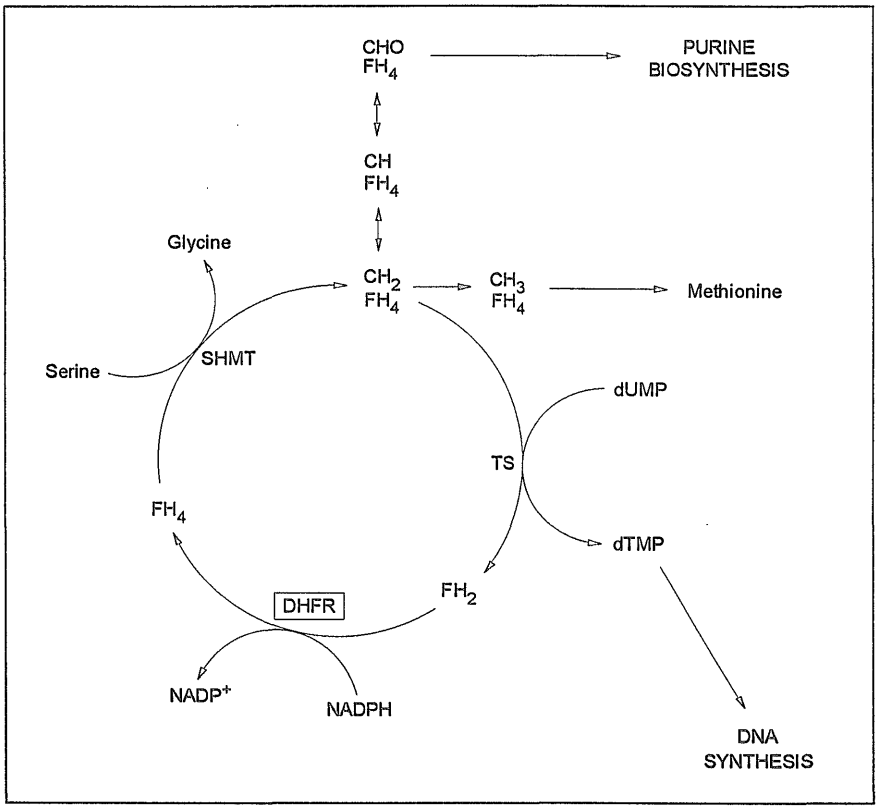

Figure 1.2 The role of tetrahydrofolate (FH_4) derivatives in the biosynthesis of thymidylate, purine nucleotides and methionine.

Key:

CH_2FH_4	5,10-methylene tetrahydrofolate
CH_3FH_4	5-methyl tetrahydrofolate
$CH{\cdot}FH_4$	5,10-methenyl tetrahydrofolate
$CHO{\cdot}FH_4$	5-formyl tetrahydrofolate
SHMT	Serinehydroxymethyl transferase
TS	thymidylate synthetase
dUMP	deoxyuridylate
dTMP	deoxythymidylate

trimethoprim (TMP) which is used specifically to treat bacterial infections (Figure 1.3). Other inhibitors of DHFR, known collectively as the "antifolates", are used to treat a wide range of disease states and include the drug methotrexate (MTX), a close structural analogue of folate which is used in the treatment of cancer and pyrimethamine (PYR) which is used as an antimalarial drug (Figure 1.3).

In addition to its importance as a pharmacological target, DHFR has been extensively studied as a model system for understanding the structure-function relationships of proteins. The enzyme has a number of attractive features which makes it an excellent candidate for such analysis:

1) Its small size (18kD-22kD) makes it particularly convenient to structural analysis by X-ray crystallographic and NMR methods.

2) Inhibitors of DHFR have greatly advanced our knowledge and understanding of the enzyme (MTX in particular has aided in the purification, structural studies and kinetics of the enzyme).

3) The reaction catalysed by DHFR can be monitored by simple spectrophotometric techniques.

4) The DHFR gene from a number of different sources has been cloned and routine mutagenesis work has been used to generate mutants. The study of such mutants (and of course the wild-type enzyme) has been greatly facilitated by the production of large quantities of the enzyme by efficient expression systems and straightforward purification protocols.

5) The complete kinetic scheme of DHFR has been elucidated in addition to a wealth of other kinetic and binding data. This allows the functional effects of individual

Figure 1.3 Structures of the inhibitors trimethoprim, pyrimethamine and methotrexate (the substrate folate is also shown for reference).

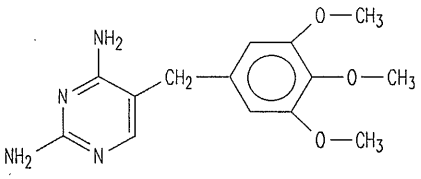

trimethoprim (TMP)

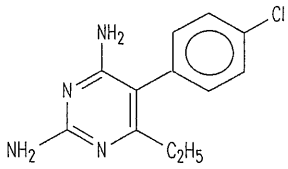

pyrimethamine (PYR)

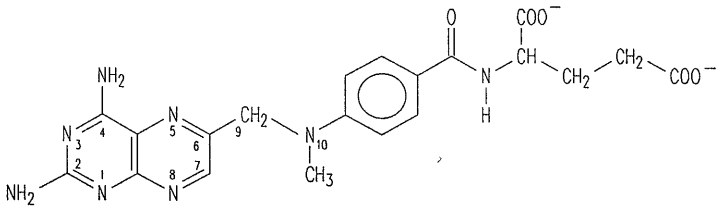

methotrexate (MTX)

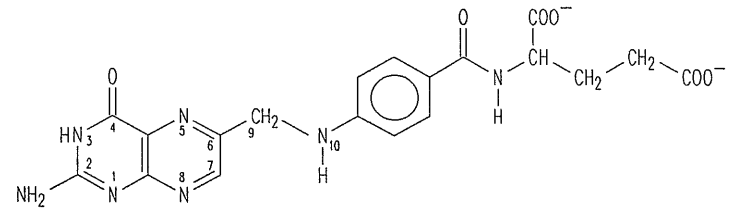

pyrimidine ring

pyrazine ring

folate

amino acid substitutions to be studied in detail and then correlated to any structural changes gleaned from NMR and X-ray crystallography.

1.2 STRUCTURAL STUDIES ON DHFR

The complete amino acid sequences of DHFRs from various bacterial and vertebrate sources have been determined; all vary in length from 159-189 residues. Examples include *E.coli* (Bennet *et al.*, 1974, Bennet *et al.*, 1978), *L.casei* (Bitar *et al.*, 1977, Freisheim *et al.*, 1978), bovine liver (Lai *et al.*, 1982), chicken liver (Kumar *et al.*, 1980) and recombinant human (Masters and Arttardi, 1983). The vertebrate sequences are highly homologous (72-89%) but there is only 25%-35% homology between vertebrate and bacterial DHFRs or between different bacterial species. Despite the low amino acid identity, the available crystal structures have revealed that the folding of the polypeptide chain is very similar in all the DHFRs and that many of the residues involved in ligand binding are conserved (Volz *et al.*, 1982).

X-ray crystallography and NMR spectroscopy have produced a great wealth of structural information on DHFR. Crystallography has not only defined the three dimensional structure of the enzyme but also revealed residues which are involved in ligand binding; thus allowing hypotheses to be put forward with regards to the importance of these residues in binding and in catalysis. Furthermore, plausible mechanisms for the manner in which in the enzyme catalyses the reaction can also be postulated. Additionally, X-ray crystallography has been used in attempts to rationalise inhibitor specificity (particularly trimethoprim since this drug is specific for bacterial DHFRs) and to understand why inhibitors such as MTX bind so tightly to DHFR compared with substrates. NMR has the advantage of not only providing structural information but also enabling the characterisation of dynamic processes such as protein-ligand interactions and conformational equilibria, in solution.

The first DHFR structures to be determined were of the *E.coli* DHFR-MTX binary complex (Matthews *et al.*, 1977) and the ternary *L.casei* DHFR-NADPH-MTX complex (Matthews *et al.*, 1978, Matthews *et al.*, 1979). The original structures were subsequently refined to a resolution of 1.7Å (Bolin *et al.*, 1982, Filman *et al.*, 1982). Figure 1.4 shows a schematic representation of the folding of the polypeptide backbone in these two structures and demonstrates the striking similarity between them, in spite of there being only 25% sequence homology. Some of the structural variance is due to the different enzyme-ligand complexes but most of the variability lies in the loop regions that join the elements of secondary structure.

Since these first bacterial structures, crystals of DHFR from several other species bound to various ligands have been obtained and their structures determined (Table 1.1). The structures of some mutant DHFRs are also available and recently the first unliganded DHFR structure was solved. Although there is species diversity, all the tertiary structures are very similar; in general the polypeptide chain folds into an 8-stranded β-sheet and four α helices. The vertebrate DHFRs are larger than the prokaryotic ones, most of the additional residues being incorporated into the loops. Figure 1.5 shows the structure of *L.casei* DHFR in complex with MTX and NADPH. MTX (a close structural analogue of the substrate FH_2) binds in a cavity that is lined with hydrophobic residues across one face of the enzyme. NADPH binds in an extended conformation in a shallow cleft where it makes numerous ionic, hydrogen bond and hydrophobic interactions. The nicotinamide ring of NADPH is in close contact with the pyrazine ring of MTX; since FH_2 binds at the same site as MTX (but with an inversion of the pteridine ring, see below) the proximity is such that hydride ion transfer can occur from the coenzyme to the substrate pyrazine ring during catalysis.

1.2.1 Inhibitor binding

From the refined crystal structures of the *E.coli* DHFR-MTX complex and the *L.casei* DHFR-NADPH-MTX complex (Bolin *et al.*, 1982, Filman *et al.*, 1982), MTX has

Figure 1.4 Backbone ribbon diagrams of the E.coli DHFR-MTX binary complex (top) and the L.casei DHFR-MTX-NADPH ternary complex (bottom). (From Bolin et al., 1982).

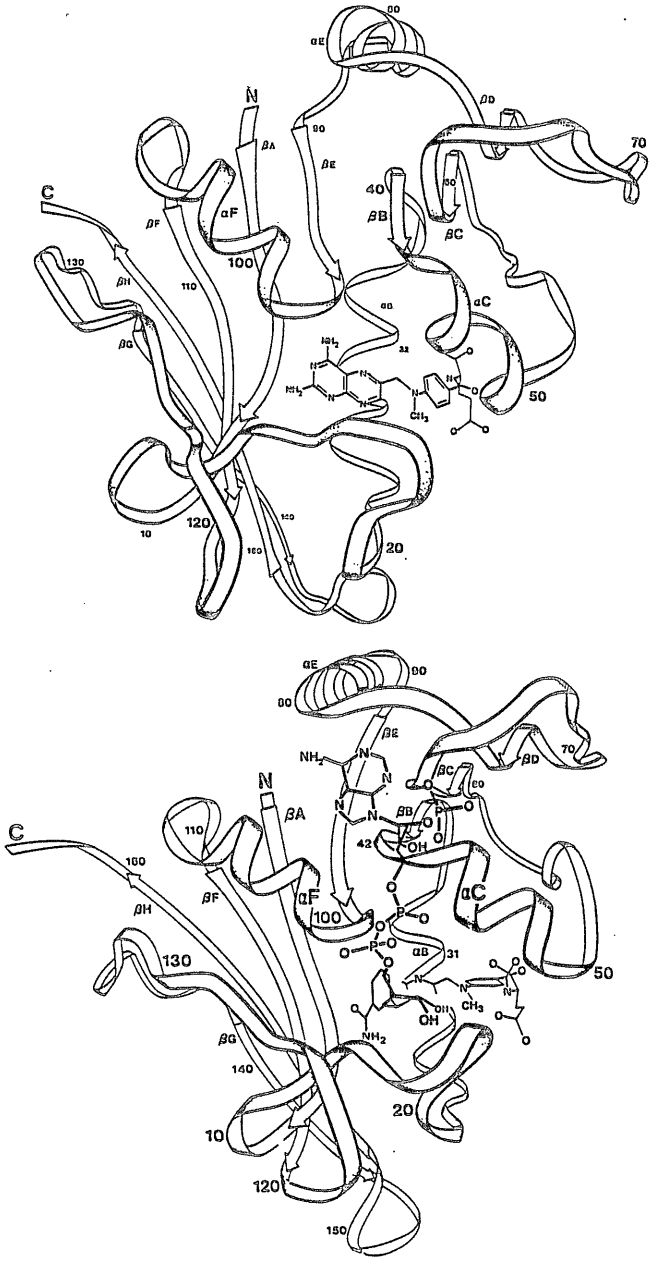

Table 1.1 Some of the available DHFR crystal structures

Species	Complex	Resolution (Å)	Reference
E.coli	enzyme alone	2.3	Bystroff and Kraut 1991
E.coli	MTX	1.7	Bolin *et al.*, 1982
E.coli	TMP	2.3	Baker *et al.*, 1981
			Matthews *et al.*, 1985a
E.coli	$NADP^+$	2.4	Bystroff *et al.*, 1990
E.coli	$NADP^+$/folate	2.5	Bystroff *et al.*, 1990
E.coli	TMP/NADPH	3	Champness *et al.*, 1986
L.casei	MTX/NADPH	1.7	Bolin *et al.*, 1982
			Filman *et al.*, 1982
Chicken	NADPH	2	Matthews *et al.*, 1985a
Chicken	NADPH/TMP	2.2	Matthews *et al.*, 1985a
Chicken	ThioNADP$^+$	2.3	McTigue *et al.*, 1993
Chicken	ThioNADP$^+$/biopterin	2.3	McTigue *et al.*, 1993
Mouse	MTX/NADPH	2.5	Stammers *et al.*, 1987
Mouse	TMP/NADPH	2	Stammers *et al.*, 1987
			Groom *et al.*, 1991
Human	folate	2	Oefner *et al.*, 1988
Human	TMP	3.5	Oefner *et al.*, 1988
Human	MTX	3.5	Oefner *et al.*, 1988
Mutants			
E.coli D27N	MTX	1.9	Howell *et al.*, 1986
E.coli D27S	MTX	1.9	Howell *et al.*, 1986
E.coli D27C	MTX	1.9	David *et al.*, 1992
E.coli D27E	MTX	1.9	David *et al.*, 1992
E.coli W22F	MTX	1.9	Warren *et al.*, 1991
mouse E30D	TMP/NADPH	1.9	Groom *et al.*, 1991
human F31S	MTX/NADPH	2.2	Chunduru *et al.*, 1994
human F31G	10-EDAM/NADPH	2.1	Chunduru *et al.*, 1994

10-EDAM, 10-deaza-10-ethylaminopterin

Figure 1.5 Structure of L.casei DHFR in complex with the coenzyme NADPH (red) and the inhibitor MTX (yellow). The four α-helices (B, C, E, F) are also marked.

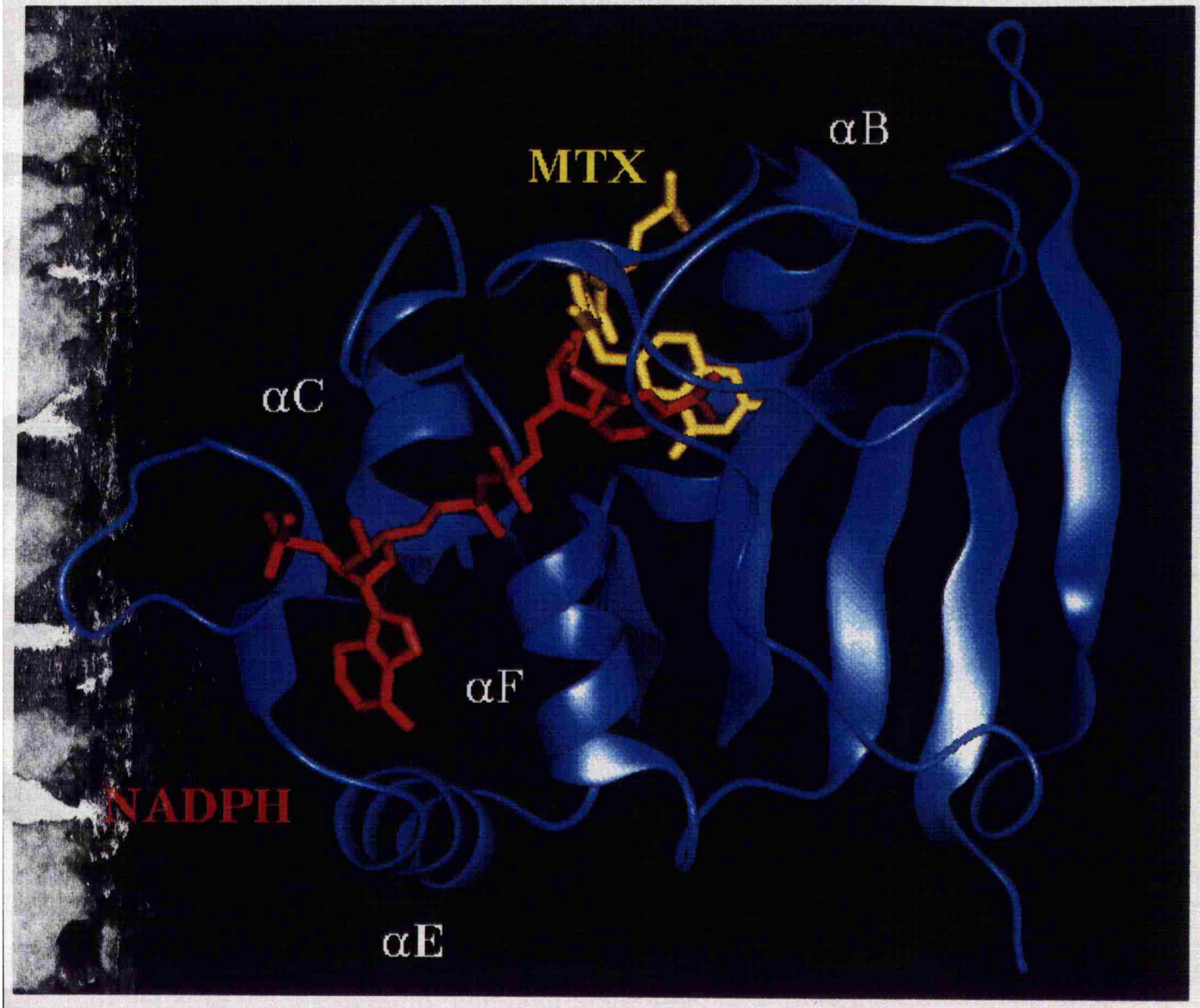

been shown to bind in a cavity 15Å deep, in a conformation where its pteridine ring is nearly perpendicular to the *p*-aminobenzoyl glutamate (PABG) moiety. The overall conformation is similar in both binary and ternary complexes. The main interactions between MTX and *L.casei* DHFR are outlined below; the numbering system is for the *L.casei* enzyme unless stated otherwise. Positions of key residues in the active site of *L.casei* DHFR are shown in Figure B1 (see Appendix B).

The α-carboxylate of the glutamic acid moiety of MTX forms an ion-pair interaction with the guanidinium group of Arg 57 which is an invariant residue found in all known DHFRs. In contrast, the interaction with the γ-carboxylate is not conserved and varies between species; in the *L.casei* enzyme it forms an ion-pair with His 28 whereas in *E.coli* DHFR Ala 29 is found in the structurally equivalent position and the γ-carboxylate interacts with solvent. The rest of the inhibitor molecule extends towards the interior of the protein. The *p*-aminobenzoyl ring binds in a cleft lined with the hydrophobic residues Leu 27, Phe 30 (conserved), Phe 49 and Leu 54 (conserved).

The 2,4-diaminopteridine ring of MTX forms several hydrogen bonds with protein backbone and side chain residues in addition to a number of non-polar contacts and a conserved ionic interaction. The main interactions between this ring and the enzyme are shown in Figure 1.6. The pyrimidine portion of the pteridine ring is deeply buried in a hydrophobic cavity where it interacts with Asp 26 (Asp 27 in *E.coli* DHFR), the only ionisable residue in the binding site. Asp 26 is strictly conserved in all bacterial DHFRs; the mammalian enzymes have a Glu at the analogous position. A variety of evidence, mainly from UV difference spectroscopy and ^{13}C NMR experiments have convincingly shown that MTX is protonated on N1 when in its complex with DHFR (Poe *et al.*, 1974, Gupta *et al.*, 1977, Hood and Roberts, 1978, Cocco *et al.*, 1981a, 1981b, 1983; London *et al.*, 1986). In these complexes the pK_a of N1 is greater than 10; some 5 units higher than its value in free MTX (pK_a is 5.7; Poe, 1977). Crystallographic studies have indicated that the raised pK_a is due to the interaction of N1 with Asp 26, which is nearly coplanar with the pteridine ring

and, in light of the results above likely to be in the ionised state (Bolin *et al.*, 1982, Filman *et al.*, 1982). This ionic interaction, which is absent in DHFR-substrate complexes (see below) is thought to contribute significantly to the tight binding of inhibitors such as MTX (Gready, 1980, Cocco *et al.*, 1981a, Blakley, 1984, Freisheim and Matthews, 1984).

Figure 1.6 Interactions between the pteridine ring of MTX and L.casei DHFR (Bolin et al., 1982).

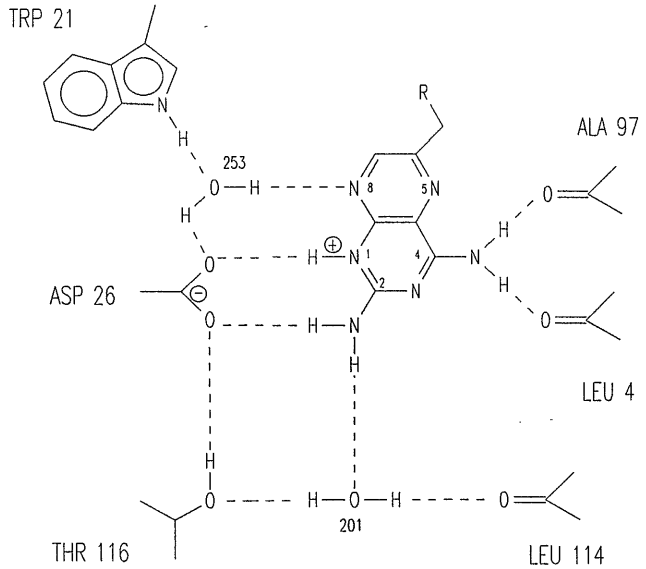

MTX also forms a number of hydrogen bonds with the protein. A water molecule (Wat 201 in *L.casei* DHFR) lies between the 2-amino group and the sidechain of Thr 116. This Thr is strictly conserved and the bridging water has also been found to be an invariant feature of all DHFR-inhibitor complexes studied to date. The 4-amino group of MTX hydrogen bonds to the backbone carbonyls of Leu 4 and Ala 97. N8 of the pyrazine ring is hydrogen bonded to a water molecule (Wat 253) which in turn hydrogen bonds to Asp 26 and Trp 21 (conserved). This second water molecule is also present in every DHFR structure solved and is thought to play an important role in the catalytic mechanism (see

Section 1.6). Leu 27 and Phe 30 make hydrophobic contacts with the pteridine ring; in the ternary *L.casei* DHFR-MTX-NADPH complex additional hydrophobic contacts are made with Leu 19 (Met 20 in *E.coli* DHFR) and the nicotinamide ring of NADPH. Interestingly, in the binary *E.coli* DHFR-MTX complex the corresponding residue, Met 20 is "folded away" and does not interact with the pteridine ring (Bolin *et al.*, 1982, Filman *et al.*, 1982). As discussed in Section 1.6 this may have mechanistic implications (Bystroff *et al.*, 1990, Brown and Kraut, 1992).

The diaminopyrimidine ring of the inhibitor trimethoprim (TMP) binds in an analogous manner to the corresponding part of MTX (Baker *et al.*, 1981, Matthews *et al.*, 1985a, Matthews *et al.*, 1985b, Champness *et al.*, 1986, Stammers *et al.*, 1987, Groom *et al.*, 1991). The trimethoxybenzyl moiety is sandwiched between, and makes hydrophobic contacts with residues including Leu 27, Phe 49, Phe 30 and Ala 97. Mammalian and bacterial DHFR-TMP complexes have been compared in order to find differences in active-site design that could account for the species selectivity of this inhibitor (for example see Matthews *et al.*, 1985a, Stammers *et al.*, 1987, Oefner *et al.*, 1988, Groom *et al.*, 1991). However, these investigations have not provided satisfactory explanations for the tighter binding of this inhibitor to bacterial DHFRs; the species specificity of TMP remains, as yet, unknown.

1.2.2 Substrate binding

It is only recently that suitable crystals of DHFR in complex with substrate rather than with inhibitors have been obtained and their structures elucidated (Oefner *et al.*, 1988, Bystroff *et al.*, 1990, Davies *et al.*, 1990, McTigue *et al.*, 1992). Nevertheless, it has been known for many years that although substrates and inhibitors bind at the same site, the pteridine ring of substrates must be in a different orientation to that adopted by inhibitors. Feeney *et al.* (1977) and Kimber *et al.* (1977) demonstrated that folate and MTX have different effects on the tryptophan and tyrosine resonances of *L.casei* DHFR which implies

a different mode of binding between substrate and inhibitor. Similar conclusions have been drawn from the effects of substrate and inhibitors on the Met resonances of *S.faecium* DHFR (Blakley *et al.*, 1978). Additionally, spectroscopic evidence has indicated that unlike inhibitors, substrates are not protonated on N1 when in complex with the enzyme (Erickson and Matthews, 1972, Hood and Roberts, 1978, Subramanian and Kaufman, 1978, Cocco *et al.*, 1981a).

The clearest evidence, however, comes from the stereochemistry of the reaction. A number of groups have demonstrated that in the reaction catalysed by DHFR a hydride ion is transferred from the 4 *pro*-R hydrogen of NADPH which is on the A side of the nicotinamide ring (Pastore and Friedkin, 1962, Blakley *et al.*, 1963, Pastore and Williamson, 1968, Poe and Hoogsteen, 1974).

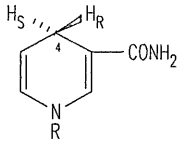

nicotinamide ring

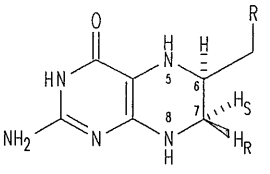

tetrahydrofolate pteridine ring

This is consistent with the *L.casei* DHFR-MTX-NADPH crystal structure which revealed that the A side of the nicotinamide ring is in contact with the pteridine binding site (Matthews *et al.*, 1978, Filman *et al.*, 1982). Charlton *et al.* (1979) showed that during enzymatic reduction of folate and FH_2 using 4R-[4-^{2}H] NADPH as coenzyme, both deuterons are added to the *si* face of the ring (i.e. the back of the pteridine ring in the structure above). However, in the crystal structure MTX binds with the *re* face of the pteridine ring turned towards the coenzyme (Matthews *et al.*, 1978, Filman *et al.*, 1982). Thus the stereochemistry of the reaction requires that the substrate pteridine ring must project the opposite face to the cofactor binding site compared with MTX.

The evidence outlined above led Bolin *et al.* (1982) to try and define interactions between the substrate pteridine ring and the enzyme. Model building experiments were carried out in which FH_2 was modelled to fit the binding site of both the *E.coli* DHFR-MTX and *L.casei* DHFR-NADPH-MTX crystal structures with minimal structural perturbations. The resulting hypothetical model is shown in Figure B2(a); see Appendix B. In order for the substrate to bind in the correct orientation for catalysis, the pteridine ring of MTX was rotated by 180° about the C6-C9 bond with an additional smaller (30°) rotation about the C9-N10 bond (see Figure 1.7). This rearrangement does not significantly alter the positioning of the PABG moiety or the C4-C6 substrate/nicotinamide ring contacts. As a result of this 180° ring inversion, the C4 carbonyl group of FH_2 makes only one hydrogen bond to the protein compared with two made by the 4-amino group of MTX. The ionic interaction between Asp 26 and N1 of MTX which contributes to the tight binding of MTX is also abolished in the substrate complex.

Confirmation that this model of substrate binding is correct came when crystal structures containing bound folate were solved (Oefner *et al.*, 1988, Bystroff *et al.*, 1990, Davies *et al.*, 1990). The structures, which were of the human DHFR-folate binary complex and the *E.coli* DHFR-$NADP^+$-folate ternary complex both verified that the substrate pteridine ring binds in an inverse orientation to that of MTX and that the proposed hydrogen bonds between substrate and protein were correct. However, a direct comparison of the *E.coli* DHFR-$NADP^+$-folate complex with the *E.coli* DHFR-MTX complex revealed that in addition to the flipping of the pteridine moiety, there was a slight "twist" of the ring; 7° counterclockwise about a perpendicular axis through N3 and a 15° rotation about the plane of the ring. The authors suggest that as a direct consequence of this "twist", hydrogen bonds to Asp 26 will be distorted and may contribute to the weaker binding of substrate compared with inhibitor (Bystroff *et al.*, 1990). As yet, however, there is still no structure available for DHFR complexed with the substrate FH_2.

Figure 1.7 Figure showing the relative orientations of the pteridine rings of MTX (blue) and folate (red).

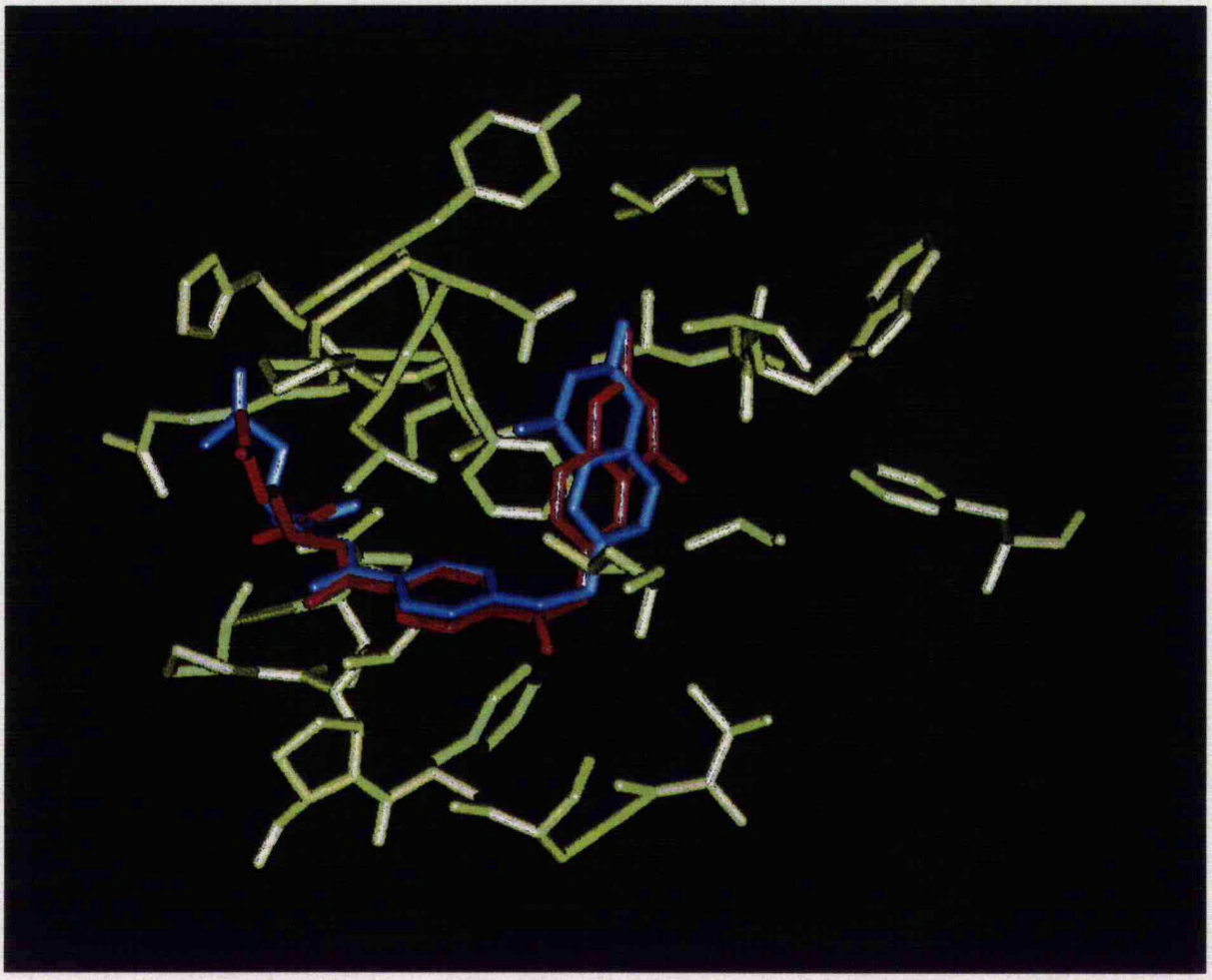

1.2.3 Coenzyme binding

In the refined crystal structure of the *L.casei* DHFR-NADPH-MTX ternary complex, NADPH was found to bind in a shallow cleft across one face of the enzyme where it makes numerous hydrogen bonds and hydrophobic interactions (Matthews *et al.*, 1978, Matthews *et al.*, 1979, Filman *et al.*, 1982). The adenine ring makes van der Waals contacts with residues including Thr 63, His 64 and the conserved Leu 62. The 2′ phosphate of NADPH interacts with Arg 43, Thr 63, His 64 and Gln 65 and there is extensive hydrogen bonding between the pyrophosphate oxygen atoms and the protein. The A side of the nicotinamide ring makes hydrophobic contact with part of the pteridine binding site including Leu 19, Trp 21 and the pyrazine ring of the pteridine moiety. The carboxamide of the nicotinamide ring hydrogen bonds to the strictly conserved Ala 6.

1.3 MULTIPLE CONFORMATIONAL STATES OF DHFR

There is a considerable body of evidence, mainly from kinetic and NMR investigations, which has convincingly demonstrated that DHFR exists in a number of conformational states that interconvert slowly. London *et al.* (1982) have carried out NMR studies on DHFR from *S.faecium* in which the Trp residues had been ^{13}C labelled. From the behaviour of some of the Trp resonances in the spectra (e.g. peak splitting and broadening) it was concluded that this enzyme exists in three slowly interconverting conformations. Dunn *et al.* and Cayley *et al.* have used the technique of stopped-flow fluorimetry to study the binding of coenzyme, substrate and inhibitors to *L.casei* and *E.coli* DHFRs (Dunn *et al.*, 1978, Dunn and King, 1980, Cayley *et al.*, 1981). From the biphasic nature of the curves obtained, it was concluded that the enzyme exists in at least two interconvertible forms which they called E_1 and E_2. Ligands (L) bind rapidly and exclusively to one form (E_1), which is followed by the slower interconversion of E_2 to E_1:

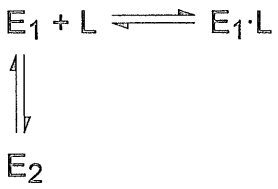

DHFR-ligand complexes as well as the free enzyme have been shown to exist in a number of conformational states; the number and nature of these conformers depends on the particular ligand. NMR has proved to be invaluable tool in characterising some of these. *L.casei* DHFR when in complex with folate and $NADP^+$ has been shown to exist in three conformations (denoted I, IIa and IIb) whose proportions are pH dependent (Birdsall *et al.*, 1981b, Birdsall *et al.*, 1982, Birdsall *et al.*, 1987, Birdsall *et al.*, 1989b, Cheung *et al.*, 1993). Conformer I predominates at low pH (< pH 5) whereas conformations IIa and IIb are present at higher pH values (> pH 7). A major difference between these conformations is in the orientation of the pteridine ring of folate. In I and IIa, the pteridine ring adopts an orientation similar to that seen for MTX in the *L.casei* DHFR-MTX-NADPH crystal structure (Filman *et al.*, 1982); this mode of binding is referred to as "non-productive". In conformation IIb, the ring is flipped over by 180° along the C2-NH_2 bond so that it is in the correct orientation for reduction ("productive" mode). The active site residue Asp 26 is thought to be responsible for the pH dependent conformational equilibria; protonated at low pH and ionised at the higher pH values. This hypothesis is consistent with results obtained on the Asp 26→Asn DHFR mutant (Jimenez *et al.*, 1989) which exists in one pH independent conformation (low pH conformer). These ternary complexes will be discussed further in Chapter 3.

The Feeney and Roberts group have also extensively characterised the *L.casei* DHFR-TMP-$NADP^+$ ternary complex (Gronenborn *et al.*, 1981a, Birdsall *et al.*, 1984, Cheung *et al.*, 1986, Searle *et al.*, 1988). This complex is present in solution as a mixture of two conformers, I and II that interconvert slowly and independently of pH. NMR has revealed that in conformation I the nicotinamide ring of $NADP^+$ is bound to the enzyme in a

similar manner as that observed in the *L.casei* DHFR-MTX-NADPH crystal structure (Filman *et al.*, 1982). However, rotations about the nicotinamide ribose C5′-O and pyrophosphate O-P bonds in conformation II have resulted in the nicotinamide ring being "swung" away from the enzyme into solution. The fact that the two conformers are equally populated is consistent with previous findings that the oxidised nicotinamide ring contributes little to the overall binding energy (Birdsall *et al.*, 1980). The *E.coli* DHFR-TMP-$NADP^+$ complex also exists in at least two conformations although these have not been characterised in any detail (Huang *et al.*, 1991).

1.4 COOPERATIVITY IN LIGAND BINDING

Equilibrium binding studies carried out on *L.casei* DHFR demonstrated that NADPH bound more tightly (670-fold) to the enzyme-MTX complex than to the enzyme alone (Birdsall *et al.*, 1980). This process, whereby the binding of the first ligand affects the binding of a subsequent ligand is termed "cooperativity". The species selectivity of the medically important drug trimethoprim (TMP) is thought to arise from the greater cooperativity between coenzyme and TMP binding exhibited by bacterial than mammalian DHFRs (Baccanari *et al.*, 1982). The cooperative effect can be either positive (as above) or negative (where the binding of the second ligand is weaker): negative cooperativity between NADPH and the product FH_4 is a crucial feature of the kinetic mechanism of DHFR (Section 1.5). The magnitude of cooperativity depends greatly upon the structure of both substrate analogue and cofactor, for instance folinic acid (5-formyl-tetrahydrofolate) binds 600-fold weaker to the *L.casei* DHFR-NADPH binary complex than to the enzyme alone but the effect is only 3-fold with $NADP^+$ (Birdsall *et al.*, 1981a).

Cooperativity in ligand binding could be the result of direct interactions between the two ligands or originate from ligand-induced conformational changes in the protein. For example, the enhanced binding of NADPH to the binary enzyme-MTX complex may result in part from the hydrophobic interaction between the pteridine ring of the inhibitor and the

nicotinamide ring of the coenzyme (Filman *et al.*, 1982). Similarly, Bystroff *et al.* (1991) have suggested that negative cooperativity could arise from a repulsion between the substrate pteridine and the NADPH nicotinamide rings. They noted that in the crystal structure of the *E.coli* DHFR-folate-$NADP^+$ ternary complex the contacts between C4 of the nicotinamide ring and C6 of the substrate pyrazine ring were close; it was postulated that further addition of hydrogen atoms to C4 and C6 would create "crowding" which would contribute to negative cooperativity. As crowding at the C4-C6 interface increases so does the magnitude of negative cooperativity, which is consistent with the fact that negative cooperativity between FH_4 and NADPH is greater than between FH_4 and $NADP^+$ (Andrews *et al.*, 1989). Inversion of the MTX pteridine ring avoids unfavourable close contact with the nicotinamide ring and hence negative cooperativity is not observed.

However, other data derived principally from NMR investigations has questioned the unique role of the nicotinamide ring in cooperativity. Birdsall *et al.* have shown that cooperativity is still observed with coenzyme analogues which either bind with the nicotinamide ring not in contact with the enzyme, or lack the ring completely (Birdsall *et al.*, 1980, Birdsall *et al.*, 1984). The binding of NADPH to *L.casei* DHFR affects residues that form part of the *p*-aminobenzoyl ring binding pocket (Leu 27, Phe 30, Phe 49 and Leu 54) which are not in contact with the coenzyme itself (Hammond *et al.*, 1986). It was postulated that these conformational changes could be transmitted through helix C (residues 42-49) which extends from the adenine ring binding site of the coenzyme to the inhibitor binding pocket. The negative cooperativity between folinic acid and NADPH mentioned above is accompanied by conformational differences located mainly at the adenine binding region of the coenzyme which is quite distant from the folinic acid binding site (Birdsall *et al.*, 1981a). These results add conviction that some contribution to cooperativity must come from effects transmitted through the protein.

1.5 KINETIC MECHANISM

A complete and detailed understanding of the kinetic mechanism for DHFR has been made more difficult by its complexity (the kinetic pathway has a number of intermediates) and other factors such as multiple enzyme conformations and submicromolar K_m values for both substrates (Kraut and Matthews, 1987). Nevertheless, complete kinetic schemes for *L.casei* (Andrews *et al.*, 1989), *E.coli* (Fierke *et al.*, 1987), mouse (Thillet *et al.*, 1990) and human (Appleman *et al.*, 1990a) DHFRs have been elucidated; these are all generally similar. The kinetic mechanism for *L.casei* DHFR is shown in Figure 1.8; the kinetically preferred reaction pathway under saturating substrate concentrations proceeds by the following steps:

1. FH_2 binds to the enzyme-NADPH binary complex
2. the reaction takes place to form the products $NADP^+$ and FH_4
3. $NADP^+$ dissociates from the enzyme-FH_4 complex
4. NADPH binds to the binary enzyme-FH_4 complex
5. the product FH_4 is released leaving the enzyme-NADPH complex to undergo another catalytic cycle

In this mechanism there are two main contributors to the rate-limiting step; the contribution that each makes is dependent upon pH. At low pH the dissociation of FH_4 is rate-limiting, but as the pH is increased hydride ion transfer becomes the slowest step in the reaction pathway. An unusual characteristic of the DHFR kinetic scheme is the negative cooperativity between NADPH and FH_4 (points 4 and 5 above); this feature has been observed in *L.casei* DHFR in the binding equilibria between the product analogue 5-formyl FH_4 and NADPH (Birdsall *et al.*, 1981a). FH_4 dissociates 80 times faster in the presence of the coenzyme than to enzyme alone; effectively NADPH facilitates the dissociation of FH_4 from the ternary enzyme-NADPH-FH_4 complex to leave the enzyme-NADPH binary complex ready for another cycle of events. It should be noted that this effect is only seen between coenzyme and product and not with the substrate, FH_2.

Figure 1.8 The kinetic scheme for L.casei DHFR (pH 6.5, 25°C).
Heavy arrows indicate the preferred pathway for steady state turnover
(From Andrews et al., 1989)

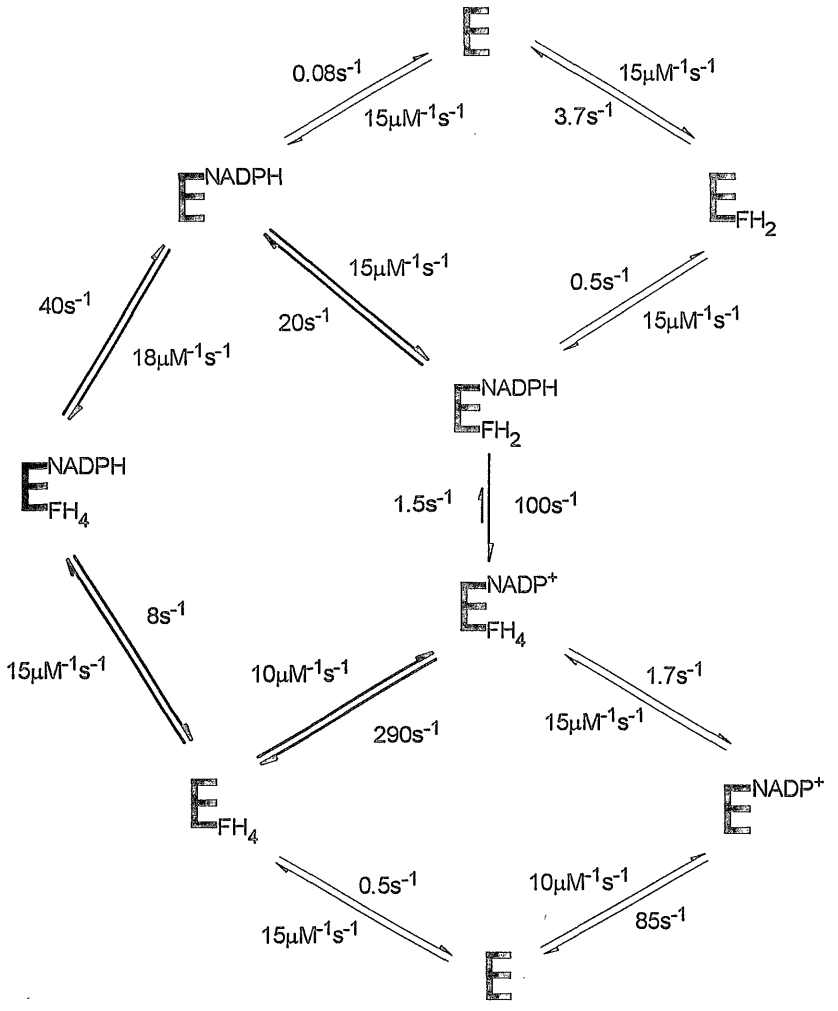

A comparison of the published kinetic mechanisms for bacterial and mouse DHFRs reveals that, despite the low sequence homology (only 28% identity between *L.casei* and *E.coli* enzymes) and evolutionary diversity, the schemes are virtually identical, in line with the close structural homology. The main differences between the two bacterial DHFR kinetic schemes is that NADPH is bound more tightly in *L.casei* DHFR complexes and the rate of hydride ion transfer is lower in the *L.casei* enzyme. There are minor variations between the bacterial and vertebrate schemes: the major distinction is that the rate of hydride ion transfer is significantly faster in the vertebrate enzymes. Mouse DHFR exists in two conformers, both of which can bind ligands to varying extents but only one is catalytically active; only one high affinity conformer exists in the bacterial enzymes. The human kinetic scheme is more complex than any of the others due to the fact that FH_4 and $NADP^+$ can both dissociate from the enzyme-$NADP^+$-FH_4 ternary complex at comparable rates.

1.6 THE CATALYTIC MECHANISM

In the reaction catalysed by DHFR it is generally accepted that reduction of the N5=C6 of FH_2 involves protonation at N5 followed by hydride ion transfer from C4 of NADPH to C6 of substrate (Huennekens and Scrimgeour 1964, Gready, 1985, Lund, 1976). In the case of those DHFRs which can utilise folate as a substrate, this also involves protonation at N8 and hydride ion transfer to C7:

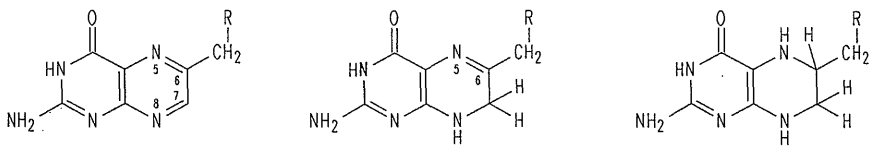

Pre-steady state kinetics have shown that the rate of hydride ion transfer increases as the pH is decreased; the pH profiles having pK_a values of 6-6.5 in different DHFRs (Fierke *et al.*, 1987, Andrews *et al.*, 1989). These results suggest that some ionisable group, either on the enzyme or the substrate must be protonated to achieve maximum activity. Free substrates do not have ionisable groups in the required pH range (Stone and Morrison, 1983, 1984; Morrison and Stone 1988). However, recently Chen *et al.* (1994) have shown (using Raman difference spectroscopy) that in the ternary *E.coli* DHFR-FH_2-$NADP^+$ complex, at least, the pK_a of N5 of FH_2 rises by some four units from its value in free FH_2 (which is 2.59; Maharaj *et al.*, 1990) to a value of 6.5. Assuming that the aforementioned ternary complex is a good model for the catalytically functional DHFR-FH_2-NADPH complex, it was suggested that the group responsible for the pH dependence of hydride ion transfer was the N5 of the substrate (Chen *et al.*, 1994).

All available crystal structures of DHFR have revealed that Asp 26 (or Glu in eukaryotic enzymes) is the only ionisable group close to the substrate pteridine ring. Hence this residue could be the source of the proton. This is in line with kinetic investigations on the *E.coli* enzyme which have implied that the group responsible is a neutral carboxyl (Stone and Morrison, 1984, Morrison and Stone, 1988). However, from the mode of binding of the substrate it is known that Asp 26 is approximately 6Å away from N5 of folate and thus proton transfer from this residue to N5 cannot be direct (Oefner *et al.*, 1988, Bystroff *et al.*, 1990, Davies *et al.*, 1990). Possible mechanisms for proton transfer from Asp 26 include proton transfer mediated via bound water molecules and/or transient protonation of O4 of the substrate (Bolin *et al.*, 1982, Gready, 1985). Alternatively, the proton may originate from the solvent, with Asp 26 either remaining protonated throughout catalysis (Uchimaru *et al.*, 1989, Bystroff *et al.*, 1990, Brown and Kraut, 1992) or in its ionised form stabilising a protonated transition state (Gready, 1985). Two mechanisms for proton transfer involving Asp 26 are described below.

Based on their measured kinetic parameters and upon the hypothetical mode of binding of FH_2, Stone and Morrison (1988) proposed the catalytic mechanism shown in Figure 1.9. In this mechanism Asp 26 is the source of the proton which is transferred to O4 of FH_2 via a strictly conserved water molecule (Wat 253, *L.casei* numbering) with the result that Asp 26 becomes negatively charged, N3 positively charged and the substrate is converted into the enol tautomer. The 4-OH group can rotate about the single bond as illustrated in Figure 1.9(b) enabling nucleophilic attack by the lone pair of electrons on N5 which would be facilitated by the movement of electrons towards the positively charged N3. As a result, N5 now becomes positively charged, which enhances the carbonium ion character at C6 and facilitates hydride ion transfer from NADPH to form FH_4. The authors propose that the hydrogen bonding network plays an important role in the catalytic scheme by decreasing the basicity of Asp 26 and at the same time increasing the basicity of N5. Theoretical studies by Gready (1985) have suggested that interaction between the ionised carboxylate of Asp 26 and the pteridine ring could significantly stabilise and hence raise the pK_a of N5 which would facilitate its protonation.

Kraut and his colleagues have proposed (based on the crystal structure of the *E.coli* DHFR-folate-$NADP^+$ ternary complex) a mechanism for proton transfer in which the proton is ultimately derived from solvent as shown in Figure 1.10 (Bystroff *et al.*, 1990, Brown and Kraut, 1992). The role of Asp 27 (*E.coli* numbering) in this mechanism is to promote enolisation of the substrate pyrimidine ring by relaying a proton from N3 to O4 via the conserved water molecule, Wat 206 (*E.coli* numbering; Figure 1.10a→b). It is then postulated that this proton is transferred to N5 by a less tightly bound water molecule (Figure 1.10c) with the concurrent return of the substrate to the keto tautomer. Although this transient water molecule is not observed in the *E.coli* crystal structure, it is present in the chicken DHFR-$NADP^+$-biopterin crystal structure (McTigue *et al.*, 1992). It should be noted that in this mechanism Asp 27 remains protonated throughout the catalytic cycle which is consistent with the findings of Stone and Morrison, that an unionised carboxyl is

Figure 1.9 Proposed chemical mechanism for the transfer of a proton from the protonated carboxyl of Asp 26 of DHFR to the N5 nitrogen of FH_2. (adapted from Morrison and Stone, 1988)

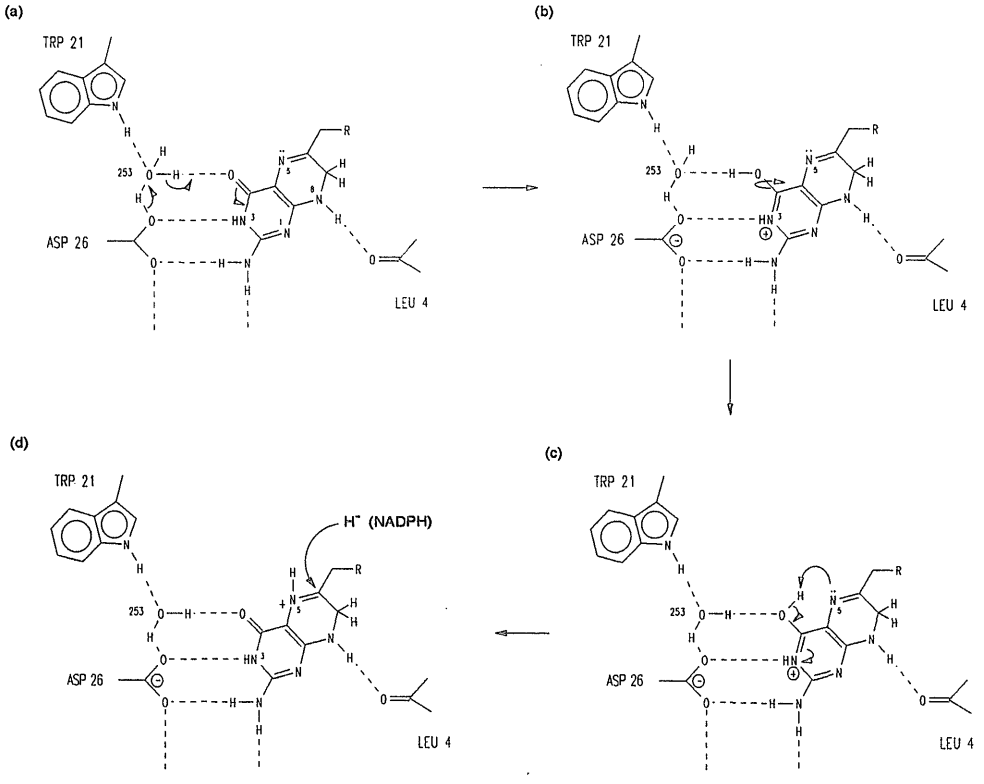

Figure 1.10 Proposed mechanism for the Asp 27 assisted protonation of FH_2 (adapted from Brown and Kraut, 1992).

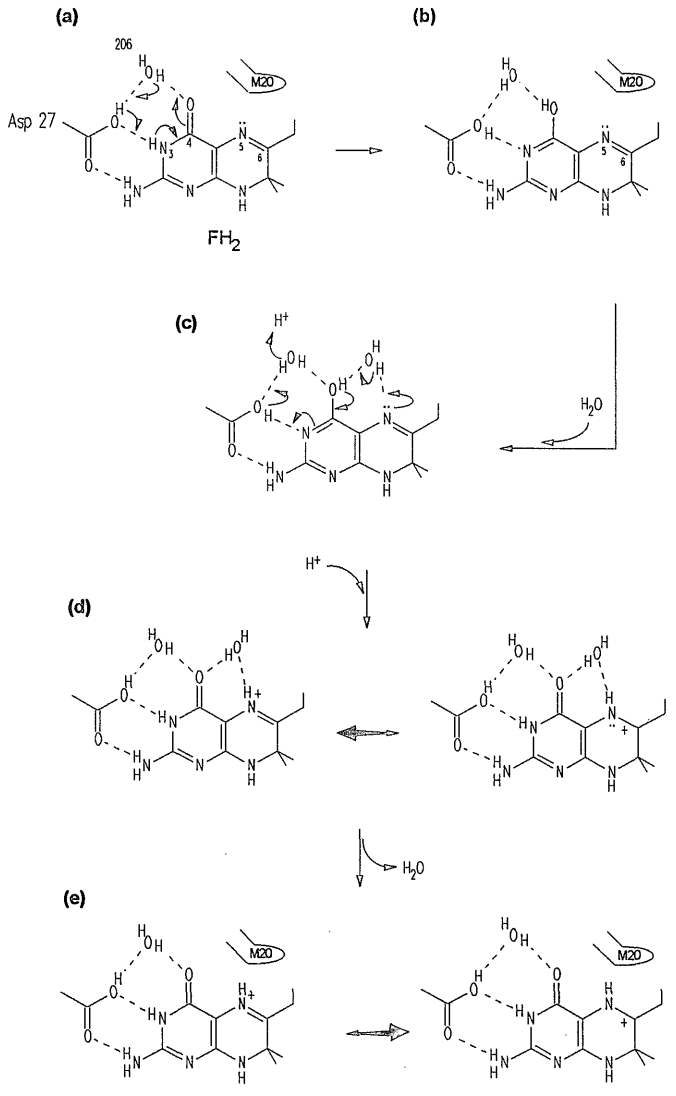

required for catalysis (Stone and Morrison, 1984, Morrison and Stone, 1988). The data is also in agreement with results obtained on an *E.coli* mutant in which replacement of Asp 27 by a nonionisable Asn residue leads to a 300-fold decrease in activity at neutral pH (Howell *et al.*, 1986). In Figure 1.10(e) it can be seen that the water molecule that stabilises the protonated N5 of FH_2 is displaced by the hydrophobic sidechain of Met 20 (this is either a Met or a Leu in other DHFRs). The authors suggest that this more hydrophobic environment would then encourage migration of the positive charge from N5 to C6, enabling hydride ion transfer from coenzyme in the transition state. As stated above, the transiently bound water molecule is not observed in the *E.coli* crystal structure but it was argued that Met 20 lies in a flexible loop region (the "teen" loop; residues 9-24) and so could move so as to enable a water molecule to bind.

1.7 MUTAGENESIS STUDIES

Site-directed mutagenesis has been used to produce a large number of mutants of DHFR from various sources. This technique has been a powerful tool in the further understanding of the structure-function relationship of DHFR and other enzyme systems (Leatherbarrow and Fersht, 1986; Shaw, 1987; Knowles, 1987). DHFR may be regarded as a "model" system for such studies due to the wealth of structural data (from X-ray crystallography and NMR) available on the enzyme in addition to the well characterised kinetic scheme. This background of knowledge enables the effects of individual amino acid substitutions on structure, conformational equilibria, ligand binding and catalysis to be analysed in great detail. Results obtained on some active site DHFR mutants are outlined below; the positions of many of the residues that have been chosen for substitution are shown in Figure B1 (see Appendix B).

Benkovic and his colleagues have made numerous mutants of *E.coli* DHFR including those of the strictly conserved residues Phe 31, Leu 54 and Thr 113 (*E.coli* numbering). Phe 31 (Phe 30 in *L.casei* DHFR) makes van der Waals contacts with the

benzoyl and pteridine moieties of substrates and inhibitors; the function of this residue was probed by replacing it with a Val and a Tyr (Taira *et al.*, 1987, Chen *et al.*, 1987). A major effect of the F31V substitution was upon the binding of MTX which was reduced by a factor of at least 40 due mainly to a 200-fold reduction in the association rate constant (k_{on}); the results suggest that the mutation has altered the accessibility of MTX to its binding site. Both mutations have a modest effect on hydride ion transfer although the overall k_{cat} was increased by a factor of two due to an increase in the rate of FH_4 dissociation which limits steady state turnover at low pH.

Leu 54 makes hydrophobic contacts with the opposite face of the benzoyl ring compared with Phe 31. A number of interesting results were obtained when this residue was substituted for a Gly (L54G), an Asn (L54N) and a Ile (L54I; Mayer *et al.*, 1986, Murphy and Benkovic 1989). In all the mutants the binding of the substrate FH_2 and the inhibitor MTX were reduced by varying extents; the largest effect was seen with L54G. In contrast to the binding results the rate of hydride ion transfer was decreased by the same factor in all three mutants (approximately 30-fold) so that it became the rate-limiting step in catalysis. Thus there appears to be no correlation between FH_2 binding affinity and the rate of hydride ion transfer. The pH dependence of hydride ion transfer in L54G now reflects the true pK_a of possibly Asp 27 observed in the wild-type enzyme (value of 6.5; Fierke *et al.*, 1987). In the case of L54N and L54I, the pK_a value is one unit lower than this suggesting that there are conformational changes around the catalytic site, some 10Å away from the mutation site. In the L54I mutant negative cooperativity between NADPH and FH_4 is abolished. The authors suggest that this may be due to conformational changes involving α-helix C which runs from the substrate benzoyl ring binding site to the adenine binding pocket of the coenzyme. The need for both structural and kinetic data on mutants was very evident from these studies; a lack of structural information on the mutants meant that many of the functional effects of the substitutions could not be directly interpreted.

Fierke and Benkovic (1989) have probed the role of the strictly conserved Thr 113 in *E.coli* DHFR by changing it to a Val (T113V). Thr 113 (Thr 116 in *L.casei* DHFR) forms a hydrogen-bond to Asp 27 and the 2-amino group of MTX through a fixed water molecule (Figure B2). Binding of coenzymes is largely unaffected by the substitution whereas that of substrates and MTX is reduced by 2.3 kcal/mol due to both an increase in the k_{off} and a decrease in the k_{on} rate constants. The changes in binding energy are greater than that expected from the simple loss of a hydrogen bond (Fersht, 1985) and hence it was proposed that small structural changes at the active site, in addition to unfavourable steric contacts between the methyl group of Val and either the bound ligand or nearby sidechains were responsible. The kinetic scheme of T113V is identical to that of the wild-type enzyme except for a decrease in the rate of hydride ion transfer in both directions. The pH dependence of hydride ion transfer revealed that the pK_a of Asp 27 had increased from 6.5 to 7 in the mutant. It was postulated that in the hydrophobic environment of the active site of wild-type DHFR, the carboxylate form of Asp 27 is stabilised more than the acid form by a hydrogen bond; in the mutant loss of this hydrogen bond results in an elevated pK_a value.

Leu 27 (*L.casei* numbering) makes hydrophobic contacts with the pteridine ring and the benzoyl group of substrates/inhibitors. This residue is conserved in prokaryotic DHFRs; eukaryotic enzymes have an aromatic residue, either a Tyr or a Phe, at the equivalent position. This structural difference between bacterial and mammalian reductases has made this residue a target for a number of mutagenic studies: for example in human DHFR, the Phe (Phe 31 in human DHFR numbering system) has been substituted by residues including Leu (Prendergast *et al.*, 1989, Tsay *et al.*, 1990), Ser (Schweitzer *et al.*, 1989, Chunduru *et al.*, 1994), Gly (Chunduru *et al.*, 1994), and Ala (Chunduru *et al.*, 1994). Intriguingly the Phe 31→Leu mutant bound FH_2 40-fold more tightly than the wild-type enzyme; this was also observed in the equivalent mutant of mouse DHFR (Wagner *et al.*, 1992). In the case of the human F31L mutant the increased binding of the substrate was due to a decrease in the dissociation rate constant. FH_2 also binds more tightly to the Gly 31, Ala 31 and Ser 31 mutants of the human enzyme. However, unlike the Leu 31 mutant, the binding of MTX is

substantially reduced in these mutants (by a factor of 80). The X-ray crystal structures of the Ser 31, Ala 31 and Gly 31 mutants demonstrated that the structural effects of the Phe substitutions were very small and localised around the site of the mutation (Chunduru *et al.*, 1994). The weaker binding of MTX was due to a loss in the van der Waals contacts made by Phe 31 in the wild-type enzyme. Hydrophobic contacts are also lost, not only because of the shorter sidechains of the substituents but, as revealed by the crystal structures, due to an additional water molecule that occupies the space vacated by Phe 31. Although a crystal structure for the F31L mutant is not available, the authors postulate that this water molecule may not be present in the Leu 31 mutant and hence the binding of MTX remains unaffected. With the Gly 31 mutant there was kinetic evidence that the reduced binding of MTX was due to an inability of the F31G DHFR-MTX-NADPH complex to undergo isomerisation to a tighter binding conformer; in the wild-type enzyme this accounts for a 60-fold increase in the binding of MTX (Appleman *et al.*, 1988b).

Trp 21 (*L.casei* numbering) interacts with the nicotinamide ring of NADPH through van der Waals contacts and indirectly with the substrate/inhibitor pteridine ring via hydrogen bonds through a bridging water molecule (Figure B2). The strict conservation of this residue in all known DHFRs has prompted a number of groups to probe the functional role of this amino acid in DHFR. Trp 21 has been substituted for a Leu in *L.casei* DHFR (W21L) and the mutant characterised by NMR and kinetic methods (Andrews *et al.*, 1989, Birdsall *et al.*, 1989a). The rate of hydride ion transfer in W21L DHFR was lower by a factor of 100 compared to the wild-type enzyme so that it became the sole contributor to the rate limiting step; the pH dependence of k_{cat} now reflects the true pK_a of the ternary enzyme-FH_2-NADPH complex (pK_a of 6.0). The binding of substrates, inhibitors and $NADP^+$ was unaffected by the mutation but the binding of NADPH was reduced 400-fold, due mainly to an increase in the dissociation rate constant. The difference between the binding of $NADP^+$ and NADPH was consistent with the fact that the oxidised nicotinamide ring of $NADP^+$ makes a much smaller contribution to overall binding of this coenzyme (Birdsall *et al.*, 1980). The only major structural effects of the Trp 21→Leu mutation occur

at the nicotinamide binding pocket. The substitution leads to loss of the hydrophobic contact with the carboxamide of NADPH which results in the nicotinamide ring binding in a different orientation to that seen in the wild-type enzyme. This different mode of binding is thought to account for the reduced rate of hydride ion transfer in W21L DHFR.

Huang *et al.* (1989) and Beard *et al.* (1991) have replaced the equivalent Trp residue in human DHFR with a Phe (W24F; human DHFR numbering system). Various experiments including thermal stability, competitive ELISA (using antibodies against DHFR) and protease susceptibility demonstrated that the W24F mutant adopts a more "open" or flexible conformation. It was concluded that Trp 24 was important in maintaining the structural integrity of the native enzyme. The W24F mutation has modest effects on the binding of substrates, coenzyme and inhibitors but a more dramatic effect on the ratio of the two rate-limiting steps which contribute to catalysis. In the catalytic mechanism of wild-type human DHFR the rate of catalysis is independent of pH throughout most of the pH range (from 5-9) and is limited by the rate of FH_4 dissociation (Appleman *et al.*, 1990a). With the W24F mutant k_{cat} at low pH is 7-fold higher than the wild-type enzyme due to an increase in the dissociation rate of FH_4. The substitution also has an effect on the rate of hydride ion transfer which is reduced by a factor of 40 and becomes totally rate-limiting at higher pH values. Thus the pH dependence of k_{cat} of W24F DHFR now closely resembles the profiles exhibited by the bacterial enzymes. The decrease in the rate of hydride ion transfer was attributed to, as in the case of most of Trp 21 (*L.casei* numbering) mutants, an unfavourable geometry for hydride transfer from C4 of NADPH to C6 of substrate.

Warren *et al.* (1991) have made the Trp 22→Phe mutant of the *E.coli* enzyme as well as the Trp 22→His mutant. Substitution by a His has no effect on the binding of coenzyme or substrates but the rate of hydride ion transfer is reduced by 100-fold so that it is the slowest step in steady state turnover. The results obtained on the *E.coli* W22F mutant were similar to those obtained on the corresponding human W24F mutant; minor effects on substrate binding and an elevated k_{cat} at low pH values due to an increase in the rate of FH_4

dissociation. The crystal structure of the *E.coli* W22F DHFR-MTX complex revealed that the effects of the mutation were very small and localised around residue 22. The rationale for creating the W22F mutant was to investigate the role of the strictly conserved water molecule that hydrogen bonds to the Trp residue in the wild-type enzyme, Asp 27 and the pteridine ring of substrates or inhibitors (Figure B2; see Appendix B). It was thought that the large hydrophobic sidechain of Phe 22 would displace this water molecule from its binding site. However, the crystal structure of the W22F mutant demonstrated that this was not the case and that the water molecule was still present. The only significant structural effect of the W22F mutation was the unanticipated 0.4Å movement of Met 20 which makes van der Waals contact with Trp 22 in the wild-type enzyme (Bolin *et al.*, 1982, Bystroff *et al.*, 1990). Met 20 has been suggested to play an important role in one of the proposed catalytic mechanisms of DHFR (Section 1.6). From the results obtained on the mutants the authors suggest that the function of Trp 22 is to correctly orientate Met 20 with respect to N5 of the substrate to enable efficient hydride ion transfer to C6. It was argued that the relatively conservative Phe substitution causes a 0.4Å movement of Met 20 and a 3-fold decrease in the rate of hydride ion transfer (from $730s^{-1}$ in wild-type to $230s^{-1}$ in W22F). Perturbation of Met 20 in the W22H mutant was anticipated to be greater than in W22F in order to account for the larger, 100-fold reduction, in the hydride ion transfer rate. However, no direct structural evidence is available for this since suitable crystals of the W22H mutant were not obtained.

Asp 26 (*L.casei* DHFR; Asp 27 in *E.coli* DHFR) is found in the substrate binding pocket of bacterial DHFRs; a Glu is present in the structurally equivalent position in mammalian reductases. The proposed importance of this residue in catalysis and inhibitor binding has been discussed throughout this chapter. It is therefore not surprising that a great deal of attention has focused on this residue. Kraut and his colleagues have made numerous substitutions of Asp 27 in *E.coli* DHFR (Villafranca *et al.*, 1983, Howell *et al.*, 1986, Appleman *et al.*, 1988a, Appleman *et al.*, 1990b, Howell *et al.*, 1990, David *et al.*, 1992), the Roberts group have mutated the equivalent Asp in the *L.casei* enzyme (Jimenez *et al.*,

1989, Birdsall *et al.*, 1989a). Both groups have studied the structural and functional effects of the Asp 26 mutations in detail, and these results will be discussed in Chapter 3.

1.8 BACKGROUND AND AIMS OF THE THESIS

At the start of the work described in this thesis a considerable amount of information was available on DHFR; the main points are summarised below:

Crystal structures of DHFR from various sources and in complex with a variety of different ligands (inhibitors and substrates) have been determined.

The kinetic scheme of some bacterial and vertebrate DHFRs have been fully characterised.

DHFR genes from different sources have been cloned and mutagenesis protocols developed.

A number of mutants of DHFR from various sources have been produced to test the models that have been put forward regarding the role of these residues in ligand binding and catalysis.

The main aim of the work covered in this study has been to investigate the function of some of the conserved residues in *L.casei* DHFR. The importance of these residues in ligand binding and/or catalysis have been inferred from crystallography, kinetic and other data. Previous methods for studying the structure-function relationship of DHFR have involved chemical modification of the protein and the use of substrate analogues. The cloning of the DHFR gene now provides the opportunity of using the technique of site-directed mutagenesis to specifically change individual amino acids in the protein. In our laboratory a combination of kinetic, binding and NMR techniques have been used to study these mutants, the ultimate goal being to relate the function of the enzyme to its structure. During the course of this thesis four mutants of *L.casei* DHFR have been studied:

1. Aspartate 26 →Asparagine	(D26N)
2. Tryptophan 21 →Histidine	(W21H)
3. Aspartate 26 →Asparagine and Tryptophan 21 →Histidine	(D26N/W21H)
4. Arginine 57 →Lysine	(R57K)

The positions of these residues in the active-site of DHFR are shown in Figure 1.11. Asp 26 and Trp 21 interact with substrate and inhibitor pteridine rings whereas Arg 57 makes contact with the glutamic acid moiety. The rationale behind each substitution will be detailed at the beginning of the relevant chapter.

Figure 1.11 Active site of <u>L.casei</u> DHFR showing the positions of Asp 26, Trp 21 and Arg 57. NADPH (white) and MTX (yellow) are also shown.

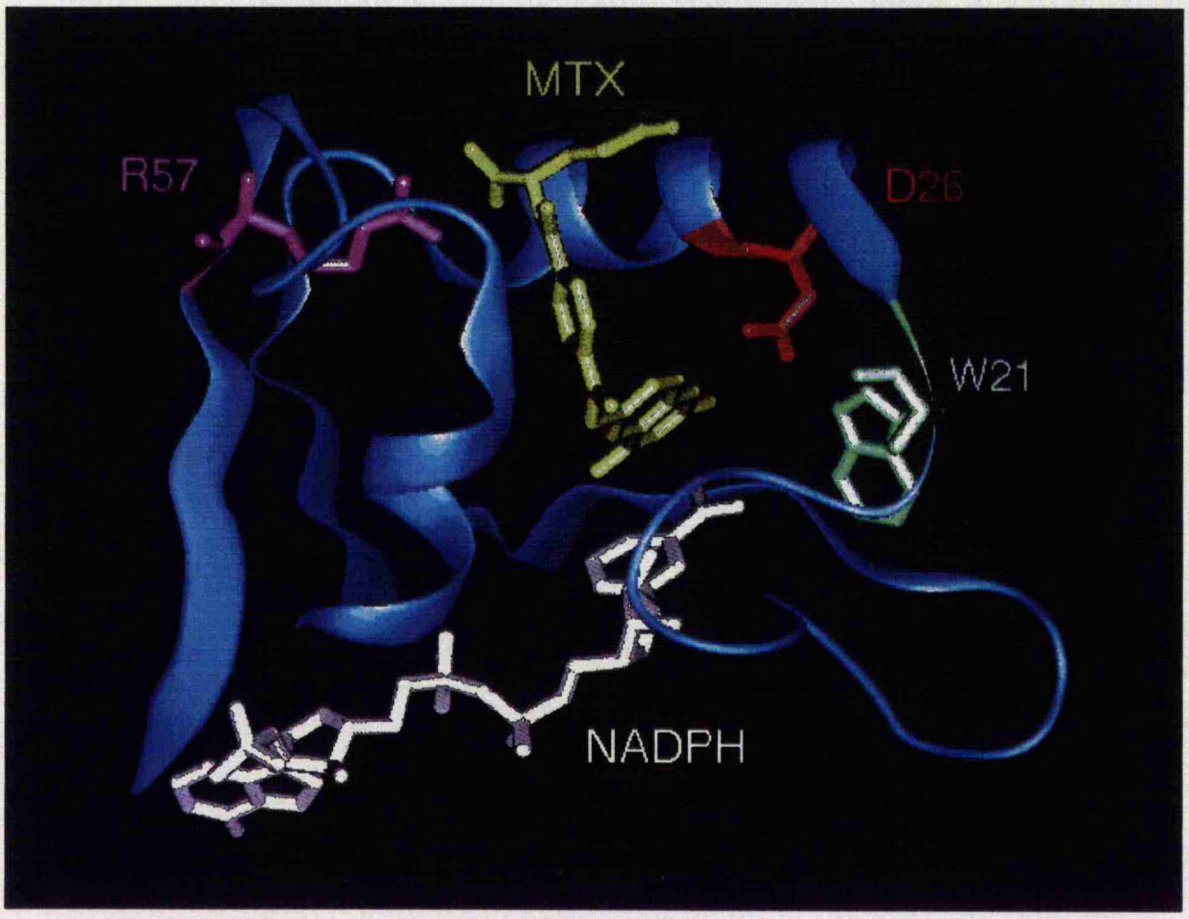

CHAPTER 2 MATERIALS and METHODS

2.1 CHEMICALS AND REAGENTS

M13mp19 RF1 DNA was purchased from Pharmacia LKB. The pET11a expression vector was purchased from Novagen through AMS Biotechnology (U.K) Ltd. as was the *E.coli* strain BL21(DE3). The GeneClean™ kit was purchased from Stratech Scientific Ltd. and the Sequenase® version 2.0 DNA sequencing kit was from United States Biochemical (USB). The Oligonucleotide-directed *in vitro* Mutagenesis System (version 2.1)™ kit and the enzymes XbaI and BamHI were purchased from Amersham International plc. The enzyme T4 DNA ligase was purchased from CP laboratories New England Biolabs. and T4 polynucleotide kinase was obtained from Cambio. Magic™ DNA purification systems were purchased from Promega. The *E.coli* strain TG1 was kindly provided by Dr. R. Frederick (Department of Biochemistry, University of Leicester). Ethanolamine, triethylamine (TEA) and deuterated ethanol were purchased from the Aldrich Chemical Co.. Deuterium oxide (99.9% and 99.96% deuterium) was from Goss Scientific Instruments Ltd. MTX-amide analogues were synthesised by Dr. H.T.A. Cheung (Antonjuk *et al.*, 1984). All other chemicals were purchased from the Sigma Chemical Co.. With the exception of NADPH and NADPD which were purified as described in Section 2.4.3, all chemicals were used without further purification.

2.2 OLIGONUCLEOTIDE-DIRECTED MUTAGENESIS

2.2.1 INTRODUCTION

DHFR mutants were created using the technique of oligonucleotide-directed mutagenesis. The mutagenesis protocol used was the M13 vector based Amersham Oligonucleotide-directed *in vitro* Mutagenesis System (version 2.1)™. The procedure is simple, quick and has efficiency levels of greater than 80% which eliminates the laborious

task of screening large numbers of plaques for mutants. An outline of the overall mutagenesis protocol is shown in Figure 2.1 and described below.

Annealing, extension and ligation

Single stranded M13mp19 DNA with the DHFR gene cloned into it (as described in Appendix A) acts as a template for the annealing, extension and ligation reactions. The mutant oligonucleotide (which carries the substitution) anneals to the complementary region of the DHFR gene and acts as a primer for the synthesis of the complementary strand. Klenow polymerase and DNA ligase carry out the extension and ligation reactions which involves the incorporation of a thio derivative of dCTP, dCTPαS, to generate a mutant heteroduplex.

Filtration

Not all of the single stranded template DNA molecules will be converted into replicative form (RF) heteroduplex DNA. It is necessary to remove these as they greatly decrease mutagenic efficiency. A simple rapid gel filtration step removes the unwanted single stranded DNA.

Removal of non-mutant strand

The next stage is the selective removal of the non-mutant (wild-type) strand by using the restriction enzyme NciI and exonuclease III. NciI cannot cleave DNA at phosphorothioate linkages. Thus the mutant strand, which will have incorporated dCTPαS (nucleotide analogue that contains a sulphur atom instead of an oxygen atom on the α phosphate of dCTP) during its *in vitro* synthesis, will be protected from the action of the enzyme. However, "nicks" will be introduced into the non-mutant strand which contains dCTP and is therefore "unprotected". The free 3'- ends produced by the action of NciI act as sites for the action of exonuclease III which digests away the non-mutant strand.

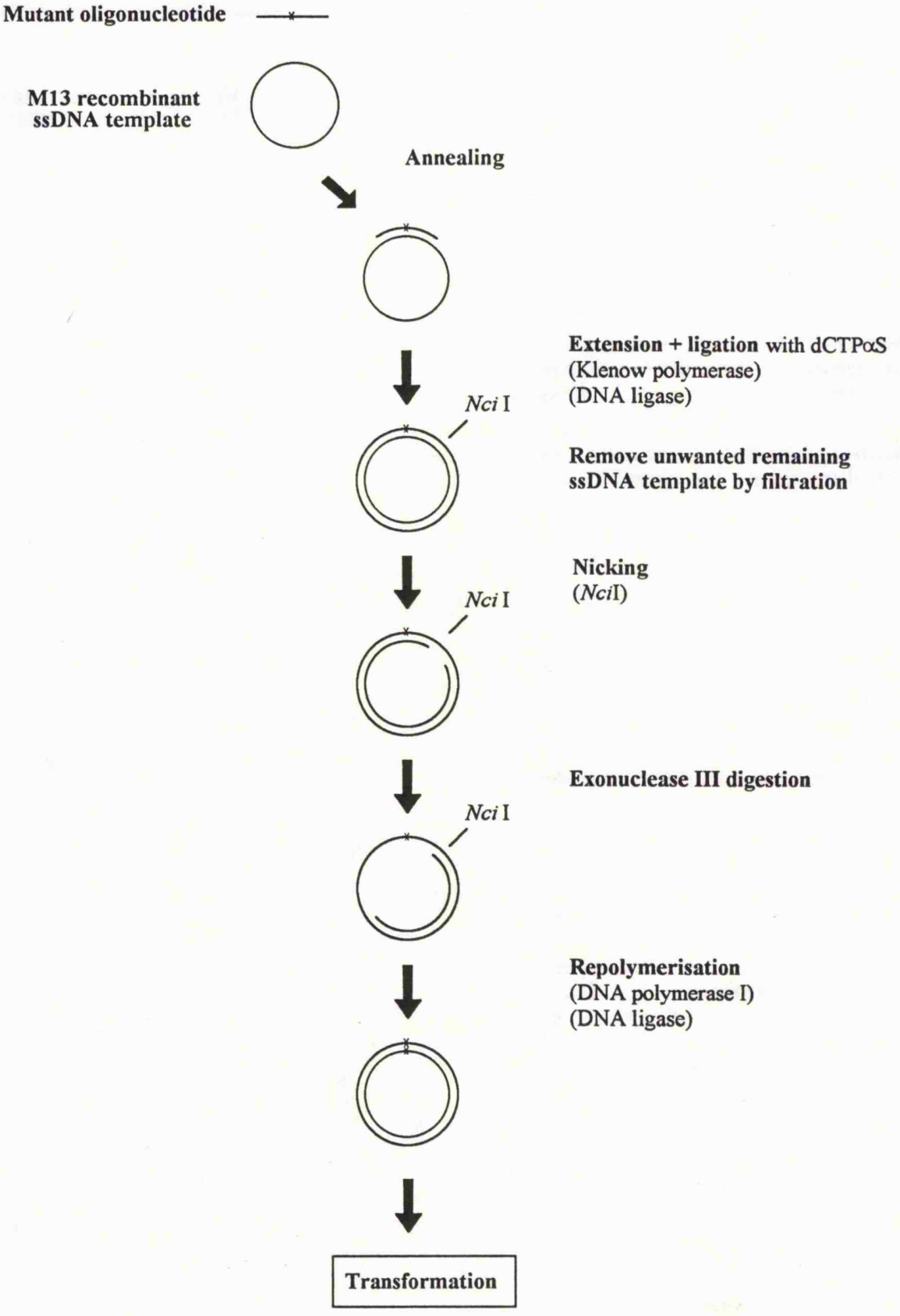

Figure 2.1 Oligonucleotide-directed in vitro mutagenesis system (adapted from the Amersham protocol)

Repolymerisation

The mutant strand is used as a template to produce a double stranded homoduplex mutant DNA molecule by the action of the enzymes DNA Polymerase I and DNA ligase. This DNA is used to transform competent *E.coli* cells and recombinants identified by blue/white selection (described below).

The high mutagenic efficiency levels of this system are due mainly to two factors:

1. The method involves specific selection and elimination of the non-mutant strand *in vitro*. The remaining mutant strand is then used to a generate a pure homoduplex mutant DNA sequence. This step increases efficiency because it avoids host-mediated repair which can remove the mutant sequence and result in poor yields.

2. A filtration step is used to remove any remaining single stranded template which reduces the level of non-mutant (i.e. wild-type) background.

Blue/white α-complementation method to select for recombinants

The bacteriophage M13 mp series of vectors (e.g. M13mp19) have a small region of *E.coli* DNA cloned into them that contains the *lac* operator and part of the *lacZ* gene (referred to as *lacZ'*). The *lacZ* gene is a structural gene that codes for the enzyme β-galactosidase. *LacZ'* is a modified version of *lacZ* which codes for only the first 146 amino acids of β-galactosidase. Host bacterial cells (e.g. the *E.coli* strain TG1) which harbour the F' plasmid carry a defective *lacZ* gene that codes for an inactive polypeptide that lacks amino acids 11-41. If host cells are transformed with this M13 vector DNA the amino terminal fragment of β-galactosidase produced by M13 DNA associates with the defective polypeptide, coded for by the F' plasmid, to form an active enzyme. This is referred to as α-complementation and can be visualised since infected cells form blue plaques when plated out on a medium containing IPTG (gratuitous inducer of β-galactosidase) and X-gal

(chromogenic substrate). Insertion of foreign DNA (e.g. the DHFR gene) into the *lacZ'* region of M13mp19 disrupts the reading frame and leads to an inactive form of the amino terminus of the enzyme being produced and hence eliminates α-complementation. These cells form colourless plaques hence providing a simple and rapid colour test that can be used to identify recombinants.

2.2.2 MUTAGENESIS OF DHFR

Mutants of DHFR produced using the Amersham Oligonucleotide-directed *in vitro* Mutagenesis System (version 2.1)™ were:

Trp 21→His	(W21H DHFR)
Trp 21→His + Asp 26→Asn	(W21H/D26N DHFR)

Oligonucleotides carrying the required mutation(s) are shown in Figure 2.2 and were designed such that the position of the mutation(s) was located near the centre of the oligonucleotide, with the rest of the sequence being complementary to the DHFR coding sequence:

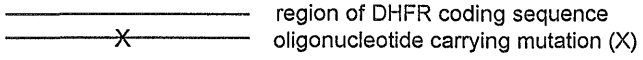

In addition, sequences which may form stable secondary structures and thus lower the efficiency with which the oligonucleotide hybridises to the target DNA were kept to a minimum.

All methods used to construct these mutants are described in detail, and in the order in which they were performed in Appendix A. The *L.casei* DHFR gene has been cloned into the pET11a plasmid and transformed into the *E.coli* strain BL21(DE3) by Dr. R. Badii. The

Figure 2.2 Oligonucleotides used in the production of mutant DHFRs (wild-type residue to be substituted and its codon are also shown).

W21H:

His21
5' C CGG TAA ATG **ATG** TGG CAA ATG ACC 3'
CCA
Trp21

W21H/D26N:

Asn26 His21
G GAA ATA ATG TAA **ATT** ATC CGG TAA ATG **ATG** TGG CAA ATG ACC ATC TTT GCC
5' ATC CCA 3'
Asp26 Trp21

pET expression system is now used to express DHFR (see section 2.3.2). However, mutagenesis and sequencing protocols used in the production of mutants are based on M13 vector systems. Hence, any DNA manipulations to be carried out require the DHFR gene to be recloned into a bacteriophage M13 vector, in this case M13mp19 RF1.

The mutagenesis procedure results in the production of M13mp19 RF1 DNA molecules some of which contain the required mutated DHFR gene. In order to select for such recombinants, the M13mp19 RF1 DNA was transformed into competent *E.coli* TG1 cells and putative mutant plaques identified by the blue/white α-complementation method. In order to ensure that recombinant (white) plaques contained mutant DHFR genes of the correct sequence (that is with no other mutations, deletions or insertions) it was necessary to sequence them. DNA sequencing was carried out using the dideoxy-mediated chain termination method and performed in two stages. Firstly, the region of the gene containing the desired mutation(s) was sequenced. Results showed that 3 out of 4 probable W21H mutant clones and 4 out of 4 putative W21H/D26N clones contained the required substitution(s), probable mutation rates of 75% and 100% respectively. Once the presence of the mutations was confirmed, the entire gene sequence of one W21H and one W21H/D26N clone was determined. A small section of an autoradiogram from a sequencing gel showing the region encompassing the mutation(s) is shown in Figure 2.3. Except for the required substitution(s) the gene sequence for each mutant was correct.

In order to express the mutant proteins it was necessary to reclone the mutant genes from M13mp19 RF1 back into the expression vector pET11a; this vector was then transformed into competent *E.coli* BL21(DE3) cells. pET11a carries the ampicillin resistance gene (*bla* gene) and hence recombinants were selected for by their ability to grow in the presence of this antibiotic. Small scale cultures of putative mutant colonies were grown and protein synthesis induced by the addition of IPTG. Expression of mutant proteins was confirmed by SDS polyacrylamide gel electrophoresis (SDS-PAGE) using wild-type DHFR as a standard molecular weight marker (Figure 2.4).

2.2.3 CONCLUSIONS

Oligonucleotide-directed mutagenesis has been successfully used to produce two mutants of *L.casei* DHFR (W21H and W21H/D26N). Sequencing of the W21H and W21H/D26N genes confirmed that, except for the required mutations they contained no other mutations. Cloning of each mutant gene into the expression vector pET11a and subsequent transformation into *E.coli* BL21(DE3) cells has enabled active mutant proteins to be produced under the control of the bacteriophage T7 promoter.

Figure 2.3 Autoradiograms showing regions of the DNA sequence encompassing the mutation site for (a) W21H DHFR
(b) W21H/D26N DHFR

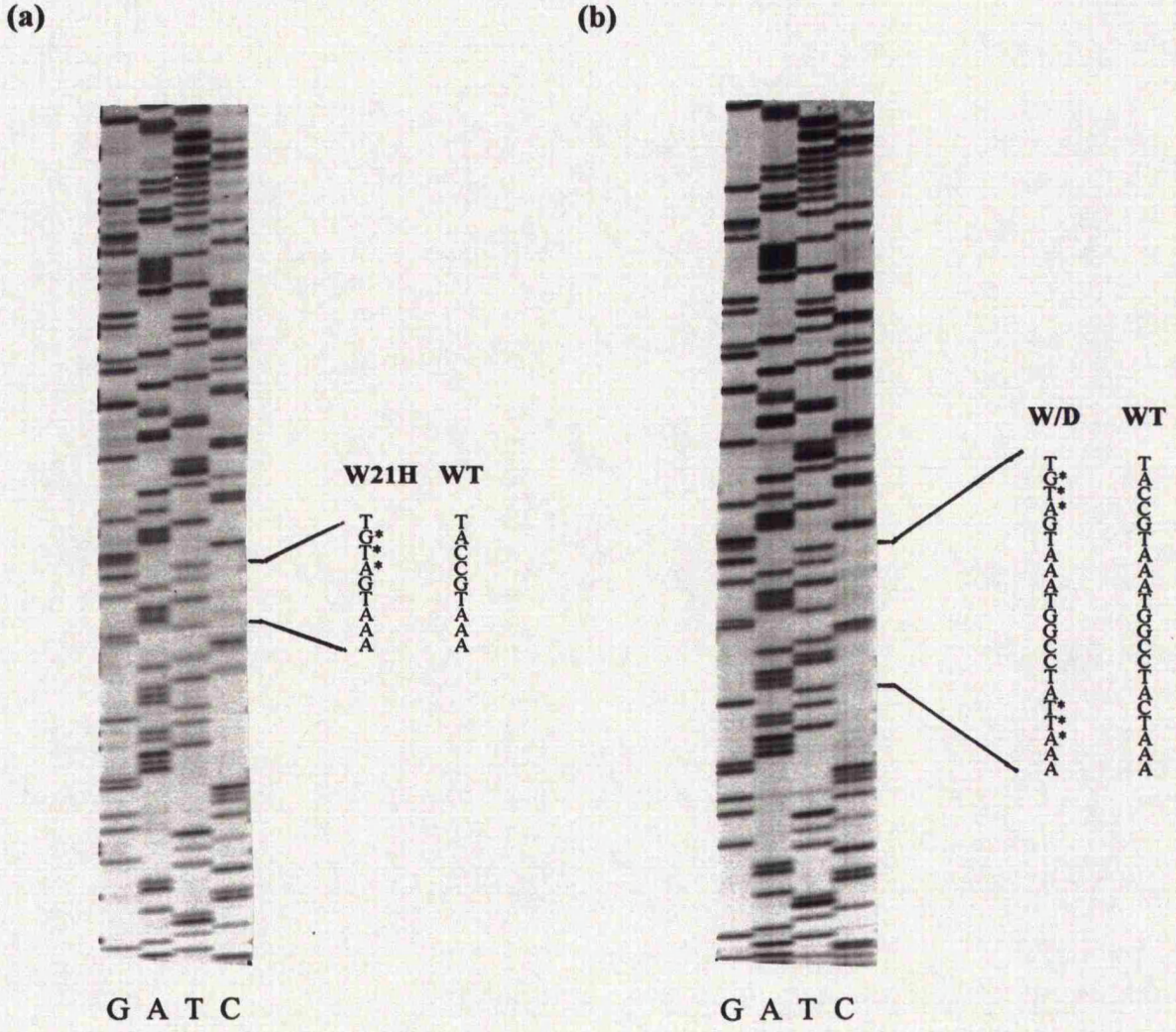

The sequence was read from the bottom to the top of the gel using the lanes labelled with the four bases (G,A,T,C) as indicated. For each mutant the region of the DNA sequence incorporating the site of the mutation is shown. The three bases that code for the mutated residue are marked with asterisks (*): ATG codes for His and ATT for Asn. WT refers to wild-type and W/D to W21H/D26N. The coding sequence for the equivalent region of wild-type DHFR is also shown. Sequencing was carried out using the dideoxy-mediated chain termination method.

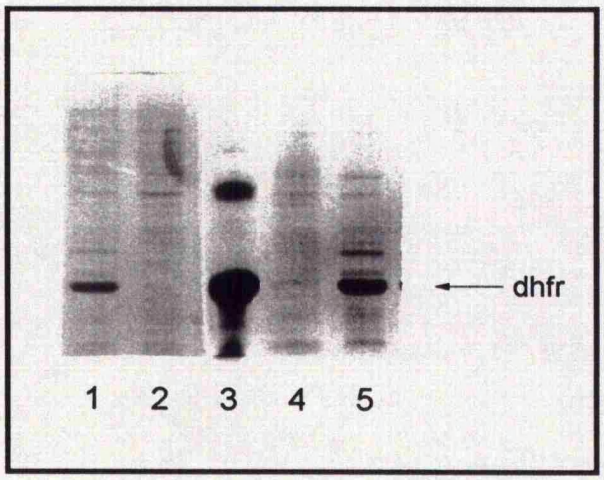

Figure 2.4 Region of a 12% SDS-polyacrylamide gel of mutant DHFR expression (stained with Coomassie Blue)

Lane 1	W21H/D26N DHFR (after 3 hour induction with 1mM IPTG)
Lane 2	W21H/D26N DHFR (non-induced)
Lane 3	wild-type DHFR
Lane 4	W21H DHFR (non-induced)
Lane 5	W21H DHFR (after 3 hour induction with 1mM IPTG)

2.3 EXPRESSION AND PURIFICATION OF DHFR

2.3.1 INTRODUCTION

L.casei DHFR was expressed in *E.coli* using two different expression vector systems, pMAC and pET:

pMAC expression system

The *L.casei* wild-type DHFR gene has been cloned into the expression vector pMAC5-14 downstream of the temperature inducible λP_L promoter (Andrews *et al.*, 1991). The P_L promoter is a strong bacteriophage λ promoter that is repressed by the cI repressor protein. The recombinant plasmid (referred to as pMA802) is transformed into a mutant host *E.coli* strain (NF1) that produces a temperature-sensitive form of the cI repressor. At 30°C the repressor binds to the P_L promoter preventing transcription of the DHFR gene. If the temperature is raised to 40°C the cI protein is unable to repress the P_L promoter, the gene is transcribed and protein is produced.

pET expression system

The *L.casei* DHFR gene has also been cloned into the pET11a plasmid next to, and under the control of the bacteriophage T7 promoter (Badii *et al.*, 1994). The recombinant plasmid (pET11a/DHFR/9) has been transformed into a host *E.coli* strain BL21(DE3). This bacterial strain has a copy of the phage T7 RNA polymerase gene in its genome which is under the control of the inducible *lac*UV5 promoter. In the presence of IPTG, synthesis of T7 RNA polymerase is induced which in turn transcribes the DHFR gene from the pET11a plasmid-based bacteriophage T7 promoter.

The D26N and R57K mutants used in this research were made by Dr. J. Andrews (Andrews *et al.*, 1991). The W21H and W21H/D26N mutants were made as described

above. DHFR produced by both the pMAC and pET expression systems was isolated and purified by following a modified version of the published protocol (Dann *et al.*, 1976). Expression and purification procedures for DHFR mutants were as for the wild-type enzyme unless stated otherwise.

2.3.2 DHFR EXPRESSION

Bacterial strains harbouring plasmids with cloned wild-type or mutant DHFR genes were maintained as described in Appendix A. All culture media (defined in Appendix A) were sterilised by autoclaving at 121°C for 20 minutes. Cultures were grown in the presence of the antibiotic ampillicin at a final concentration of 100μg/ml.

2.3.2.1 pMAC expression system

E.coli NF1 harbouring the pMA802 plasmid was used to inoculate 250ml of Luria Bertini (LB) broth and grown overnight at 30°C in a shaker. This fresh overnight culture was used to inoculate 12x 500ml 2YT broth in 2 litre flasks (approximately 20ml of overnight culture per flask). The cells were grown at 30°C until the optical density at 595nm (OD_{595}) was 0.7 (cells are in mid-log phase of growth). At this point the temperature was increased to 40°C to induce protein synthesis. After 6 hours, cells were harvested by centrifugation using a Beckman J2-21 centrifuge. The supernatant was discarded and the cell pellet stored at -20°C until the protein was to be purified.

2.3.2.2 pET expression system

Inoculation (with *E.coli* BL21(DE3) containing the pET11a/DHFR/9 plasmid) and cell growth was as for the pMAC expression system. The cells were grown at 30°C until the OD_{595} was 0.7; DHFR expression was then induced by the addition of IPTG (final concentration of 1mM). The cells were grown for a further 3 hours and then harvested by

centrifugation using a Beckman J2-21 centrifuge. The supernatant was discarded and the cell pellet stored at -20°C until the protein was to be purified.

2.3.3 PURIFICATION OF DHFR

All purification steps were carried out at 4°C or on ice to minimise protein loss. During the purification procedure the purity and presence of DHFR was assessed by SDS-PAGE, UV absorbance spectroscopy and by assaying for DHFR activity (section 2.3.3.1). An outline of the purification protocol is shown in Figure 2.5 and the steps are described in detail below.

The cell pellet was resuspended in a minimum volume of 0.05M Tris-HCl pH 7.4 buffer. Cells were broken open by passing the suspension twice through a cold French press. Cell debris was removed by centrifugation at 10,000 rpm for 40 minutes using a MSE Prespin 50 centrifuge and the supernatants pooled.

Nucleic acids were removed by precipitation with streptomycin sulphate. A 20% streptomycin sulphate solution was added in a dropwise manner to the protein sample to give a final streptomycin sulphate concentration of 4%. The solution was left to stir for 10 minutes and the DNA precipitate then removed by centrifuging at 10,000 rpm for 40 minutes. The supernatant was transferred to a fresh tube.

DHFR was concentrated by the addition of ammonium sulphate (600g per litre). The salt was added to the protein solution and stirred overnight at 4°C. The resultant precipitate was centrifuged as above, the supernatant removed, and the pellet stored at -20°C until required.

The ammonium sulphate pellet was resuspended in a minimal volume of 25mM KH_2PO_4 pH 6.5 buffer, and dialysed against the same buffer in 3x 2 litre batches and then

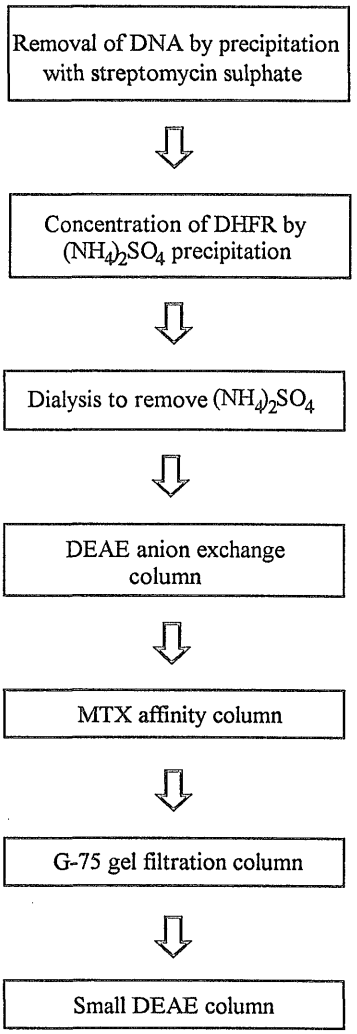

Figure 2.5 Purification scheme for DHFR

against 5 litres overnight. Any remaining protein was removed by spinning at 10,000 rpm for 30 minutes.

A DEAE (diethylaminoethyl) anion exchange column was the first chromatographic step in the purification procedure. A 200ml DEAE Sephacel column was prepared and equilibrated with 25mM KH_2PO_4 pH 6.5 buffer. The dialysed protein was pumped onto the column (2ml/min) and eluted with a salt gradient of 0-100mM KCl in 25mM KH_2PO_4 pH 6.5. Fractions containing DHFR (as judged by SDS-PAGE and enzyme assay) were pooled and lyophilised.

The next stage of the purification protocol was a methotrexate (MTX) affinity column. The column was prepared by Dr. R. Badii and is composed of EAH Sepharose 4B resin which has six carbon (1,6 diaminohexane) spacer arms that have been coupled to MTX using the method described by the Pharmacia protocol. A 50ml MTX column was washed extensively with 50mM KH_2PO_4/100mM KCl pH 6.5 (MTX equilibration buffer) and the absorbance of the effluent monitored at a wavelength of 302nm (A_{302}). When A_{302} was less than 0.01 the column was deemed clean from free MTX or folate from previous usage.

The protein sample from the DEAE step was dialysed against MTX equilibration buffer and loaded on to the MTX column. The column was washed with one column volume of equilibration buffer and then with high salt buffer (50mM KH_2PO_4/2M KCl pH 6.5) which removes most of the impurities. The flow was reversed (since this is known to give a sharper DHFR elution peak; Dann, 1975, Dann *et al.*, 1976) and DHFR eluted with folate elution buffer (50mM Tris-HCl/1M KCl/2mM folate pH 8.5). The protein-folate fractions were pooled and immediately dialysed against 10mM KH_2PO_4/100mM KCl pH 6.5 buffer to remove as much of the folate as possible (typically against 20 litres over 24 hours). The protein was then lyophilised and the MTX column re-equilibrated with MTX equilibration buffer.

DHFR was dissolved in a small volume (usually 5-10ml) and loaded onto a 200ml Sephadex G-75 column in order to remove the remaining folate and a high molecular weight impurity. The enzyme was eluted from the column with 10mM KH_2PO_4/100mM KCl pH 6.5 buffer. UV absorbance spectra of fractions from the Sephadex G-75 column showed that some fractions still contained trace amounts of folate. The remaining folate was removed by passing the protein through a small final DEAE Sephacel column which was run under the same conditions as the first DEAE Sephacel column. The protein was pooled, lyophilised and stored at -20°C.

2.3.3.1 Assessment of DHFR presence and purity

During the purification procedure DHFR activity was measured as described in Section 2.4.7.1. SDS-PAGE and UV absorbance spectroscopy were used to assess protein purity:

SDS-PAGE was carried out using the Bio-Rad Mini-PROTEAN II gel electrophoresis kit and protocol. An equal volume of Sample Buffer (62.5mM Tris-HCl (pH 6.8), 2% SDS, 10% glycerol, 5% β-mercaptoethanol, 0.025% w/v bromophenol blue) was added to the protein sample, mixed and then heated at 100°C for 3 minutes. The protein samples were loaded onto a 12% SDS polyacrylamide gel (containing 0.1% SDS) alongside pure wild-type DHFR which was used as a standard marker. The gel was run in 25mM Tris-192mM glycine buffer pH 8.3 (1% SDS) at 200V until the dye front had reached the bottom of the gel (approximately 45 minutes). The gel was stained with Coomassie Blue for 30 minutes, destained and then examined.

Contamination of DHFR with low molecular weight impurities such as NADPH and folate was determined by recording UV absorption spectra. NADPH and folate absorb in the 340-350nm wavelength region of the UV spectra whereas proteins do not. Hence, DHFR was deemed clean (i.e. free from such impurities) when the protein had no significant absorption (less than 5% of the A_{280}) in this region.

2.3.4 SUMMARY

Table 2.1 lists typical protein yields for wild-type and mutant DHFRs obtained after the purification procedure. Purification of all mutants was carried out as for the wild-type enzyme with the exception of the double mutant W21H/D26N. The affinity of the double mutant for the MTX column was reduced, but retarded sufficiently to afford a good purification; the mutant was eluted with the first traces of folate. The final DEAE anion exchange column was not used in the purification of W21H/D26N DHFR since the UV spectra of fractions from the G75 column revealed no absorption at A_{350} i.e. there was no contamination with folate. This may suggest weaker binding of this substrate to W21H/D26N DHFR.

Table 2.1 Typical yields of pure wild-type and mutant DHFRs after purification

DHFR	Expression system	Yield mg/litre[a]
wild-type	pMAC	5
	pET	50
D26N	pMAC	4
R57K	pMAC	2.5
W21H	pMAC	0.1
	pET	1
W21H/D26N	pET	0.5

[a] milligrams of pure protein obtained after purification from one litre of 2YT media inoculated with the appropriate bacterial strain and protein expression induced as described in the text

Yields of the D26N mutant produced using the pMAC system were comparable to those of wild-type DHFR. R57K DHFR yields were 50% of that of the wild-type enzyme.

With both the pMAC and pET expression systems levels of the Trp 21 mutants are lower than the wild-type enzyme (by a factor of 50). It is thought that DHFR in the cell is stabilised by the coenzyme NADPH. It is feasible that if the binding constant of NADPH to these mutants has been decreased, then they will not be stabilised to the same extent as the wild-type enzyme and this may contribute to lower protein yields. In the case of the double mutant low levels of protein may also be attributed to losses (particularly at the MTX column stage) of protein during the purification procedure.

2.4 KINETIC METHODS

All ligand binding and kinetic experiments were carried out at 25°C unless stated otherwise. Experiments were performed on mutant and wild-type DHFRs to allow a direct comparison of the data.

2.4.1 Determination of ligand concentrations

Ligand concentrations were determined by absorbance spectroscopy using the following extinction coefficients: folate, 27,600 M^{-1} cm^{-1} at 282nm, pH 7.0; FH_2, 28,000 M^{-1} cm^{-1} at 282nm, pH 7.0; FH_4, 28,000 M^{-1} cm^{-1} at 297nm, pH 7.5; NADPH, 6200 M^{-1} cm^{-1} at 340nm, pH 7.5 (all the above from Dawson *et al.*, 1986); MTX, 22,100 M^{-1} cm^{-1} at 302nm in 0.1M KOH (Seegar *et al.*, 1949); TMP, 6060 M^{-1} cm^{-1} at 271nm in 0.1M acetic acid (Roth and Strelitz, 1969).

Folate, FH_2 and FH_4 were dissolved in KMB buffer pH 7 while NADPH which is stable at higher pH values was dissolved in 20mM Tris-HCl pH 8.5.

KMB buffer:	MES	50mM
	Tris-HCl	25mM
	KCl	500mM
	Ethanolamine	25mM

MES = 4-morpholinoethane sulphonic acid

2.4.2 Production of [4(R)-^{2}H] NADPH (NADPD)

Deuterated coenzyme (NADPD) was prepared by reducing $NADP^+$ in the presence of $^2H_6$-ethanol using $NADP^+$ dependent alcohol dehydrogenase (ADH) (Stone and Morrison, 1982):

50mg $NADP^+$, 20 units of ADH and 1ml of $^2H_6$-ethanol were added to 8ml of 20mM triethylamine (TEA) and adjusted to pH 9. The solution was kept in the dark, mixed by occasional swirling and the reaction allowed to proceed until there was no further increase in absorbance at 340nm (approximately 4 hours). The reaction mix was stored at -70°C until the coenzyme was ready to be purified.

2.4.3 Purification of NADPH and NADPD

Preparations of NADPH and NADPD either purchased from the Sigma Chemical Co. or prepared as described above contain a breakdown product that is a potent inhibitor of DHFR (Fawcett *et al.*, 1961). The coenzymes were therefore purified by ion exchange chromatography (Orr and Blanchard, 1984) prior to use in order to achieve accurate kinetic results.

Purification was carried out by FPLC using a Pharmacia Mono Q 10/10 anion exchange column. A salt gradient was made from 20mM triethylamine bicarbonate (TEAB) pH 9 (Buffer A) and 20mM TEAB/1M KCl pH 9 (Buffer B). Buffers were made by bubbling carbon dioxide through a solution of TEA until a pH of 9 was reached and then filtered through a 0.2μM filter. 10mg of NADPH was loaded onto the Mono Q 10/10 column and washed with 8ml (one bed volume) of Buffer A. NADPH was eluted using a gradient from 25% Buffer B to 35% Buffer B over 35ml during which time it was separated from $NADP^+$ and other impurities. The column was then washed with 8ml of 100% Buffer B and re-equilibrated with Buffer A.

NADPD was purified in a similar manner. However, since enzymatic preparations of NADPD contain more impurities than do commercial preparations of NADPH it was necessary to wash the column with two bed volumes of Buffer A once NADPD had been loaded; NADPD was eluted with a gradient from 25-35% Buffer B over 40 ml.

In both cases 1ml fractions were collected and the absorbance at 260nm and 340nm (A_{260} and A_{340} respectively) measured. Fractions with an A_{260}:A_{340} ratio of less than 2.3 were deemed pure and were pooled. The purified coenzyme was lyophilised, stored at -70°C and used within a week.

2.4.4 Determination of DHFR concentration

Absorbance spectroscopy

The concentration of DHFR was estimated by measuring the A_{280}, using an extinction coefficient (ε) of 30,500 M^{-1} cm^{-1} (Andrews *et al.*, 1989). When calculating the concentration of mutants lacking Trp 21 an ε of 23,500 M^{-1} cm^{-1} was used (Andrews *et al.*, 1989).

Fluorescence spectroscopy

The concentration of DHFR can be accurately determined by performing a MTX titration in which the quenching of protein fluorescence is measured as MTX binds. MTX binds tightly and stoichiometrically to wild type DHFR (K_d less than 1nM) so that almost all of the inhibitor is bound to the enzyme in the early stages of the titration. A plot of protein fluorescence against MTX concentration therefore yields two straight lines, the intersection of which gives the enzyme concentration. Figure 2.6 shows a typical graph obtained from such a titration. Provided that the binding constant of MTX has not been significantly reduced by the mutation, this method provides a very accurate active-site concentration for the protein.

The MTX titration was performed as follows:

3ml of 50mM KH_2PO_4/500mM KCl (1% lactose) pH 6.5 buffer containing 0.2-0.5μM DHFR was pipetted into a 1cm path length quartz cuvette. Microlitre (μl) volumes of an appropriately diluted MTX solution were added to the cuvette and mixed by inversion. Fluorescence measurements were made at an excitation wavelength (E_x λ) of 290nm and an emission wavelength (E_m λ) of 340nm until no further quench in protein fluorescence occurred.

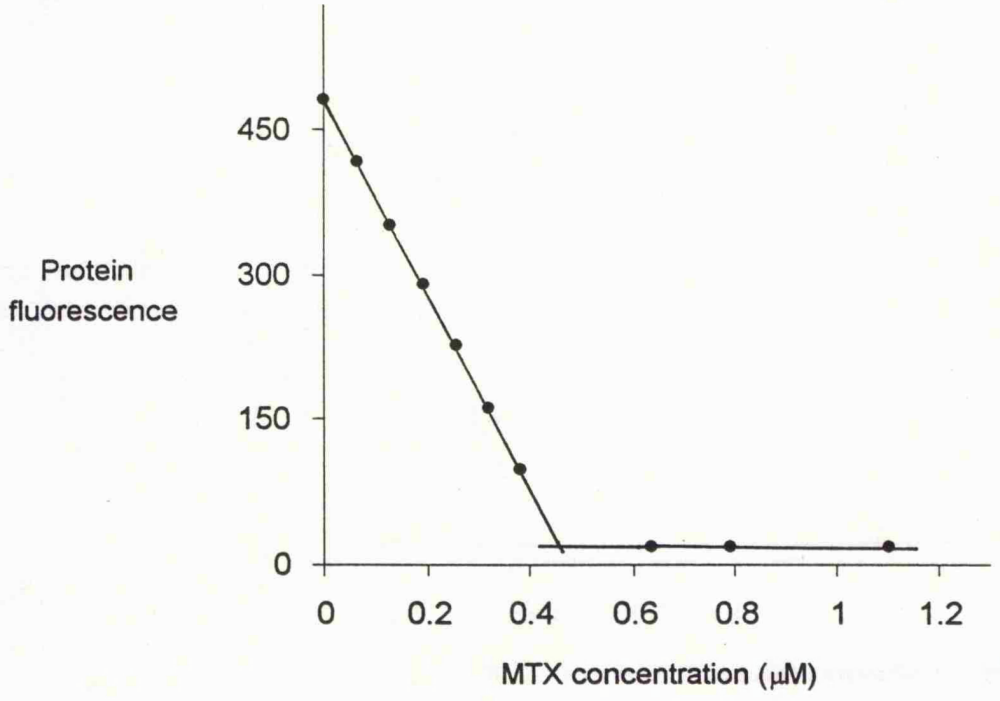

Figure 2.6 Determination of DHFR concentration by titration with MTX

2.4.5 Determination of equilibrium binding constants

Excitation of DHFR at a λ of 290nm produces a fluorescence emission spectrum with a maximum at 340-350nm. The addition of coenzyme, substrates or inhibitors quenches this fluorescence (essentially all of which is due to Trp residues) to varying extents. Titration curves obtained from such experiments can then be used to determine equilibrium binding constants of various ligands (Birdsall *et al.*, 1980, Birdsall *et al.*, 1978, Dunn *et al.*, 1978).

All fluorescence measurements were carried out on a Perkin-Elmer LS-5 Luminescence spectrometer at 25°C using an E_x λ of 290nm and an E_m λ of 340-350nm. The buffer used was 50mM KH_2PO_4/500mM KCl pH 6.5 containing 1% lactose which prevented the small quantities of DHFR from adsorbing to the sides of the cuvette. Microlitre volumes of the appropriately diluted ligand solution were added to a cuvette containing the protein and mixed by inversion. The solution was allowed to equilibrate for a few minutes and then fluorescence readings taken. This procedure was repeated until no further change in fluorescence occurred upon addition of ligand.

To correct for light absorption by the ligand, a tryptophan solution was titrated using the same wavelengths and slit widths as used for the titration of protein fluorescence. Absorption of the excitation light by the ligand leads to a decrease in the amount of fluorescence emitted, this is referred to as an "inner filter effect" (Birdsall *et al.*, 1983, Bagshaw and Harris, 1987). This effect "mimics" fluorescence quenching due to ligand binding and, if uncorrected, can lead to errors when calculating binding constants. Correction for the inner filter effect and the subsequent determination of binding constants from the corrected fluorescence data were carried out as described previously (Birdsall *et al.*, 1980, Birdsall *et al.*, 1983) and is outlined below.

2.4.6 Calculation of equilibrium binding constants

Data obtained from the fluorescence titrations were fitted by non-linear regression to equations programmed into the Enzfitter software package (Leatherbarrow, 1987).

To correct for the inner filter effect the tryptophan fluorescence titration data (see above) was fitted to equation 1 and estimates for the correction factors *a* and *d* obtained. Equation 1 relates the observed fluorescence (F_{obs}) to the "true" fluorescence (F):

$$F_{obs} = F[(\exp(-aL_T d) - \exp(-aL_T) / aL_T(1-d))] \qquad \text{eqn. 1}$$

where L_T = ligand concentration

Parameters *a* and *d* were then used in equation 1 to calculate the correction factor F_{obs}/F, and this was then used to correct the measured fluorescence intensities of the enzyme solution. The corrected enzyme fluorescence is related to the fractional saturation of the enzyme with ligand by equation 2:

$$[EL] / E_T = (F_o - F) / (F_o - F_\infty) \qquad \text{eqn. 2}$$

where [EL] = concentration of the complex at a ligand concentration giving a fluorescence intensity F
E_T = total enzyme concentration
F_o = fluorescence intensity at zero ligand concentration
F_∞ = fluorescence intensity at saturating ligand concentration

Combining equation 2 with the mass action equation (eqn. 3) produces equation 4:

$$K_d = [E][L] / [EL] \qquad \text{eqn. 3}$$

$$[EL] / E_T = [K_d + E_T + L_T - [(K_d + E_T + L_T)^2 - 4E_TL_T]^{1/2}] / 2E_T \qquad \text{eqn. 4}$$

where K_d = equilibrium dissociation constant

Combination of equation 4 with equation 2 produces equation 5 from which the equilibrium binding constant was estimated.

$$F_o - F = (F_o - F_\infty / 2E_T) [K_d + E_T + L_T - [(K_d + E_T + L_T)^2 - 4E_TL_T]^{1/2}] \qquad \text{eqn. 5}$$

2.4.7 STEADY STATE KINETICS

2.4.7.1 Measurement of DHFR activity

DHFR activity can be measured by following the decrease in A_{340} which accompanies the conversion of folate or FH_2 + NADPH into FH_4 + $NADP^+$. Assays were carried out using KMB buffer because the ionic strength of this buffer remains constant over the pH range 5 to 9, thus eliminating the need to change buffer when activity was measured at different pH values (Ellis and Morrison, 1982).

FH_2 reduction

KMB buffer was pipetted into a 1ml quartz cuvette and preincubated at 25°C. NADPH and enzyme were then added to the cuvette, mixed by inversion and left to equilibrate for two minutes. The reaction was initiated by the addition of FH_2 which had also been incubated at 25°C. The rate of the reaction was measured on a Hewlett Packard 8452A Diode array spectrophotometer by monitoring the change in A_{340}. The difference extinction coefficient for the reaction is 11,800 M^{-1} cm^{-1} (Stone and Morrison, 1982).

For the wild-type enzyme, substrate concentrations of 50μM NADPH and 50μM FH_2 were used. In the case of the mutants, if the K_m for the substrate(s) had changed, then assays were performed using substrate concentrations of 10x K_m.

Wild-type and mutant enzymes were assayed in the pH range 5.2 to 8.6 using the above procedure. At low pH values the coenzyme oxidises at quite measurable rates in the absence of enzyme. This rate was measured and subtracted from the enzyme-catalysed reaction.

Folate reduction

Measurement of enzyme activity using folate as the substrate was performed as previously noted for FH_2 reduction albeit with minor modifications. Enzyme activity was measured in the pH range 4.5 to 5.5 using 15mM sodium acetate/500mM KCl buffer. The difference extinction coefficient for the reaction was 18,900 M^{-1} cm^{-1} (Matthews and Huennekens, 1963).

In order to calculate apparent pK_a values, data was fitted by non-linear regression to the appropriate equations using the GraFit software package (Leatherbarrow, 1990). When the pH dependence of k_{cat} was described by the ionisation of a single group, the apparent pK_a of this group was calculated using the following equation:

$$y = (k_{cat1} + k_{cat2} \cdot 10^{(pH - pK_a)}) / (10^{(pH - pK_a)} + 1) \qquad \text{eqn I}$$

where $y = k_{cat}$ at a particular pH value
$k_{cat1} = k_{cat}$ at low pH
$k_{cat2} = k_{cat}$ at high pH
$pK_a = -\log K_a$

When the variation of k_{cat} with pH was dependent on the ionisation of two groups, both of which had to be protonated to achieve maximum velocity, equation II was used to calculate the two pK_a values:

$$y = (k_{cat1} + k_{cat2} \cdot 10^{(pH - pK_a1)}) / (10^{(pH - pK_a1)} + 1) - [((k_{cat2} - k_{cat3}) \cdot 10^{(pH - pK_a2)}) / (10. (pH - pK_a2) + 1)] \qquad \text{eqn II}$$

where $y = k_{cat}$ at a particular pH value
$k_{cat1} = k_{cat}$ at low pH
$k_{cat2} = k_{cat}$ at middle pH
$k_{cat3} = k_{cat}$ at high pH
$pK_a = -\log K_a$

For the cooperative ionisation of two groups, pK_a values were calculated using the following equation (Tipton and Dixon, 1983):

$$y = 1 / [(1 + 10(pH - pK_a1)) + (10(pH - pK_a1) . 10(pH - pK_a2))] \qquad \text{eqn III}$$

2.4.7.2 Determination of K_m values

K_m values that are submicromolar cannot be determined by absorbance spectroscopy because the technique is not sensitive enough to measure absorbance changes accurately at such low substrate concentrations. For this reason, a fluorimetric assay has been developed (Dann, 1975, Dann *et al.*, 1976) in which the course of the reaction is followed by monitoring the change in fluorescence that accompanies oxidation of NADPH and reduction of FH_2.

Assays were carried out on a Perkin-Elmer LS-5 Luminescence Spectrometer using an E_x λ of 360m and an E_m λ of 450nm. The buffer used was KMB (adjusted to the required pH) containing 1% lactose. When measuring the K_m value for a substrate its concentration was varied, whilst keeping the concentration of the second substrate constant and at saturating levels. The enzyme catalysed reaction was monitored by measuring the decrease in fluorescence of the nicotinamide ring as NADPH is converted to $NADP^+$. Background rates due to instability of substrates were measured and subtracted from the enzyme catalysed reactions.

K_m values of substrates which were not submicromolar were measured using the spectrophotometric assay. In cases where relatively high substrate concentrations were used, the absorbance at 340nm was high. Therefore, assays were performed at longer wavelengths of 360, 370 and 380nm depending on the concentration of substrate being used. Rates were then calculated using the following difference extinction (ε) coefficients: $\varepsilon_{360} = 6140\ M^{-1}\ cm^{-1}$, $\varepsilon_{370} = 3190\ M^{-1}\ cm^{-1}$ and $\varepsilon_{380} = 1180\ M^{-1}\ cm^{-1}$ (Thomas, 1990).

The kinetic parameters K_m and k_{cat} were calculated by fitting the data to the Michaelis-Menten equation by non-linear regression using the GraFit software package (Leatherbarrow, 1990):

$$v = \frac{k_{cat}[S]}{K_m + [S]}$$

where v = rate at a particular [S]
[S] = substrate concentration

2.4.7.3 The kinetic isotope effect

The kinetic isotope effect (k_{cat}NADPH/k_{cat}NADPD) was calculated by measuring DHFR activity using normal and deuterated coenzyme at saturating concentrations. The pH dependence of the isotope effect was determined by measuring k_{cat} values at a range of pH values (between pH 5 and 8.5).

2.4.7.4 The solvent isotope effect

When carrying out solvent isotope effect experiments all proteins, substrates and buffers were dissolved in ^2H_2O (D_2O). Buffer salts were dissolved in D_2O and the pD of the buffers was calculated by adding 0.4 to the observed pH meter reading. DHFR activity was measured in D_2O and in H_2O and the solvent isotope effect (k_{cat} H_2O/k_{cat} D_2O) calculated. The pH(D) dependence of the solvent isotope effect was measured for the pH range 5.5-8.5.

2.4.8 PRE-STEADY STATE KINETICS

Pre-steady state kinetic measurements were made by using an Applied Photophysics (model SF.17 MV) stopped flow spectrometer operating in either a fluorescence or

absorbance mode with a 2mm sample cell. All data were analysed using an iterative, non-linear regression package supplied by Applied Photophysics; the average of at least 4 runs was used for data analysis at each point.

2.4.8.1 Measurement of the rate of hydride ion transfer

The rate constant for hydride ion transfer from NADPH to FH_2 when bound to the enzyme can be measured from the burst of product formation that occurs after mixing the DHFR-NADPH complex with FH_2 (Fierke *et al.*, 1987, Andrews *et al.*, 1989):

DHFR (1μM) was preincubated with NADPH (20μM) in KMB buffer. The reaction was initated by mixing with an equal volume of FH_2 (50μM) and monitored by measuring the decrease in A_{340}. Data were collected by a computer over a given time interval following a trigger impulse. Reaction rates were recorded in the pH range 5-9.

2.4.8.2 Measurement of the dissociation rate constant (k_{off}) for FH_4 by competition experiments

In this technique the enzyme-ligand complex ($E{\cdot}L_1$) is mixed with a large excess of a second ligand that competes for the binding site (see scheme I). The formation of the new enzyme-ligand complex ($E{\cdot}L_2$) is monitored by a fluorescence change due to the different fluorescence quenching properties of the two ligands.

Scheme I:

$$E{\cdot}L_1 \underset{k_1}{\overset{k_{-1}}{\rightleftharpoons}} E + L_1$$

$$E + L_2 \underset{k_{-2}}{\overset{k_2}{\rightleftharpoons}} E{\cdot}L_2$$

When $k_1[L_1] << k_2[L_2] >> k_{-1}$, k_{obs} for the reaction is equal to the dissociation rate constant for L_1, k_{-1}. The validity of these conditions is checked by showing that k_{obs} does not change when the concentration of L_2 is doubled.

The dissociation rate constant (k_{off}) for FH_4 from the ternary enzyme-FH_4-NADPH complex was measured by using MTX as the competing ligand (Fierke *et al.*, 1987, Andrews *et al.*, 1989). FH_4 is sensitive to oxygen and light and solutions were therefore purged with argon and kept in the dark during the course of the experiments. Buffers were also purged with argon.

DHFR (1μM) was preincubated with FH_4 (5μM) and NADPH (5μM) in KMB buffer. The ternary complex (DHFR-NADPH-FH_4) was then mixed with an equal volume of the competing ligand, MTX (20μM) and the change in fluorescence (in this case a decrease) monitored using E_X λ of 290nm and a 350nm cut-off filter. Data were collected by a computer over a given time interval following a trigger impulse. Product dissociation rates were measured at a range of pH values.

2.5 UV DIFFERENCE SPECTROSCOPY

UV difference spectra were recorded on a Hewlett Packard 8452A Diode array spectrophotometer. The buffer used was 50mM KH_2PO_4/500mM KCl pH 7. The spectrum of free enzyme (8μM) and free MTX (30μM) were recorded separately and stored. Enzyme and MTX were then mixed (final concentrations 8μM and 30μM respectively) and the spectrum of the enzyme-MTX complex recorded. Difference spectra were obtained by subtracting the free enzyme and the free MTX spectra from the enzyme-MTX binary complex spectra. The protonation difference spectra of free MTX was generated by recording the spectrum of a MTX solution at pH 2 and at pH 7 and then subtracting the two.

2.6 ^{1}H NMR SPECTROSCOPY

Proton (^{1}H) NMR spectra were recorded using a Brüker AM500 spectrometer at 298K. Typical parameters included 16K data acquisition points and a sweep width of 7042 Hz. Prior to Fourier transformation the free induction decay was multiplied by a Gaussian function. Samples contained 1mM enzyme with one molar equivalent of MTX or MTX-α-amide that had been dialysed against 50mM KH_2PO_4/200mM KCl pH 6.5. The protein sample was lyophilised and then dissolved in 500µl of 99.96% D_2O. The pH of the sample was measured (uncorrected for the isotope effect on the glass electrode), the spectrum collected and the pH of the sample remeasured. Spectra were recorded at a variety of pH values, the pH of the sample was adjusted by the careful addition of ^{2}HCl or $NaO^{2}H$.

CHAPTER 3 D26N DHFR

3.1 INTRODUCTION

Asp 26 is a conserved residue found in all known prokaryotic DHFRs; eukaryotic enzymes have a Glu at the equivalent position (Volz *et al.*, 1982). The rationale for the Asp26→Asn mutant (D26N) was two fold:

Crystal structures of various DHFR-ligand complexes have shown that Asp 26 (or the corresponding Glu residue) is the only ionisable group in an active site that is otherwise lined with hydrophobic residues (for example see Bolin *et al.*, 1982, Filman *et al.*, 1982, Matthews *et al.*, 1985a, Oefner *et al.*, 1988, Bystroff *et al.*, 1990, McTigue *et al.*, 1992, 1993). This, and the fact that it lies close to the substrate pteridine ring (Figure B2) has led to its postulated role as the proton donor in the reaction catalysed by DHFR (see section 1.6 of the Introduction chapter). However, it is known that Asp 26 is not close enough to N5 of FH_2 to protonate it directly, and hence mechanisms for indirect substrate protonation, all involving Asp 26, have been put forward (Bolin *et al.*, 1982, Gready, 1985, Uchimaru *et al.*, 1989 Bystroff *et al.*, 1990, Brown and Kraut, 1992). In order to probe the role of Asp 26 as the proton donor, it was replaced by an Asn residue (D26N DHFR). This substitution would eliminate the ionisable sidechain and at the same time have minimum effects on the structure of the protein.

Inhibitors such as MTX bind very tightly to DHFR (K_d of less than 1nM). Crystallography and NMR spectroscopy have shown that a major difference between the binding of MTX and substrates is that the pteridine ring of the inhibitor is flipped over by 180° along the C2-NH_2 bond (see section 1.2 of the Introduction chapter). In the case of MTX (and other N1 protonated inhibitors), this "ring flipping" enables the N1 of the MTX pteridine ring to form an ion-pair interaction with Asp 26 (Figure B2). It is this ionic interaction, which is absent in substrate complexes, that is believed to be the main

contributor to the tight binding of MTX (Gready, 1980, Cocco *et al.*, 1981a, Blakley, 1984, Freisheim and Matthews, 1984). As a result of the Asp 26→Asn mutation, the ion-pair will be abolished in D26N-inhibitor complexes hence allowing the contribution that it makes to the overall tight binding of inhibitors to be determined.

3.2 RESULTS

In the study of a mutant such as D26N in which the importance of a residue in catalysis is being elucidated, it is necessary that the protein is of the highest possible purity. In the case of D26N DHFR there is also the additional risk (although very small) of contamination with wild-type DHFR from deamidation of Asn 26 back to Asp. For these reasons numerous efforts were made to confirm the purity of D26N DHFR.

Although *L.casei* DHFR and its mutants are expressed in an *E.coli* host, they are conveniently and completely separated from *E.coli* DHFR by the first anion exchange step of the purification procedure. Protein purity was assessed by running non-denaturing native and denaturing SDS-PAGE gels; D26N DHFR appeared as one band on both types of gel indicating the presence of a single species. As a final check of protein purity, the powerful and sensitive technique of isoelectric focusing was used (carried out by Dr G. Mason and Dr. M.G. Casarotto; Biochemistry Department, University of Leicester). The isoelectric point (pI value) of wild-type DHFR was calculated to be 6.2±0.1 which is identical with the previously reported value (Dann *et al.*, 1976). The Asp 26→Asn substitution results in a pI value for the D26N mutant of 6.9±0.1. This difference in pI values between mutant and wild-type enzymes, together with the appearance of the D26N mutant as a single band on the native gel confirmed that there was no contamination by deamidation and that D26N DHFR is indeed pure.

3.2.1 Equilibrium binding constants

The equilibrium dissociation constants for ligands binding to D26N and wild-type DHFRs are given in Table 3.1. The binding of NADPH to D26N DHFR was the same as to the wild-type enzyme. There is a small decrease in the binding constant of FH_2 (7-fold) while the binding of the other substrate, folate, is unchanged. For D26N and wild-type DHFR the dissociation constant of MTX was too low to measure using the fluorescence

quenching technique; a maximum value of 1nM is quoted for the wild-type enzyme. When determining a binding constant, the enzyme concentration should ideally be at, or lower, than the K_d value. However, in the case of determining a K_d value for MTX this would require very low protein concentrations (10nM or less) where the signal to noise ratio was very poor, and thus accurate titrations could not be carried out. In an attempt to assess if the binding of MTX had been affected by the mutation, the binding of an analogue of MTX, MTX-αγ-diamide (K_d of 0.15μM for wild-type DHFR) was measured (see section 5.1 of the R57K chapter for the structure of this analogue). The dissociation constant of MTX-αγ-diamide to D26N DHFR was found to be only 4-fold higher than that to the wild-type enzyme.

Table 3.1 Equilibrium dissociation constants of ligands binding to wild-type and D26N DHFR.

Ligand	K_d (μM)	
	Wild-type DHFR	D26N DHFR
NADPH	0.01±0.001	0.01±0.001
FH_2	0.24±0.02	1.6±0.2
folate	7.8±0.3	10±0.8
MTX	<0.001	0.003±0.001
MTX-αγ-diamide	0.15±0.004	0.6±0.06

3.2.2 Determination of the N1 protonation state of MTX in enzyme-MTX complexes using UV difference spectroscopy

Subtraction of the UV spectrum of free MTX at pH 7 from that at pH 2 produces the protonation difference spectrum of free MTX shown in Figure 3.1(a). Similarly, the

Figure 3.1(a) Difference spectrum between MTX at pH 2 and pH 7.

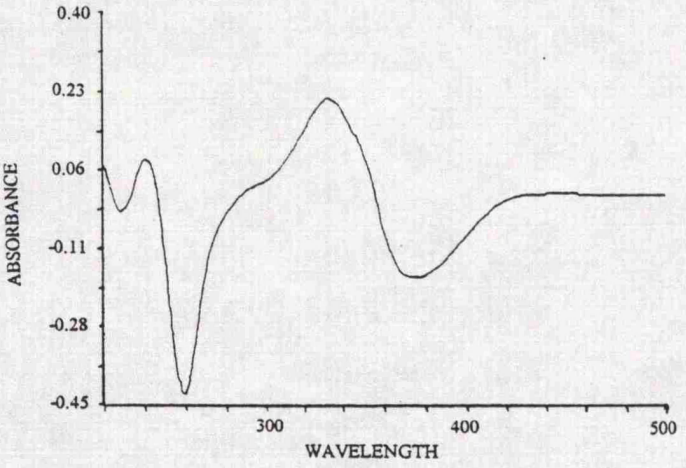

(b) Difference spectrum generated on MTX binding to wild-type DHFR

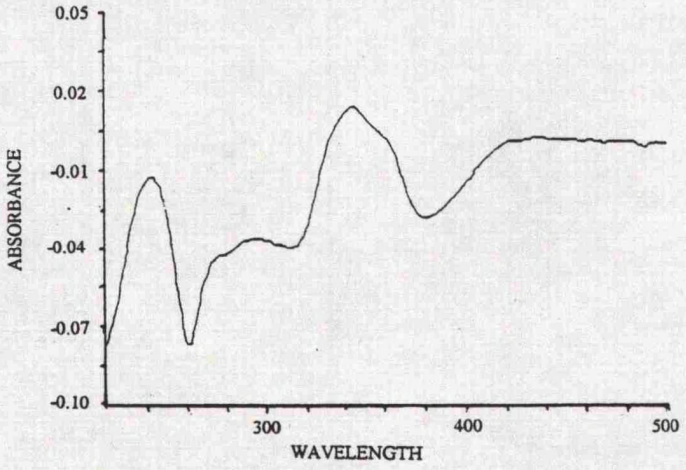

(c) Difference spectrum generated on MTX binding to D26N DHFR

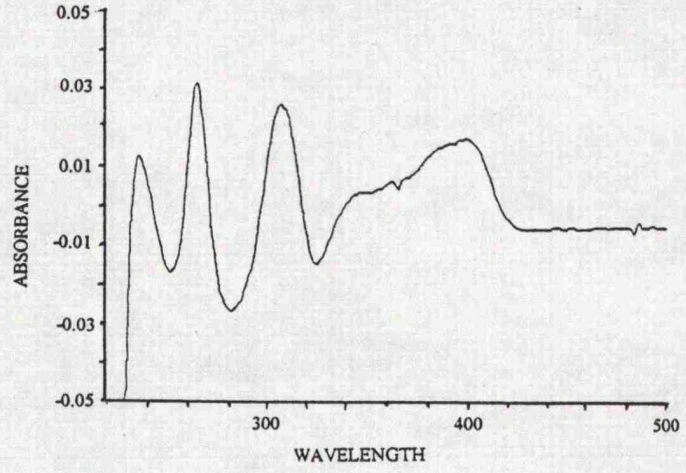

Difference spectra were obtained at 25°C in 50mM KH_2PO_4/100mM KCl pH 7. Enzyme and MTX concentrations were 8μM and 30μM respectively.

difference spectra obtained when MTX binds to wild-type and D26N DHFR (obtained by subtracting the spectra of free MTX and free enzyme at pH 7 from that of the enzyme-MTX complex at the same pH) are shown in Figure 3.1(b) and (c). The MTX protonation difference spectrum and the difference spectrum generated on MTX binding to wild-type DHFR at pH 7 are similar. Both have large negative bands at wavelengths of 260nm and 380nm and a positive band at approximately 340nm. These results have previously been interpreted as indicating that the MTX pteridine ring is in a similar protonation state when in complex with the wild-type enzyme as it is in free solution at low pH (Erickson and Mathews, 1972, Poe *et al.*, 1974, Gupta *et al.*, 1977, Hood and Roberts, 1978, Stone and Morrison, 1983). These spectra however, bear little resemblance to the difference spectrum obtained when MTX binds to the mutant suggesting that the pteridine ring of MTX is not protonated when bound to D26N DHFR.

3.2.3 Steady state kinetic parameters with FH_2 as the substrate

The K_m value of FH_2 for D26N DHFR was not significantly different from that for wild-type DHFR at pH 5.5 and pH 7.5 (Table 3.2). The results imply that the mutation has not affected the affinity of the enzyme for FH_2.

Table 3.2 Kinetic parameters of FH_2 reduction for wild-type and D26N DHFR.

Kinetic parameter	Wild-type DHFR	D26N DHFR
K_m (μM)		
pH 5.5	1±0.5	1.6±0.3
pH 7.5	1±0.5	1.4±0.2
k_{cat} (s^{-1})		
pH 5.5	25±0.8	5.5±0.1
pH 7.5	10±0.5	1.1±0.02

At pH 7.5, the value of k_{cat} was $10s^{-1}$ for the wild-type enzyme and $1.1s^{-1}$ for D26N DHFR, hence the mutant has only suffered a 9-fold decrease in catalytic activity at this pH; at pH 5.5 this difference is only 5-fold. The pH dependence of k_{cat} for both enzymes was measured over the pH range 5.2 to 8.6 and the resulting profiles are shown in Figure 3.2. The wild-type pH dependence has an apparent pK_a of 7.3±0.1, the D26N mutant shows a rather different pH profile in which the catalytic rate increases almost linearly as the pH is decreased. This curve could not be fitted to the ionisation of a single group.

3.2.3.1 Deuterium isotope effect experiments

Deuterium isotope effect experiments were carried out to determine the extent to which hydride ion transfer limits the rate of the DHFR catalysed reaction. k_{cat} values for wild-type and D26N DHFR were measured at a range of pH values using NADPH and NADPD as the coenzymes; the deuterium isotope effect (k_{cat}NADPH/k_{cat}NADPD) was then calculated at each pH value for both enzymes and the results are shown in Figure 3.3. In the case of wild-type DHFR, FH_4 dissociation is the major contributor to the rate-limiting step at low pH (Fierke *et al.*, 1987, Andrews *et al.*, 1989). As the pH is increased, the rate of hydride ion transfer begins to slow down and starts to contribute to the rate-limiting step; this is evident by an increase in the magnitude of the isotope effect which reaches a maximum value of 2.9 at high pH values. The apparent pK_a value of 7.3±0.1 seen in the pH dependence of the deuterium isotope effect for the wild-type enzyme thus reflects a change in rate-limiting step with pH. In the D26N mutant the pH dependence of the deuterium isotope effect was abolished and a large isotope effect of approximately 2.7 across the whole pH range was observed. The results suggest that for the D26N mutant hydride ion transfer is rate-limiting.

3.2.3.2 Solvent isotope effect experiments

In order to assess the role of proton transfer in the rate-limiting step the pH dependence of k_{cat} was measured in H_2O and D_2O for both wild-type and D26N DHFR

Figure 3.2 pH dependence of k_{cat} (FH_2) for D26N and wild-type DHFR.

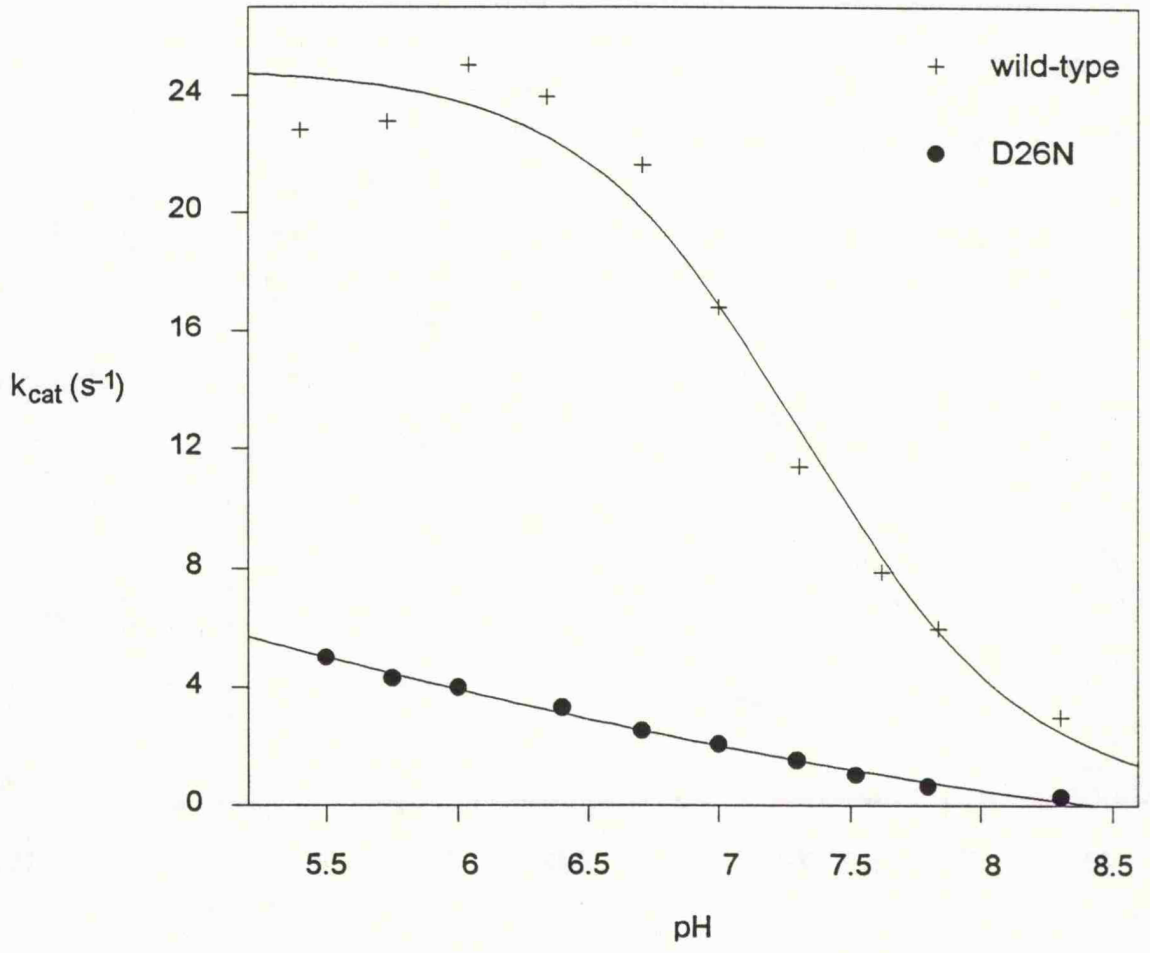

Figure 3.3 pH dependence of the deuterium isotope effect for D26N (•) *and wild-type* (+) *DHFR.*

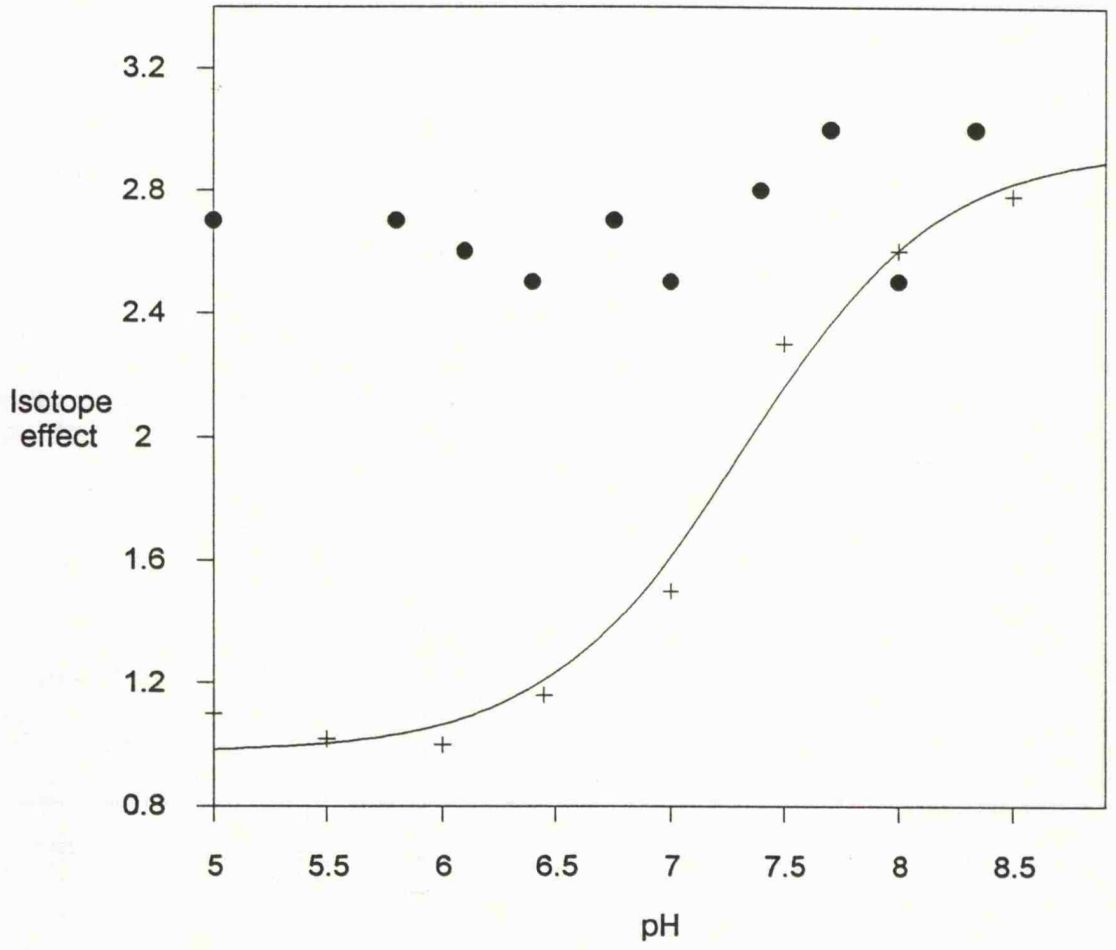

(Figure 3.4). With both enzymes the rate of catalysis is very similar in H_2O and D_2O across the measured pH range implying that proton transfer is not rate-limiting.

3.2.4 Steady state kinetic parameters with folate as the substrate

K_m values of folate for both wild-type and D26N DHFR were measured at pH 5 and pH 7.5 and the results are shown in Table 3.3. The K_m values of folate for both enzymes at pH 5 are identical (approximately 0.6μM). As the pH is increased to pH 7.5, the value of K_m increases for both mutant and wild-type DHFR to 16μM and 29μM respectively. The K_d (folate) is independent of pH (data not shown). The D26N mutation leads to a 25-fold decrease in folate reduction (k_{cat}) at pH 7.5. The pH dependence of k_{cat} for wild-type and D26N DHFR is shown in Figure 3.5. The wild-type k_{cat}-pH profile fits well to the ionisations of two groups with pK_a values of 5±0.36 and 7.3±0.2. However, the pH dependence of the D26N mutant reflects the ionisation of only a single group with a pK_a of 6.9±0.1.

Table 3.3 Kinetic parameters of folate reduction for wild-type and D26N DHFR

Kinetic parameter	Wild-type DHFR	D26N DHFR
K_m (μM)		
pH 5	0.59±0.1	0.63±0.1
pH 7.5	29±4	16±2
k_{cat} (s^{-1})		
pH 7.5	0.06±0.003	0.0024±0.0001
pK_a from pH dependence of k_{cat}	5±0.36 7.3±0.2	6.9±0.1

Figure 3.4a. pH dependence of k_{cat} (FH_2) for wild-type DHFR in H_2O (+) and D_2O (•)

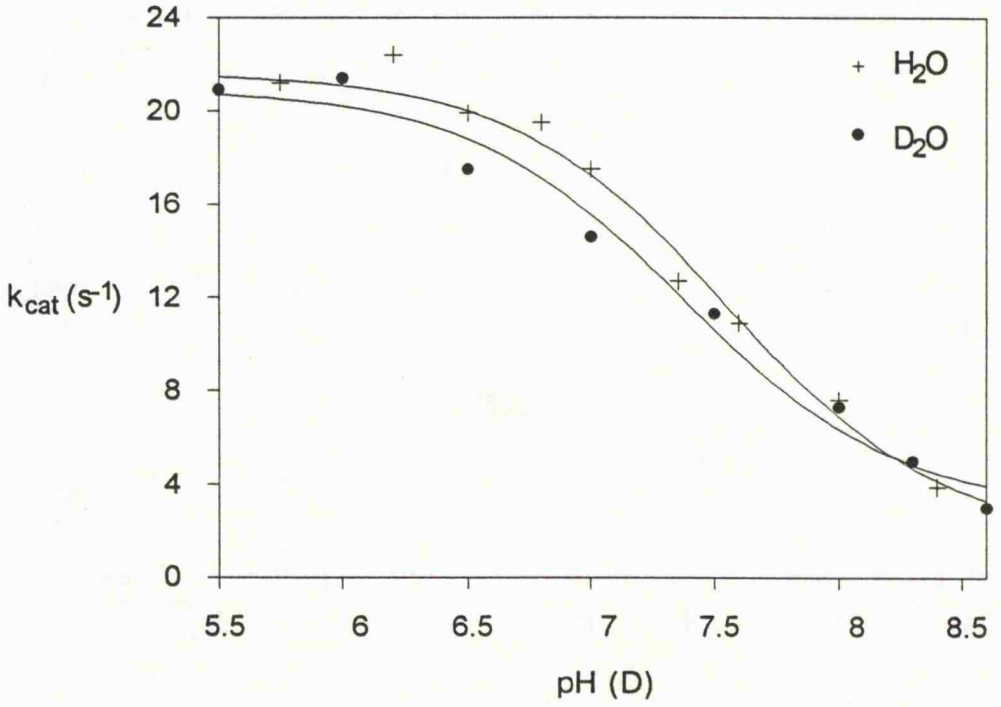

Figure 3.4b. pH dependence of k_{cat} (FH_2) for D26N DHFR in H_2O (+) and D_2O (•)

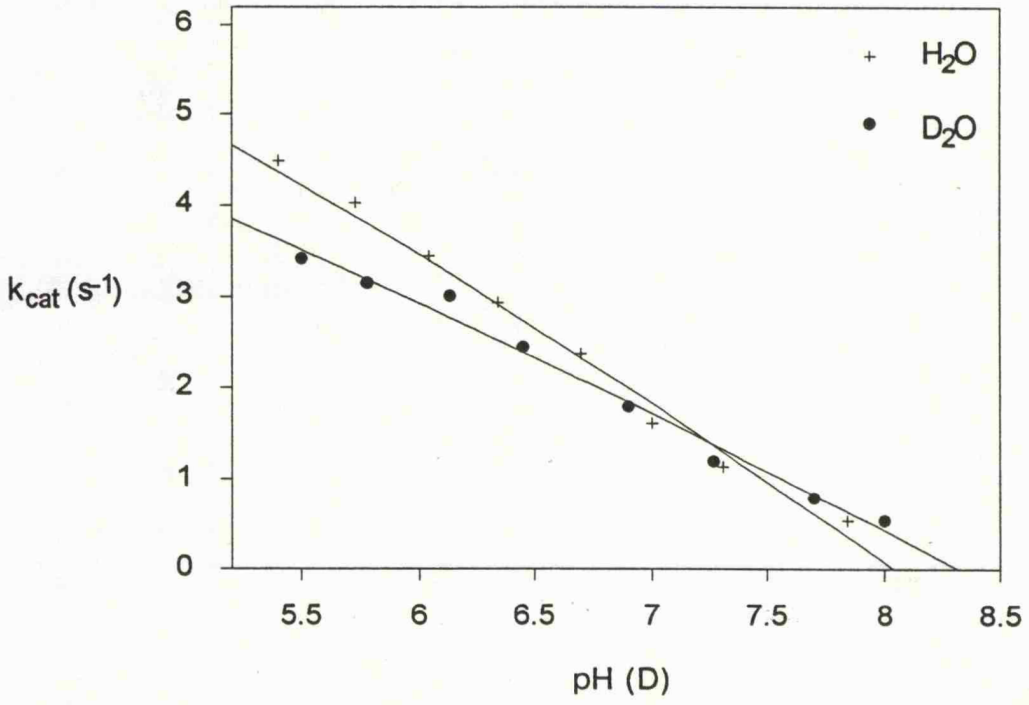

Figure 3.5a. pH dependence of k_{cat} (folate) for wild-type DHFR.

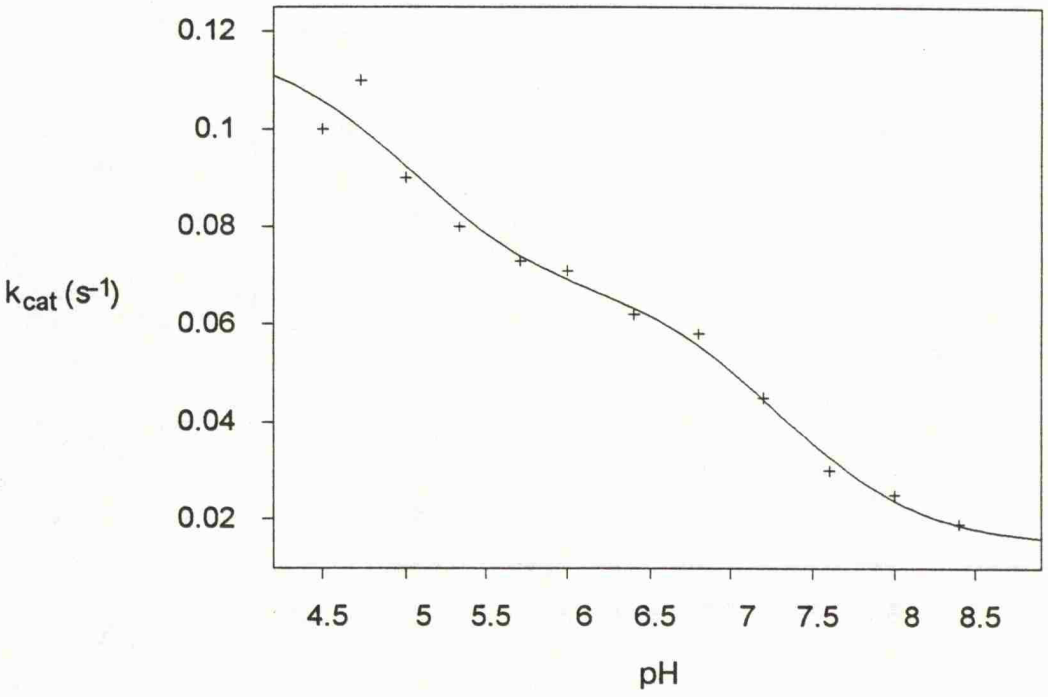

Figure 3.5b. pH dependence of k_{cat} (folate) for D26N DHFR.

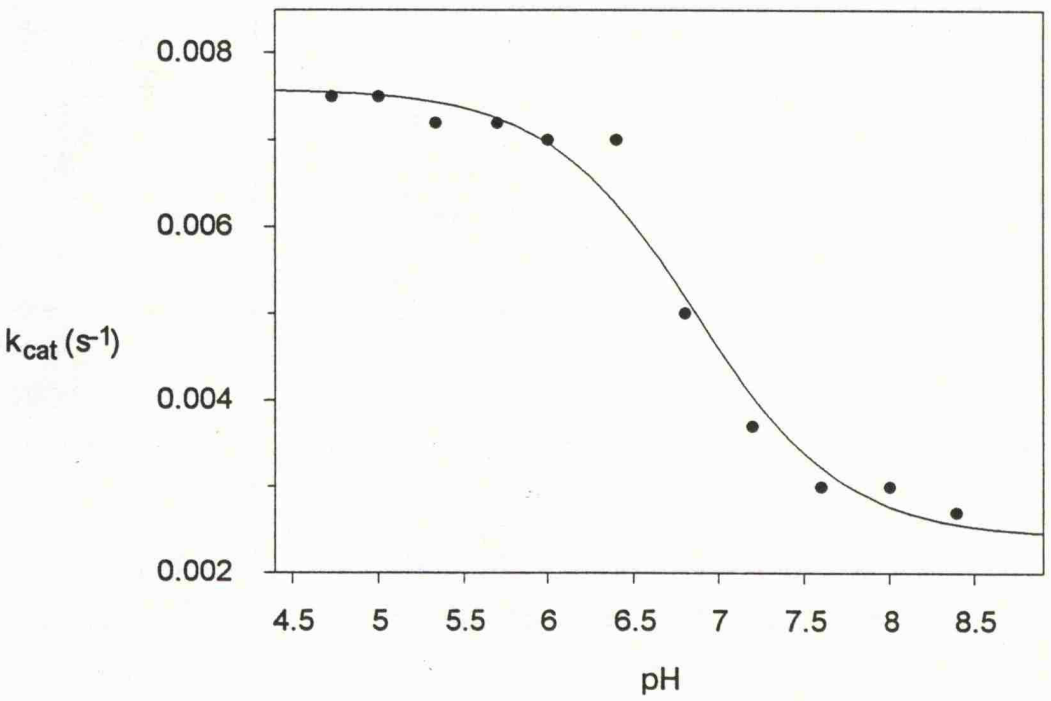

3.2.5 PRE-STEADY STATE KINETICS

3.2.5.1 Hydride ion transfer

The rate of hydride ion transfer (k_{hyd}) for wild-type DHFR has been measured from the "burst" of product formation which is equivalent to the first turnover of the enzyme by Andrews *et al.* (1989). Similar experiments carried out on the D26N mutant over the pH range 5-8.5 showed that there was no "burst". Instead a linear rate was observed suggesting that in the mutant hydride ion transfer is rate-limiting, as already indicated by the magnitude of the isotope effect observed with NADPD.

3.2.5.2 Dissociation rates (k_{off}) for FH_4 from ternary enzyme-FH_4-NADPH complexes

Dissociation rate constants of FH_4 from ternary enzyme-NADPH-FH_4 complexes were measured by competition experiments with MTX at a variety of pH values and the results are shown in Table 3.4. The rate of product release is slightly faster in the D26N mutant than in the wild-type enzyme, although the effect is never greater than 4-fold. The results suggest that the mutation has not had a major effect on this process. It is important to note that for D26N DHFR the rate of product dissociation is always at least 20 times faster than the value of k_{cat} at each pH value.

Table 3.4 Dissociation rate constants (k_{off}) for FH_4 from enzyme-NADPH-FH_4 ternary complexes.

pH	Wild-type DHFR (s^{-1})	D26N DHFR (s^{-1})
5.5	29±0.8	112±2
6.0	44±1	174±5
7.0	97±4	162±4
8.0	76±2	121±2
9.0	73±2	132±2

3.3 DISCUSSION

E.coli D27N DHFR is the equivalent Asp mutant of the *E.coli* enzyme (the numbering system between the two enzymes is different: Asp 26 in *L.casei* DHFR corresponds to Asp 27 in the *E.coli* enzyme). The *E.coli* D27N mutant has been studied by Kraut and co-workers (Howell *et al.*, 1986) using X-ray crystallography and kinetic methods. The results obtained for both mutants will be compared wherever possible.

3.3.1 Structural effects of the D26N mutation

In order to assess the structural effects of the Asp 26→Asn mutation NMR work has been carried out in this laboratory on the D26N-MTX binary complex (I. Barsukov and M.G. Casarotto, personal communication). This complex was chosen because unlike those containing bound substrates, the wild-type DHFR-MTX complex forms a single stable species (Birdsall *et al.*, 1982). More importantly, most of the proton assignments of the wild-type DHFR-MTX complex are complete (Birdsall *et al.*, 1990, Carr *et al.*, 1991, Soteriou *et al.*, 1993) so that comparison with spectra of the MTX complex of the mutant enables any structural changes to be identified. Results of such experiments on the D26N-MTX complex have shown that the Asp26→Asn substitution is accompanied by only minor structural perturbations localised around the MTX binding site (Figure 3.6). The figure shows the region of the MTX pteridine ring binding site which encompasses the site of the mutation (marked in blue); the positions of residues with chemical shift differences of ±0.1 ppm in the mutant (when compared to the wild-type enzyme) are shown in red. Residues affected include Leu 4, Trp 5, Ala 6, which are part of the βA strand, the loop region extending from Leu 12-Leu 23, and Tyr 29 and Phe 30 which are present in α-helix B. The most prominent chemical shift difference involves the indole ring of Trp 21 which can be seen in the figure. In the wild-type enzyme the indole ring of this strictly conserved residue interacts with Asp 26 via a conserved water molecule (Figure B2). Although the structural effects of the substitution were determined for the D26N-MTX complex, these are modest

Figure 3.6 The L.casei DHFR MTX pteridine ring binding site showing the chemical shift changes that have occurred as a result of the D26N mutation

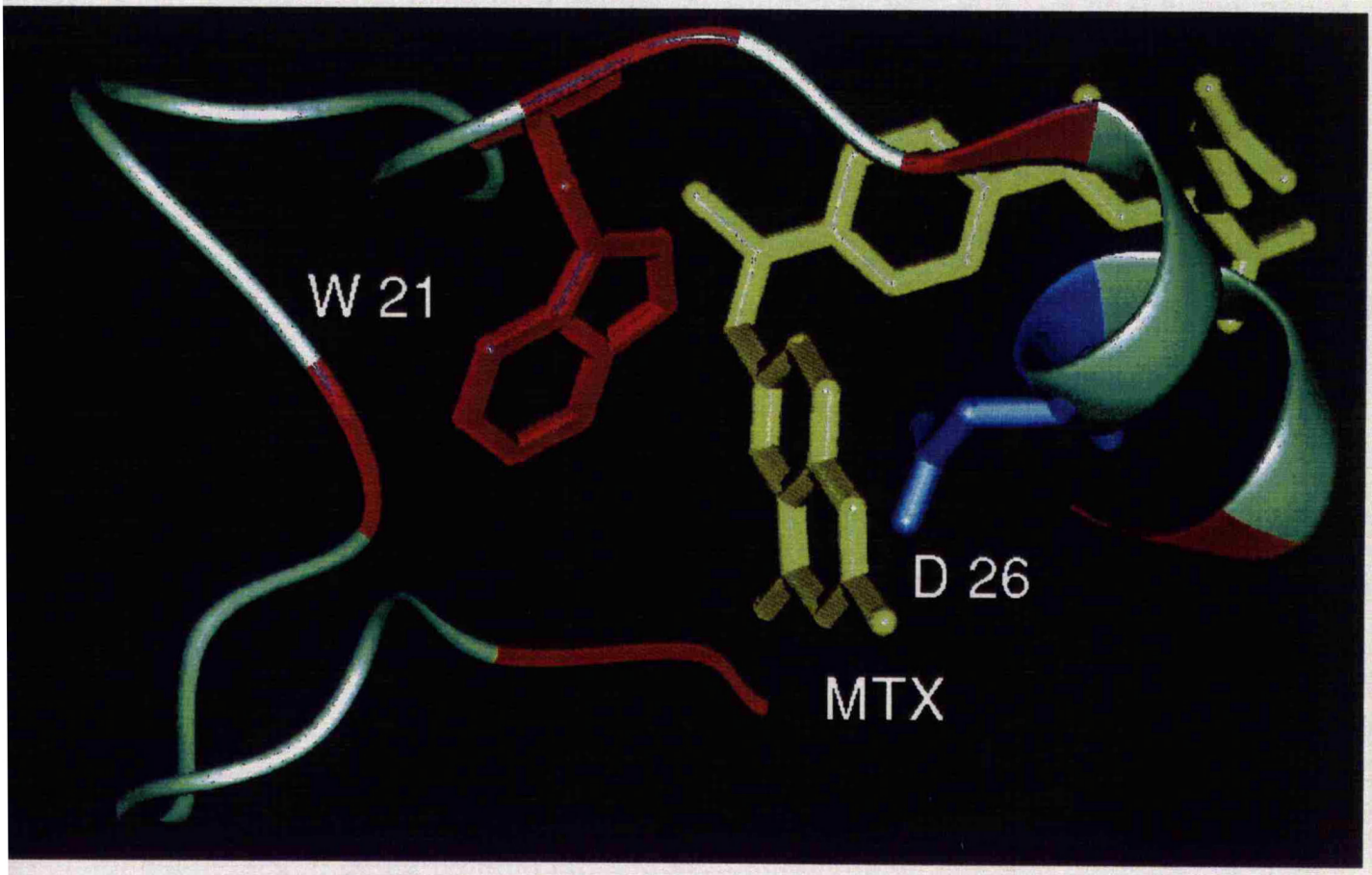

The inhibitor MTX is coloured in yellow and the site of the mutation in blue. Regions of the protein which contain residues whose chemical shifts differ by ±0.1ppm when compared to the wild-type DHFR-MTX complex are shown in red.

and imply that the effects could also be small in D26N-substrate complexes.

Structural data are also available on the *E.coli* D27N mutant which has been crystallised in complex with MTX and the structure compared with the wild-type enzyme (Howell *et al.*, 1986). It was found that, with the exception of the reorientation of two internally bound water molecules, Wat 403 (Wat 253 in *L.casei* DHFR) and Wat 567 necessary to accommodate the new Asn side chain (Figure 3.7), there were no other significant (> 0.2Å) changes in protein structure.

3.3.2 Ligand binding

The *L.casei* D26N mutation has no effect on the binding of the substrate folate and leads to only a minor decrease (7-fold) in the binding of FH_2. These results are consistent with the modest structural effects of the Asp 26→Asn substitution seen in the D26N-MTX binary complex. The binding of the inhibitor MTX to both wild-type and mutant enzymes was too tight to be measured accurately by fluorescence quenching and therefore the binding constant of MTX-αγ-diamide (K_d of 0.15μM for wild-type DHFR) was determined. This analogue binds only 4-fold weaker to the D26N mutant than to the wild-type enzyme. The results imply that the ionic interaction does not make a significant contribution to the binding energy. However, as outlined below the use of D26N DHFR in an attempt to determine the importance of the ion-pair interaction to MTX binding is not as straightforward as first anticipated.

Binding constants of MTX to *E.coli* wild-type and D27N DHFRs were determined by equilibrium dialysis with ^{3}H-labelled MTX and found to be 0.07nM and 1.9nM respectively (Howell *et al.*, 1986). This is a difference of only 27-fold which corresponds to a decrease in binding energy of 1.8 kcal/mol. Kraut *et al.* concluded that the small reduction in the MTX binding constant was consistent with previous results which hypothesised that there would be only an 11-fold difference in binding constant between

Figure 3.7 Probable hydrogen bonding between the MTX pteridine ring and
a) E.coli wild-type DHFR
b) E.coli D27N mutant (from Howell et al., 1986)

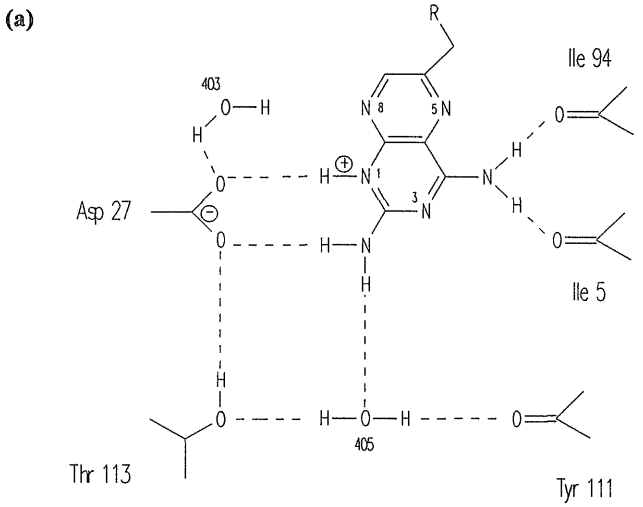

Wild-type:MTX

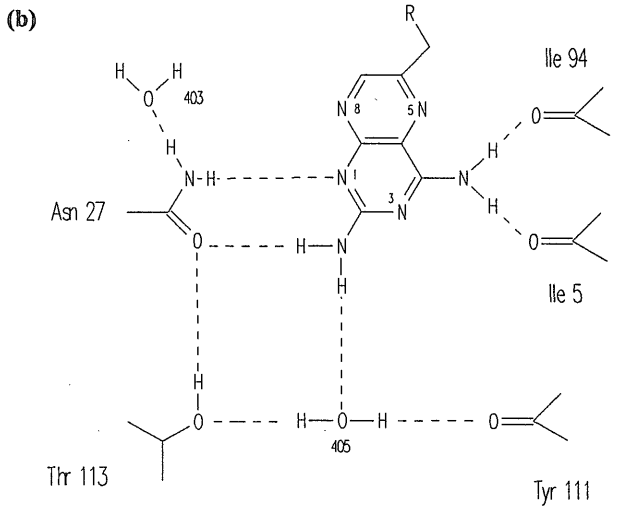

D27N:MTX

protonated MTX and an ionised DHFR (presumably Asp 26) and between neutral MTX and a non-ionised DHFR (Stone and Morrison, 1983).

It is difficult to assess the contribution that the ion-pair makes to inhibitor binding using the D26N mutant since MTX has been shown to exist in different protonation states when in complex with wild-type and mutant enzymes (Howell *et al.*, 1986, London *et al.*, 1986 and work in this thesis). Comparison of the UV difference spectra generated when MTX binds to wild-type *L.casei* DHFR with that of the protonation difference spectrum of free MTX shows a clear resemblance. This similarity has generally been accepted to indicate that MTX is protonated on N1 when bound to the wild-type enzyme at neutral pH (Erickson and Mathews, 1972, Poe *et al.*, 1974, Gupta *et al.*, 1977, Hood and Roberts, 1978, Stone and Morrison, 1983). This was substantiated by ^{1}H NMR which demonstrated that the pK_a of N1 of the inhibitor was greater than 10 when in complex with wild-type DHFR (Cocco *et al.*, 1981a, 1981b and 1983; M.G. Casarotto, personal communication). In contrast, the lack of resemblance between the UV difference spectrum obtained when MTX binds to D26N DHFR and the protonation difference spectrum of free MTX suggests that the inhibitor is not protonated on N1 when in complex with the mutant. Further evidence has been obtained from ^{1}H NMR experiments carried out in this laboratory (M.G. Casarotto, personal communication) on the D26N-MTX complex. Comparison of wild-type and mutant spectra demonstrated the absence of the very low field MTX N1 proton resonance in the mutant, again indicating that N1 is not protonated when MTX is in complex with D26N DHFR. Analogous results have been obtained with the *E.coli* D27N-MTX complex where the pK_a of N1 in this complex was estimated to be less than 4 (London *et al.*, 1986). Hence, when in complex with the Asn mutants, MTX is in its high pH state (i.e. non protonated) whereas the Asn sidechain "mimics" the low pH form of Asp (i.e. protonated). Therefore essentially two different species are being compared which makes it difficult to assess the contribution of the Asp 26-N1 MTX ion-pair to the overall tight binding of MTX.

Apart from the contribution of the ionic interaction, other hypotheses have been put forward to account for the tight binding of MTX compared with substrates. It has been suggested that the additional hydrogen bond made by the 4-NH_2 group of MTX to backbone protein carbonyls may be important to the binding of the inhibitor (Freisheim and Matthews, 1984, Howell *et al.*, 1986). Binding studies on the *S.faecium* DHFR-MTX complex and the *E.coli* DHFR-TMP binary complex demonstrated that after the initial inhibitor binding step, an isomerisation step occurs which results in much tighter binding of the inhibitors (Blakley and Cocco, 1985, Cayley *et al.*, 1981, Williams *et al.*, 1980); this is a general phenomenon for all DHFRs. In the case of the *S.faecium* enzyme the authors noted that the isomerisation step was not observed with the DHFR-folate complex.

3.3.3 Kinetics of FH_2 reduction

The K_m value of FH_2 for the D26N mutant was the same as for wild-type DHFR at pH 5.5 and 7.5. The Asp 26→Asn substitution has not affected the affinity of FH_2 for the enzyme-NADPH complex; this is consistent with the small effect on K_d. These results are in contrast to those obtained on the *E.coli* D27N mutant in which the 40-fold increase in K_m for FH_2 was interpreted as implying that Asp 27 plays an important role in the binding of FH_2 (Howell *et al.*, 1986).

The D26N mutation has only a modest effect on the rate of catalysis (k_{cat}); the mutant is surprisingly active having suffered at maximum a 10-fold decrease in k_{cat} at pH 7.5 when compared to the wild-type enzyme. If Asp 26 was the ultimate proton donor in the reaction catalysed by the wild-type enzyme, then the D26N mutant would have expected to be much less active. The ability of D26N DHFR to reduce FH_2 at quite measurable rates is clearly not compatible with mechanisms which propose that Asp 26 is the primary source of the proton in the DHFR catalytic mechanism. However, the results may be more consistent with a mechanism in which Asp 26 remains in a protonated state throughout the

catalytic cycle as discussed below (Taira *et al.*, 1987, Uchimaru *et al.* 1989, Bystroff *et al.*, 1990, Brown and Kraut, 1992).

The deuterium isotope effect and its pH dependence are different in the D26N mutant to that seen in the wild-type enzyme; the results imply that the mutation has altered the rate-limiting step. With wild-type DHFR a full isotope effect (approximately 2.9) is only observed at high pH values where the rate of hydride ion transfer is rate-limiting (Fierke *et al.*, 1987, Andrews *et al.*, 1989). At low pH values, product (FH_4) dissociation is the main contributor to k_{cat} and hence no isotope effect is apparent. In the D26N mutant, an isotope effect of approximately 2.7 throughout the pH range 5-8.5 indicates that the reaction catalysed by the mutant is limited solely by the rate of hydride ion transfer. This was confirmed by pre-steady state kinetics. In the wild-type enzyme the rate of hydride ion transfer has been calculated from the "burst" of product formation that occurs after mixing enzyme with substrates (Andrews *et al.*, 1989, Fierke *et al.*, 1987). No such "burst" was observed in the D26N mutant, in fact the rate was linear throughout the measured pH range. Furthermore, in the D26N mutant the rate of FH_4 dissociation from the D26N mutant-NADPH-FH_4 complex is at least 20 times faster than k_{cat} at every pH measured; for example, $112s^{-1}$ compared with $5.5s^{-1}$ at pH 5.5. The results therefore show that in the mutant, hydride ion transfer is the rate-limiting step that governs catalysis. A comparison of the k_{cat} value (D26N DHFR) with the rate of hydride ion transfer for the wild-type enzyme at pH 5.5 ($350s^{-1}$; Andrews *et al.*, 1989) indicates that the rate of this process has been decreased by a factor of 60. These results are in contrast to those obtained on the *E.coli* D27N mutant. The *E.coli* D27N mutation had a more drastic effect on catalysis; k_{cat} is reduced by a factor of 300 at neutral pH, while direct comparison of the rate of hydride ion transfer at pH 5.5 demonstrated that this is 1500-fold lower than seen for the wild-type enzyme (Howell *et al.*, 1986).

The Asp 26→Asn mutation has altered the pH dependence of k_{cat}. In wild-type DHFR the rate of catalysis depends upon protonation of some residue, presumed to be Asp

26 for maximal activity (Stone and Morrison, 1984, Morrison and Stone, 1988). Pre-steady state kinetics have shown that the pH dependence of hydride ion transfer requires a group with a pK_a of 6.0-6.5 in different DHFRs to be in the protonated state (Fierke *et al.*, 1987, Andrews *et al.*, 1989, Thillet *et al.*, 1990). Since hydride ion transfer is thought to be dependent on the protonation state of N5 of FH_2, this pK_a has been attributed to Asp 26 in the enzyme-NADPH-FH_2 ternary complex. In *L.casei* DHFR the steady state pH dependence of k_{cat} has a pK_a value of 7.3 (Andrews *et al.*, 1989), with *E.coli* DHFR it is 8.4 (Fierke *et al.*, 1987, Morrison and Stone, 1988). From Figure 3.8 it can be seen that Fierke *et al.* (1987) have shown that this is an apparent pK_a that arises due to a change in rate-limiting step from FH_4 dissociation at low pH to hydride ion transfer at higher pH values (Andrews *et al.* (1989) have also demonstrated this for the *L.casei* enzyme).

Figure 3.8 Observed rate constants for hydride ion transfer (– • –), ***FH_4 dissociation*** (– – –) ***and k_{cat}*** (——) ***as a function of pH for E.coli DHFR (from Fierke et al., 1987).***

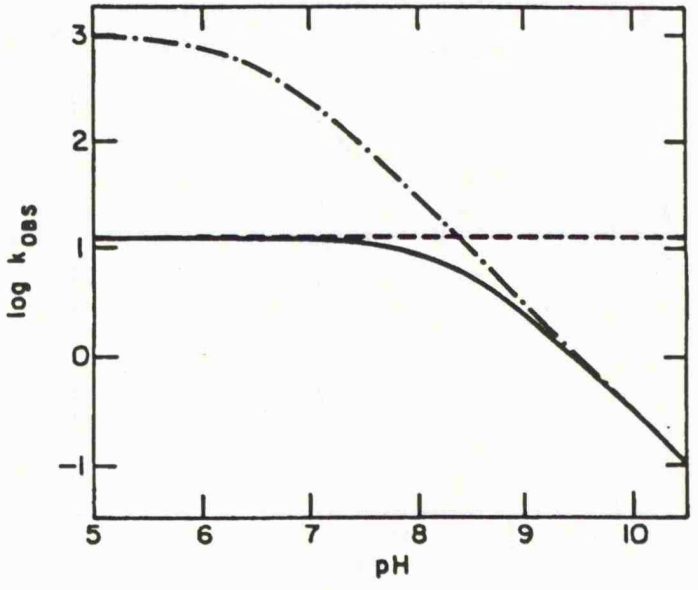

In the D26N mutant k_{cat} (which is equivalent to the rate of hydride ion transfer) continues to increase as the pH is decreased in an almost linear fashion. A similar pH dependence was observed with the *E.coli* D27N mutant. The Kraut group have postulated

that the form of the *E.coli* D27N DHFR pH-activity profile was due to the mutant binding FH_2 that was preprotonated (from solvent) on N5. In free solution, N5 of FH_2 has a pK_a value of 2.6 (Maharaj *et al.*, 1990). If protonation was from solvent then a much sharper increase in activity should be observed as the pH is decreased. This is not in accord with the *L.casei* D26N mutant data or the *E.coli* D27N mutant results.

The exact source of the proton in the catalytic mechanism of DHFR is still unclear. Gready (1985) proposed that the function of Asp 26 is not to protonate substrate, but to stabilise a transition state in which the N5 of FH_2 has been directly protonated from solvent. Stabilisation would raise the pK_a of N5 which in turn would enhance carbonium ion character at C6 and hence facilitate hydride ion transfer from NADPH. A mutant such as D26N would therefore still be capable of catalysing the reaction although at a much reduced rate. In an attempt to investigate the role of proton transfer in the reaction catalysed by DHFR, the rate of catalysis was measured in D_2O. It was believed that the protonation step would be slower in D_2O than in H_2O with the result that hydride ion transfer would also be reduced and hence a solvent isotope effect (k_{cat} H_2O/k_{cat} D_2O) would be observed. In the case of wild-type DHFR this effect would only be seen at higher pH values where the rate of hydride ion transfer is totally rate limiting (Andrews *et al.*, 1989). The results showed that for both wild-type and mutant enzymes the rates of catalysis in H_2O and in D_2O were very similar, implying that in both cases proton transfer is not rate-limiting.

The high catalytic activity of D26N DHFR may be more compatible with a mechanism in which Asp 26 remains protonated throughout the catalytic cycle (see Section 1.6 of the Introduction chapter). In this mechanism the function of Asp 26 is to promote enolisation of the substrate with the aid of a conserved water molecule, Wat 253 as depicted in Figure 3.9.

Figure 3.9 Enolisation of the FH_2 pteridine ring by Asp 26 (adapted from Bystroff et al., 1990)

Wild-type DHFR

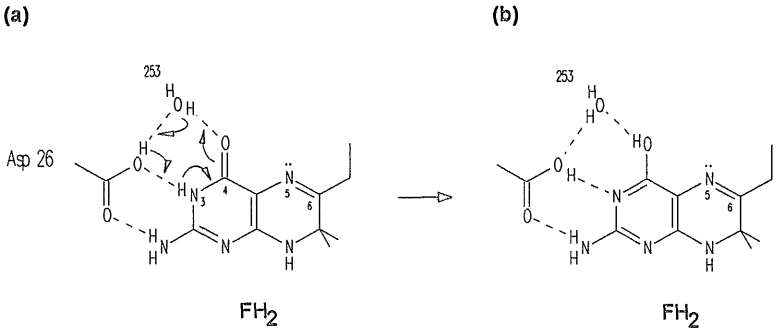

A proton is transferred from N3 to O4 of FH_2 to produce the enol form of the substrate (Figure 3.9b) and is stabilised by Wat 253. The proton is then transferred from O4 to N5 either directly or by a transiently bound water molecule (Brown and Kraut, 1992); this would then promote hydride ion transfer to C6. It has been suggested that the enol tautomer shown in Figure 3.9(b) may occur in the ground state of the reaction and indeed work on *L.casei* DHFR-folate complexes have demonstrated that this is possible (Cheung *et al.*, 1993). In the case of the D26N mutant, although it cannot promote enolisation of the keto tautomer of FH_2, it may bind the enol form of the substrate:

D26N DHFR

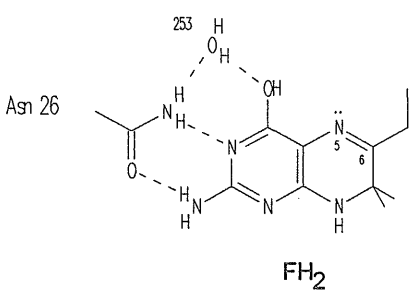

In fact the interaction between the Asn 26 sidechain and the enol tautomer is likely to be more favourable than that with the keto tautomer. If enolisation of FH_2 is important in catalysis then the Asp 26→Asn substitution is a favourable one. However, in solution FH_2 exists largely in the keto form and so the concentration of the enol tautomer will be small (Zakrzewski, 1963, Blakley, 1969, Gready, 1980). Additionally, substitution for an Asn may result in reorientation of one or more water molecules (including Wat 253) that may be crucial in proton transfer. Indeed, evidence for this has been provided by X-ray crystallographic studies on the *E.coli* D27N-MTX complex (see Figure 3.7). The net result of both these factors is that the D26N mutant is unable to catalyse the reaction as effectively as wild-type DHFR. The difference in catalytic activity of the *E.coli* and *L.casei* Asn mutants may therefore be due to one of two factors. Firstly, there may be a difference in the keto-enol equilibrium position of bound FH_2 in the two enzymes; for instance the *E.coli* D27N mutant may stabilise the keto tautomer to a larger extent than the *L.casei* D26N mutant. If enolisation is important in catalysis then the D27N mutant would have significantly reduced activity. Secondly, and probably more importantly, any change in the orientation or location of the bound water molecules which may transfer a proton to N5 could have a substantial effect on the rate of the reaction catalysed by the mutants.

A better understanding of the catalytic mechanism of *L.casei* DHFR will no doubt come from studies on the enzyme which are currently in progress. These include direct measurement of the pK_a of Asp 26 using γ-^{13}C Asp labelled DHFR and determination of the tautomeric state of FH_2 in complexes which closely resemble the enzyme-FH_2-NADPH complex.

3.3.4 Kinetics of folate reduction

L.casei DHFR catalyses the reduction of folate in two steps:

$$\text{folate} + \text{NADPH} + H^+ \rightleftharpoons FH_2 + NADP^+$$

$$FH_2 + \text{NADPH} + H^+ \rightleftharpoons FH_4 + NADP^+$$

Steady state kinetic parameters for folate reduction have been measured and shown to be much slower than any of the rate constants for FH_2 reduction (Andrews *et al.*, 1989). The results imply that the overall rate-limiting step must occur in the conversion of folate to FH_2; a large deuterium isotope effect on k_{cat} (5.1 at pH 5) demonstrated that this step is hydride ion transfer from NADPH to folate. Folate is a poor substrate for *L.casei* DHFR; the rate of hydride ion transfer to FH_2 at pH 5 is $450s^{-1}$ compared with $0.075s^{-1}$ for folate (Andrews *et al.*, 1989).

The slow reduction of folate has been attributed to a number of factors: as in the case of FH_2 reduction, hydride ion transfer proceeds from the A side of the nicotinamide ring to the C7 *si* face of the folate pteridine ring, presumably preceded by protonation of N8 (see Section 1.6 of Introduction chapter). Although the pK_a of N8 in free folate is very low (less than -1.5; Poe, 1977) crystal structures of enzyme-folate complexes have shown that a proton on N8 could hydrogen bond to the backbone of Ile 5 (Leu 4 in *L.casei* DHFR) which may effectively stabilise and hence raise its pK_a value (Oefner *et al.*, 1988, Bystroff *et al.*, 1990). There also seems to be no direct route for proton transfer from either protein sidechains or bound water molecules. Modelling studies based on the crystal structure of the *E.coli* DHFR-folate-$NADP^+$ complex have indicated that hydride ion transfer from C4 of NADPH is directed at a point midway between C6 and C7 of folate (Bystroff *et al.*, 1990). This would result in inefficient hydride ion transfer from the nicotinamide ring and may contribute to the slow reduction of this bond.

The D26N mutation has little effect on the K_m for folate at pH 5 or 7.5 when compared to the wild-type enzyme, which is consistent with the observation of no change in the K_d for this substrate. These results are also in line with those obtained with FH_2 except that the K_m for folate appears to be pH dependent. The K_m of folate for wild-type *E.coli* DHFR does not show a pH dependence; K_m is 22μM at pH 5 and 16μM at pH 7 (Baccanari *et al.*, 1975, Howell *et al.*, 1990). At pH 7.5 the *L.casei* Asp 26→Asn substitution leads to a 25-fold reduction in catalytic activity. Because a full isotope effect is

observed on k_{cat} with the wild-type enzyme (Andrews *et al.*, 1989), k_{cat} (folate) is a direct measure of the rate of hydride ion transfer. No comparison can be made with *E.coli* DHFR since folate is a very poor substrate for this enzyme and folate reduction by the *E.coli* D27N mutant was not detectable (Howell *et al.*, 1986).

The kinetics of folate reduction may be complicated by the ability of *L.casei* DHFR to bind the folate pteridine ring in a nonproductive as well as in a productive manner. NMR studies on the *L.casei* DHFR-folate-$NADP^+$ ternary complex have shown that it exists in solution as a mixture of three slowly interconverting conformations (denoted I, IIa and IIb; see Scheme I) whose proportions are pH dependent (Birdsall *et al.*, 1981b, Birdsall *et al.*, 1982, Birdsall *et al.*, 1987, Birdsall *et al.*, 1989b, Cheung *et al.*, 1993). Conformer I predominates at low pH (< pH 5) whereas IIa and IIb are present at higher pH values (> pH 7). A major difference between the conformations is in the orientation and tautomeric state (discussed later) of the pteridine ring. In forms I and IIa the folate pteridine ring is bound in a similar way to that of the MTX pteridine ring in the *L.casei* DHFR-MTX-NADPH crystal structure (Filman *et al.*, 1982). This mode of binding is therefore referred to as "nonproductive". In conformation IIb, however, the ring is turned over by 180° ("productive" binding) and is in the correct orientation for reduction by NADPH.

It is not known if the two modes of folate binding exist in the catalytically functional DHFR-folate-NADPH complex although similar conformational equilibria have been observed in the binary *L.casei* DHFR-folate complex and hence are not dependent on the presence of $NADP^+$ (Birdsall *et al.*, 1987). The Asp 26→Asn DHFR mutation abolishes this pH dependent conformational equilibria (Jimenez *et al.*, 1989); the results strongly suggest that Asp 26 is responsible for this equilibrium. The mutant appears to exist in only one conformation which does not change with pH. This is the low pH form (conformer I) in the wild-type enzyme in which Asp 26 is thought to be protonated. It was suggested that this conformation was adopted by the mutant because an Asn sidechain may "mimic" a

protonated Asp residue. Alternative modes of folate binding have not been observed with *E.coli* DHFR (Falzone *et al.*, 1990).

Scheme I

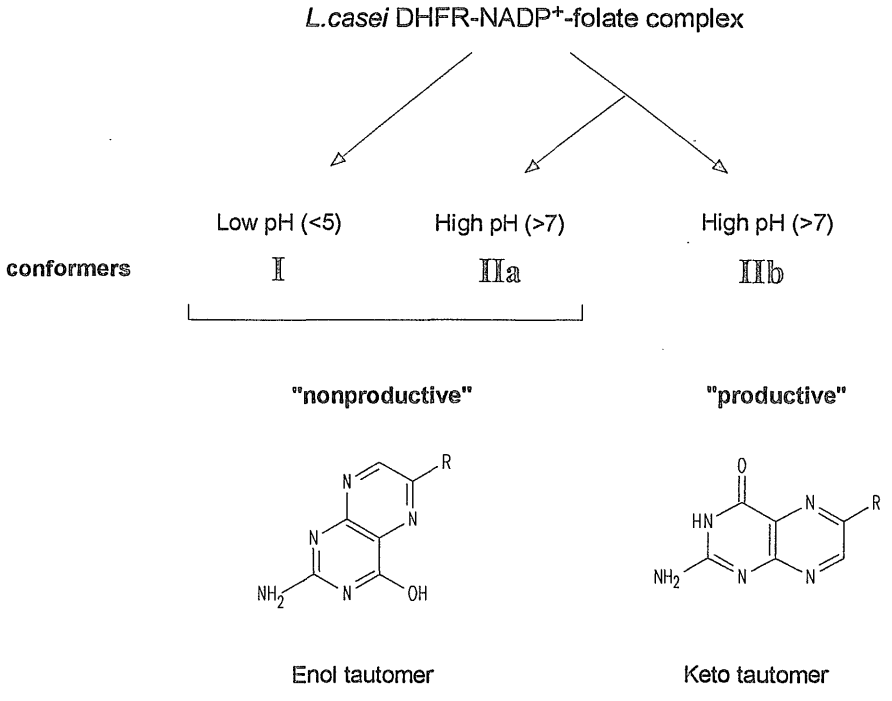

The pH dependence of k_{cat} (folate) has also been affected by the D26N mutation. The wild-type k_{cat} profile reflects the ionisation of two groups (pK_a values of 5±0.36 and 7.3±0.2); the enzyme having maximum activity when both groups are protonated. In contrast, the pH dependence of k_{cat} for D26N DHFR can be fitted to a single ionisation with a pK_a of 6.9±0.1. The absence of the group with a pK_a of 5 in the D26N mutant pH dependence suggests that this could be the pK_a of Asp 26. Since with folate reduction hydride ion transfer is rate-limiting across the pH range, this pK_a should be a true pK_a value

for this residue. In an attempt to directly measure the pK_a of Asp 26, NMR experiments on various wild-type DHFR-folate complexes in which the Asp residues have been ^{13}C labelled in the γ-position have been carried out (M.G. Casarotto, personal communication). Results have implied that Asp 26 could have a pK_a of less than 5.0 although confirmation will have to await resonance assignment using the D26N mutant.

The ionisable group with a pK_a of 7.3 in the wild-type enzyme and 6.9 in the mutant must belong to folate since apart from Asp 26, DHFR does not have an ionisable group close to the pteridine ring. However, as mentioned above, the pH dependence of folate reduction may be complicated by the ability of the substrate pteridine ring to bind in alternative conformations. The fact that a pK_a of 6.9 is still observed in the mutant, in which this conformational equilibria is abolished (Jimenez *et al.*, 1989) suggests that this ionisation is not responsible for the conformational equilibria. A possible candidate for the pK_a of 7.3 (wild-type) and 6.9 (D26N DHFR) could be the N3 of folate which in free solution has a pK_a of 8.4 (Poe, 1977). Further characterisation of the *L.casei* DHFR-folate and DHFR-folate-$NADP^+$ complexes has recently been carried out by Cheung *et al.* (1993) using ^{13}C labelled folate. They have shown that in the productive conformation folate is bound as the keto tautomer (see Scheme I) and that N3 remains protonated up to pH 7.3; that is, N3 does not ionise in the pH range suggested by the kinetic experiments. However, it may be possible that this ionisation may only occur in the transition state of the enzyme-folate-NADPH complex and therefore will not be observed in the ground state complexes studied by NMR.

3.4 SUMMARY

The Asp 26→Asn mutation in *L.casei* DHFR has only minor (less than 7-fold) effects on the binding of the substrates FH_2 and folate. The binding of the inhibitor MTX remains tight to the D26N mutant (K_d less than 10nM) and is not protonated when in complex with the mutant. However, as discussed in this chapter the D26N mutant is probably not the best mutant for assessing the contribution that the ionic interaction makes to the overall strong binding of MTX to wild-type DHFR. The binding results are consistent with NMR studies carried out on the D26N mutant in this laboratory (I. Barsukov and M.G. Casarotto, personal communication) which have shown that the substitution results in only local minor structural perturbations.

Steady state deuterium isotope effect experiments and pre-steady state kinetics have revealed that the reaction catalysed by the Asp 26→Asn mutant is limited by the rate of hydride ion transfer from NADPH to FH_2. The ability of D26N DHFR to catalyse the reduction of FH_2 at appreciable rates (10% of the rate of wild-type DHFR at pH 7.5) implies that Asp 26 is not the source of the proton in the wild-type catalytic mechanism. The results are more consistent with a mechanism in which the function of Asp 26 is to promote enolisation of the substrate, the proton being derived from the solvent.

The Asp 26→Asn substitution also leads to a 25-fold decrease in k_{cat} (pH 7.5) with folate as the substrate; in this case this is a direct effect on the rate of hydride ion transfer. The folate kinetic data (and NMR work; M.G. Casarotto, personal communication) suggests that the pK_a of Asp 26 in complexes with this substrate is no greater than 5. However, the mechanism of folate reduction by DHFR is unclear and could be complicated by the existence of nonproductive binding of the substrate.

CHAPTER 4 W21H and W21H/D26N DHFR

4.1 INTRODUCTION

Trp 21 is an evolutionarily conserved residue that lies close to both substrate and coenzyme in the active site of DHFR. Various DHFR crystal structures containing either bound substrate or substrate analogue have shown that the NH of the Trp 21 indole ring interacts with the pteridine ring of these ligands and Asp 26 (or the corresponding Glu) via a fixed water molecule (Wat 253; *L.casei* DHFR numbering) as shown in Figure B2 (Bolin *et al.*, 1982, Filman *et al.*, 1982, Oefner *et al.*, 1988, Bystroff *et al.*, 1990, Davies *et al.*, 1990). Trp 21 has also been shown to make hydrophobic contacts with the nicotinamide rings of $NADP^+$ and NADPH in complexes containing bound cofactor (Matthews *et al.*, 1979, Filman *et al.*, 1982, Bystroff *et al.*, 1990).

Site-directed mutagenesis has been used to replace Trp 21 of *L.casei* DHFR with a Leu residue (W21L DHFR; Andrews *et al.*, 1991, Birdsall *et al.*, 1989a, Andrews *et al.*, 1989). This quite drastic substitution was made in order to abolish the interaction with the substrate pteridine ring and the hydrophobic contact with the nicotinamide ring of the coenzyme. The results of the W21L mutation have been outlined in Section 1.7 of the Introduction chapter and will be discussed further in relation to the mutant studied in this chapter, the Trp 21→His (W21H) mutant. In W21H DHFR the imidazole ring of His replaces the 5-membered ring of Trp 21 and, when protonated, should maintain the interaction with the pteridine ring of the substrate via hydrogen bonding to Wat 253 (Figure B2). However, the smaller size of the His sidechain means that hydrophobic contact with the nicotinamide ring of the coenzyme will be reduced, hence allowing us to probe the importance of this interaction in the binding of NADPH. The W21H mutation is thus a more "conservative" substitution than the W21L one.

The double mutant, Trp 21→His and Asp 26→Asn (W21H/D26N DHFR) was created in order to try and clarify some of the results obtained on the single W21H mutant.

4.2 RESULTS

4.2.1 Equilibrium binding constants

Table 4.1 shows the equilibrium dissociation constants for ligands binding to W21H, the double mutant and wild-type DHFR. For W21H (as with wild-type DHFR) the dissociation constant of the inhibitor MTX was too low to measure accurately using the fluorescence titration method. One of the most dramatic effects of the W21H mutation is upon the binding of the antibacterial drug trimethoprim (TMP). This inhibitor binds nearly 200-fold more weakly to W21H DHFR than to the wild-type enzyme.

Table 4.1 Equilibrium dissociation constants of ligands binding to wild-type, W21H and W21H/D26N DHFR.

Ligand	K_d (μM)		
	Wild-type	W21H	W21H/D26N
MTX	<0.001	0.005±0.001	nd
TMP	0.15±0.01	29±1.9	nd
FH_2	0.24±0.02	0.75±0.03	2.83±0.23
folate	7.8±0.3	17±1.9	nd
NADPH	0.01±0.001	12±0.25	9.2±0.54

nd = not determined

The binding constants for the substrates folate and FH_2 to the single W21H mutant were similar to wild-type DHFR, although the double substitution (Trp 21→His and Asp 26→Asn) does lead to a 12-fold increase in the binding constant for FH_2. By far the largest

effect of the W21H substitution in both single and double mutants is upon the affinity of the coenzyme NADPH, which is reduced by a factor of approximately 1000 in each mutant when compared to the wild-type enzyme.

4.2.2 Steady state kinetic parameters

The K_m of FH_2 for the W21H/D26N mutant was 12-fold higher than that for the wild-type enzyme; this is in line with a similar increase in the K_d for this substrate (Table 4.2). There is virtually no change in the K_d of FH_2 for W21H DHFR and this suggests that the K_m of FH_2 for the W21H mutant should also be largely unaffected. This is consistent with the fact that there was no increase in W21H activity when the FH_2 concentration was varied from 50μM to 150μM, indicating that the substrate is at saturating levels.

Table 4.2 K_m and k_{cat} kinetic parameters for wild-type, W21H and W21H/D26N DHFR (pH 6.0).

Kinetic parameter	Wild-type	W21H	W21H/D26N
K_m (μM)			
FH_2	1±0.4	nd	12.4±1.7
NADPH	3.7±1	27±2.3	15±2
k_{cat} (s^{-1})	25±0.8	6.5±0.17	3±0.08

nd = not determined

The K_m of NADPH has increased by factors of 7 and 4 for W21H and W21H/D26N DHFR respectively, when compared to the wild-type enzyme; this is in marked contrast to the effects on K_d (see above). With wild-type DHFR, K_m (NADPH) is a reflection of the affinity of the coenzyme for the enzyme-FH_4 binary complex whereas K_d (NADPH) reflects

binding to the enzyme alone (Fierke *et al.*, 1987, Andrews *et al.*, 1989). With wild-type DHFR Andrews *et al.* have measured the K_m/K_d (NADPH) ratio to be 100 which has been attributed to the negative cooperativity between the binding of NADPH and FH_4 (see section 1.5 of Introduction chapter). In this study the K_m/K_d ratio has been calculated to be 2.3 for W21H and 1.6 for W21H/D26N DHFR. The results suggest that the negative cooperative effect has been greatly reduced by mutation of Trp 21.

The rate of catalysis is 4-fold lower in W21H DHFR and 8-fold lower in W21H/D26N DHFR when compared to the wild-type enzyme. However, deuterium isotope effect experiments have shown that k_{cat} reflects different processes in wild-type and mutant enzymes and hence a direct comparison of the k_{cat} values is not valid. Figure 4.1 shows the pH dependence of the deuterium isotope effect (k_{cat}NADPH/k_{cat}NADPD) for wild-type DHFR and the Trp 21 mutants. These experiments were carried out in order to determine if the Trp 21 mutations had affected the rate of hydride ion transfer. The pH dependence of the isotope effect observed in the wild-type enzyme (which reflects a change in rate-limiting step, see Section 3.2.3.1 of the D26N chapter) is abolished in W21H DHFR. Instead, a large isotope effect of approximately 2.6 is seen throughout the measurable pH range. The results imply that in the reaction catalysed by the W21H mutant, hydride ion transfer is the rate-limiting step in steady state turnover. In the case of the double mutant, a full isotope effect is only observed at higher pH values, at lower pH values it varies between 2.0-2.4. The results suggest that some other step, in addition to hydride ion transfer, must be contributing to catalysis at these pH values.

4.2.3 The pH dependence of k_{cat} for W21H DHFR

The pH dependence of k_{cat} was measured for wild-type and mutant enzymes over the pH range 5-8.5 and the resulting profiles are shown in Figure 4.2. With wild-type DHFR the pH dependence of k_{cat} has an apparent pK_a of 7.3±0.1 due to a change in rate-limiting step (see Section 3.3.3 of the D26N chapter). However, from Figure 4.2(b) it can be seen

Figure 4.1 pH dependence of the deuterium isotope effect

(a) W21H DHFR (•) and wild-type DHFR (+)

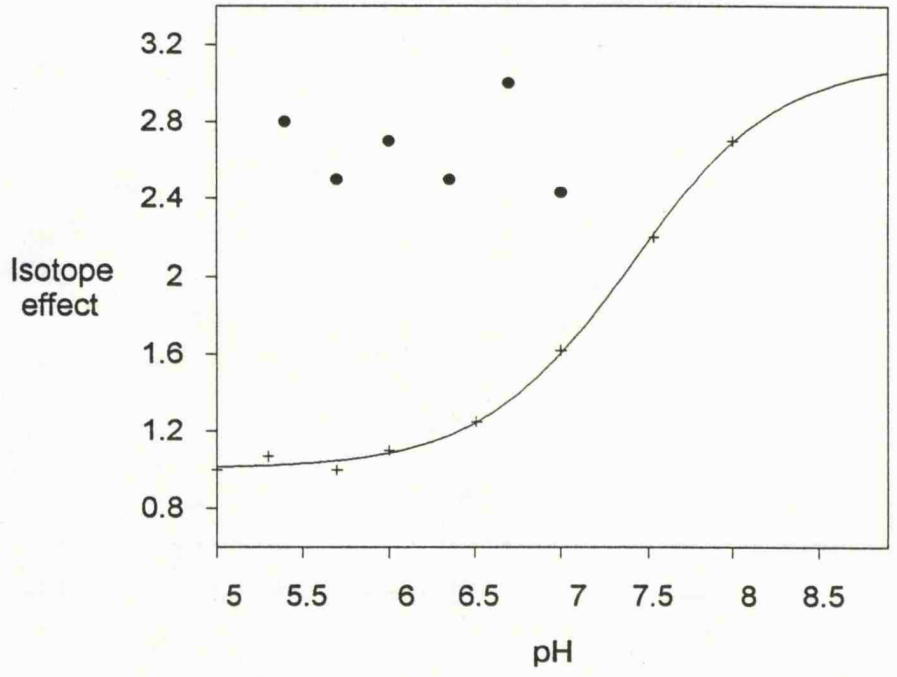

(b) W21H/D26N DHFR (•) and wild-type DHFR (+)

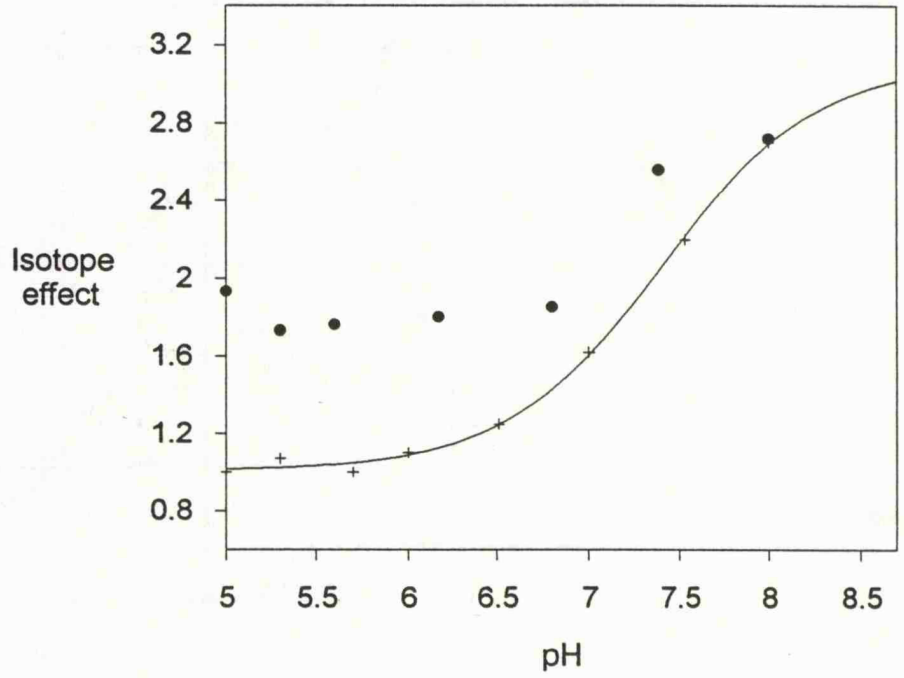

Figure 4.2 pH dependence of k_{cat}

(a) Wild-type DHFR

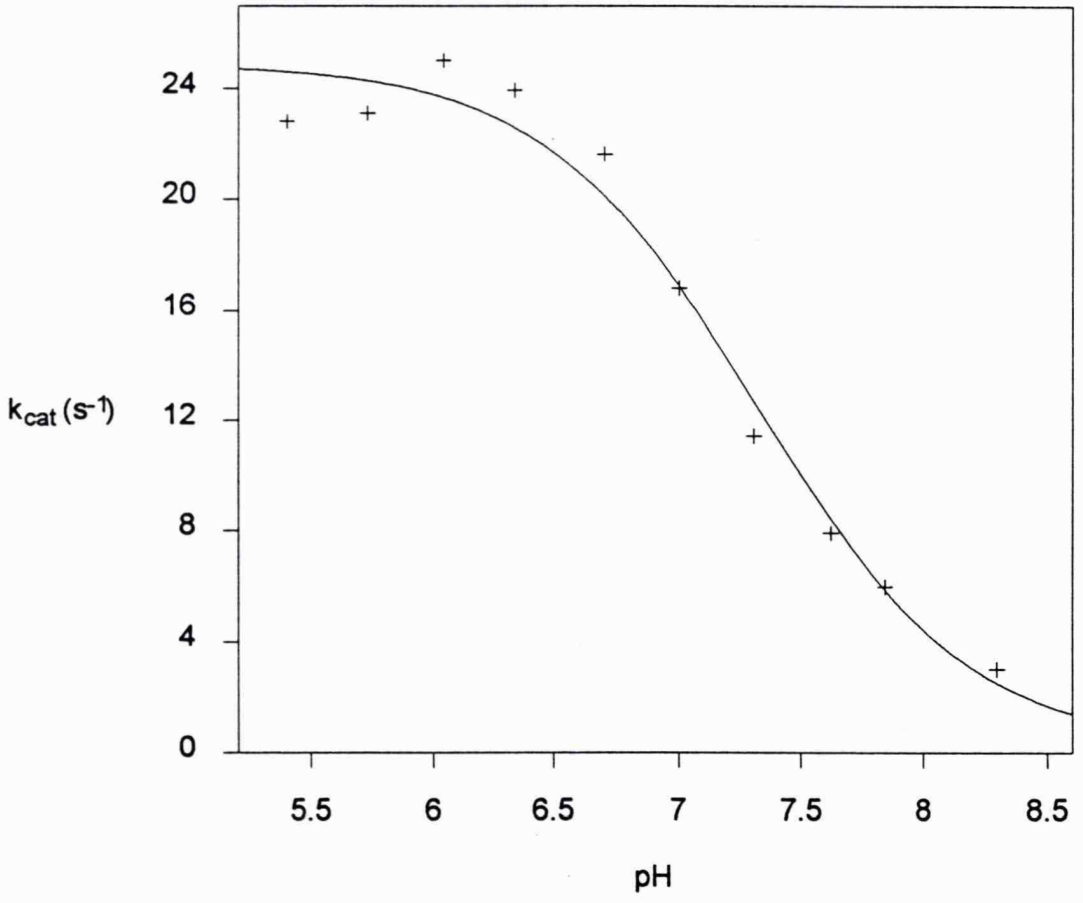

(b) W21H DHFR

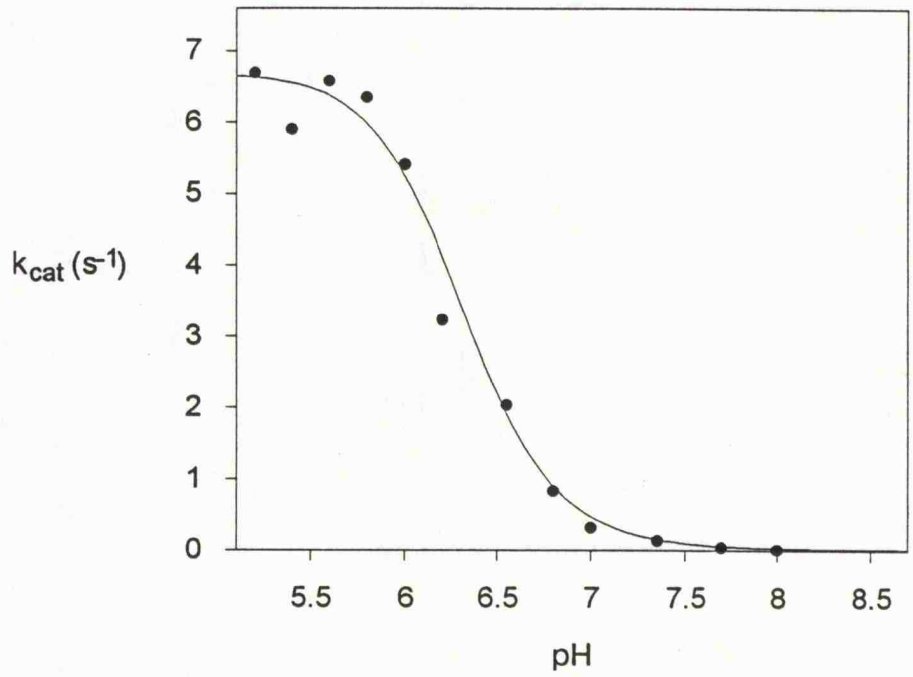

(c) W21H/D26N DHFR

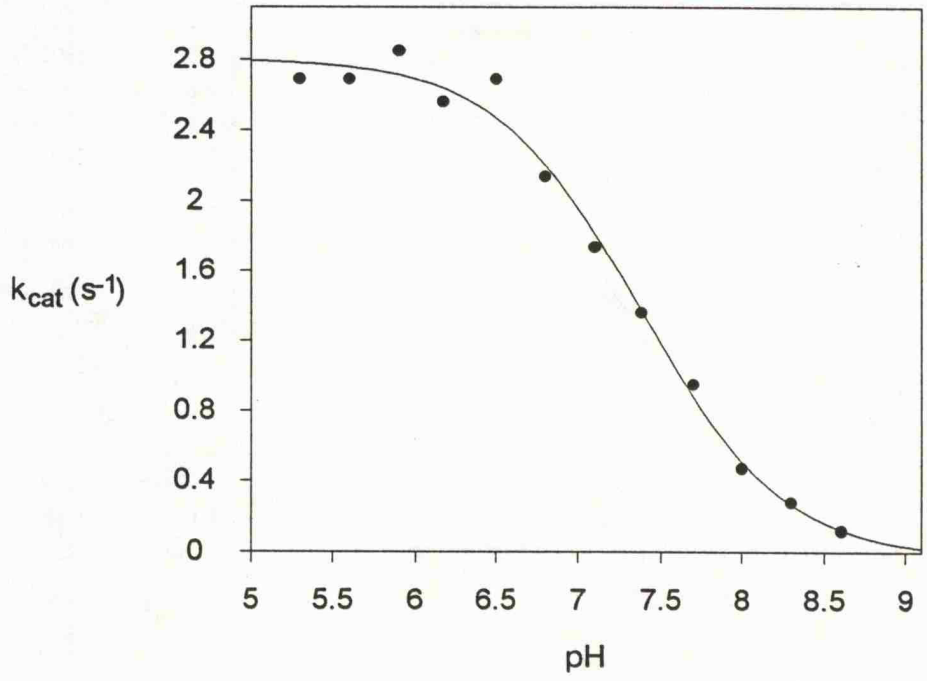

that the form of the pH-k_{cat} profile in W21H DHFR is very different; after pH 6 there is a steep fall in catalytic activity as the pH is increased further. In order to establish if the rapid decrease in activity was due to inactivation of the W21H mutant at higher pH values, the pH dependence of k_{cat} was repeated using mutant enzyme which had been preincubated at pH 5 and pH 7.5. In both instances the variation of k_{cat} with pH was identical to that seen in Figure 4.2(b) and hence was not the result of enzyme inactivation.

The pH dependence of k_{cat} for W21H DHFR could not be fitted to the ionisation of a single group but could be fitted to an equation which describes the cooperative ionisation of two groups (Dixon, 1976; Tipton and Dixon, 1983; Dixon, 1992). This is illustrated by Schemes I and II and discussed below.

Scheme I Ionisation of a dibasic acid

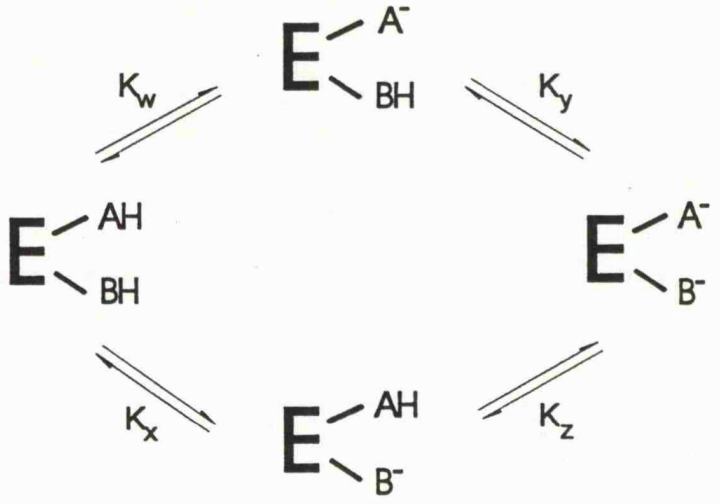

In this scheme "E" is the enzyme and can be considered as a dibasic acid with A and B representing two ionisable groups. K_w, K_x, K_y and K_z are *group* dissociation constants for each proton in the particular enzyme complex. In this scheme $K_x \neq K_y$, even though both represent dissociation of a proton from the same group, namely BH. This is because the ionised form of A (A^-) will have an effect on the ionisation of BH in EA^-BH (see the Discussion section) with the result that the value of K_x will not be the same as K_y (similar

arguments apply to K_w and K_z). Since there are often difficulties in determining values for individual group dissociation constants, the singly protonated complexes EA^-BH and $EAHB^-$ are treated as a single species (Scheme II) and *molecular* dissociation constants (K_1 and K_2) are often calculated.

Scheme II Molecular dissociation constants of a dibasic acid

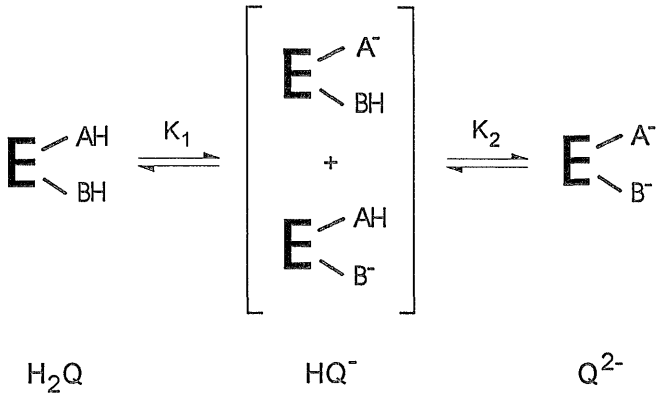

In this scheme EAHBH is referred to as H_2Q, which dissociates first to HQ^- and then to Q^{2-}. The molecular dissociation constants K_1 and K_2 are defined as:

$$K_1 = [H^+][HQ^-]/[H_2Q] = K_w + K_x$$

$$K_2 = [H^+][Q^{2-}]/[HQ^-] = K_z \cdot K_y/(K_z + K_y)$$

The pH dependence of k_{cat} for W21H DHFR has been fitted to an equation that describes Scheme II and the values $pK_1 = 6.7 \pm 0.22$ and $pK_2 = 6.0 \pm 0.4$ have been obtained.

The pH dependence of k_{cat} for W21H/D26N DHFR is shown in Figure 4.2(c). The curve fits well to a single pK_a value of 7.4±0.06. The cooperative ionisation of the two groups observed in W21H DHFR is abolished in the double mutant.

4.2.4 Measurement of pK_a values of His residues in the W21H DHFR-MTX complex

The chemical shifts of the His C2-protons were measured for both wild-type and W21H DHFR when in complex with MTX over the pH range 5-8.5. The resonances of all seven histidines in *L.casei* DHFR have been assigned (Carr *et al.*, 1991). The pH dependence of the His C2 proton resonances of the W21H DHFR-MTX complex are shown in Figure 4.3. For each His residue a titration curve was obtained by plotting its C2-proton chemical shift against pH, and a pK_a value calculated by fitting the titration data to an equation that describes the ionisation of a single group. pK_a values calculated in this manner are listed in Table 4.3.

Table 4.3 pK_a values of His residues in wild-type DHFR-MTX and W21H-MTX complexes

Histidine	pK_a of His in complex with:	
	wild-type-MTX	W21H-MTX
18	7.34±0.05	7.34±0.1
21	-	6.33±0.07
22	6.0±0.02	6.44±0.05
28	7.56±0.03	7.42±0.08*
64	7.47±0.08	6.76±0.07*
77	7.3±0.07	7.51±0.1
89	7.73±0.04	7.9±0.08
153	nd	nd

nd= not determined (see text)

* = tentatively assigned

Figure 4.3 His C2 proton chemical shifts as a function of pH for the W21H-MTX complex.

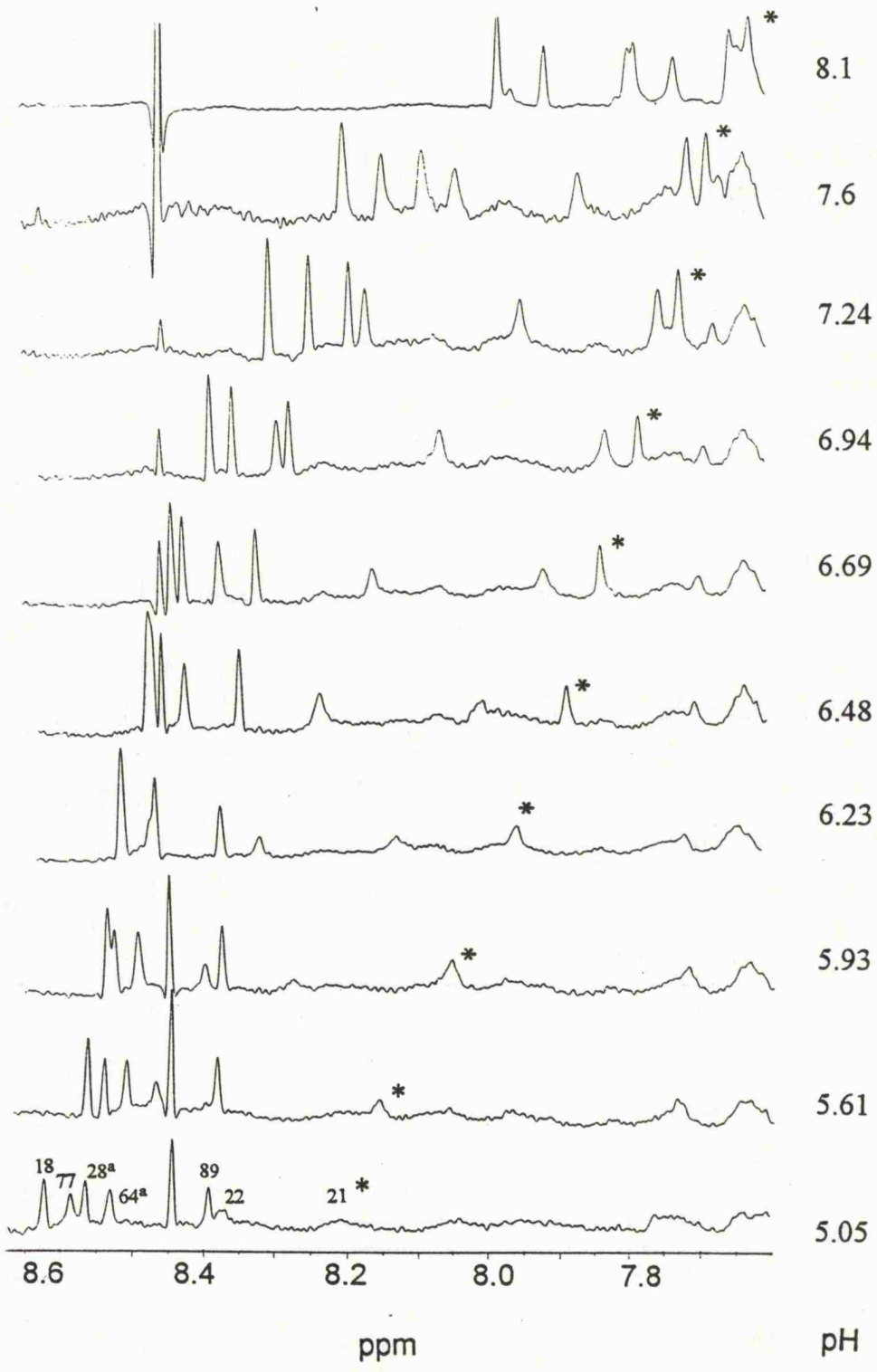

Numbers refer to the particular His C2-proton resonance
New His 21 C2-proton resonance is marked with an asterisk (*)
[a] tentatively assigned (see text)

For wild-type DHFR, with the exception of His 18 and His 22 (which were incorrectly assigned), pK_a values are similar to previously published values (Gronenborn *et al.*, 1981b, Antonjuk *et al.*, 1984). pK_a values for only six of the seven histidine residues in *L.casei* DHFR are given in Table 4.3. The His residue not shown is His 153 which forms an ionic interaction with Asp 25 of *L.casei* DHFR (Filman *et al.*, 1982) resulting in an elevated pK_a value (greater than 8; Wyeth *et al.*, 1980, Antonjuk *et al.*, 1984) that gives an incomplete titration curve in the pH range used.

The pH dependence of the His C2 proton chemical shift for His 21 is shown in Figure 4.4; the pK_a of the new His was calculated to be 6.33±0.07. Ionisations of other His residues have been affected by the W21H mutation, in particular that of His 22 which has an increased pK_a from 6.0 (in the wild-type enzyme) to 6.4 in W21H (Table 4.3). The resonances of His 64 and His 28 appear very close to each other in the W21H-MTX ^1H NMR spectrum (pH 6.5) and cannot be unambiguously assigned in the W21H mutant. Hence it is not clear which one of these two His residues has a pK_a of 6.76 in the mutant; a value approximately 0.7 units lower than that seen in the wild-type DHFR-MTX complex.

Figure 4.4 pH dependence of the chemical shift of the C2 proton of His 21 in the W21H-MTX complex

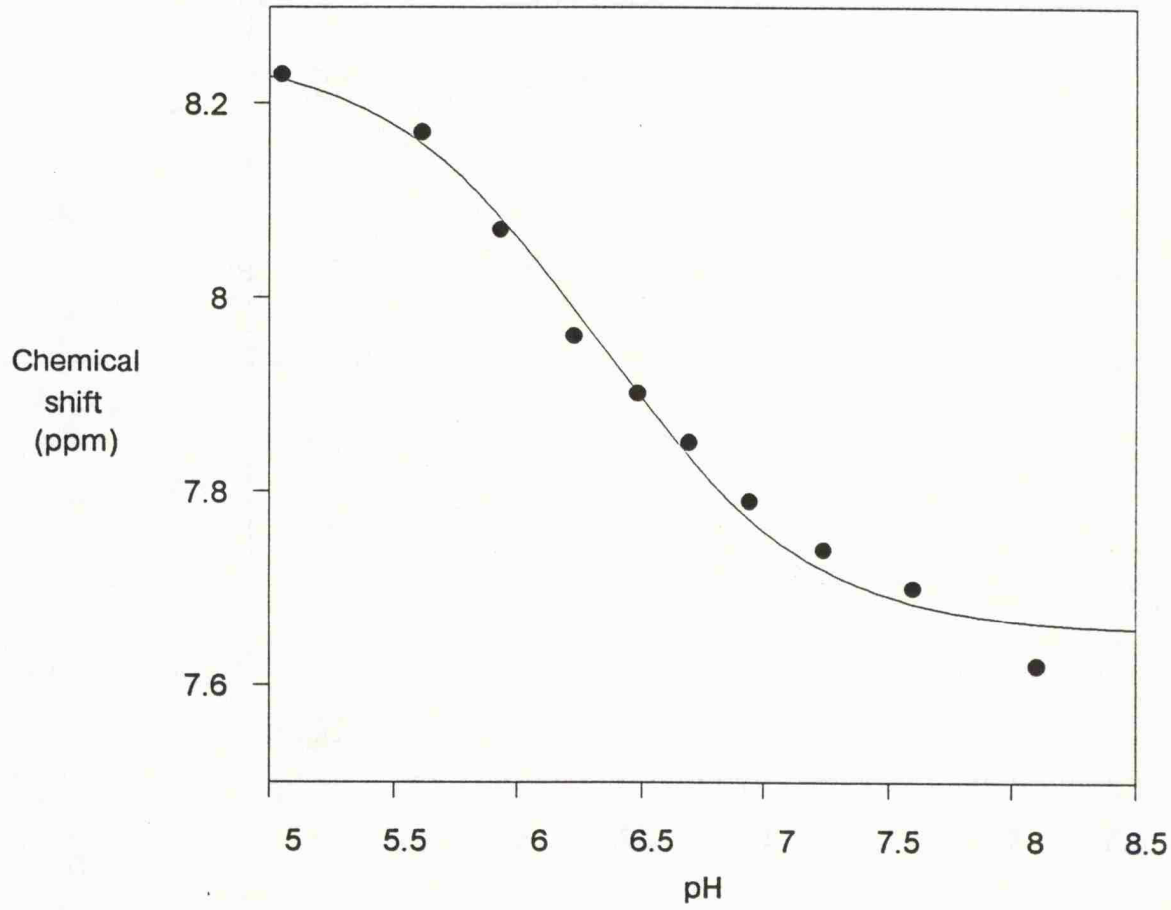

4.3 DISCUSSION

4.3.1 Ligand binding

The binding of the inhibitor MTX to W21H DHFR was found to remain tight (K_d less than 10nM), while the W21H mutation has only a modest effect on the binding of substrates (less than 4-fold). The results suggest that any structural changes accompanying the Trp 21→His mutation do not have a major effect on the binding of MTX or the substrates folate and FH_2. These results are very similar to those obtained on the *L.casei* Trp 21→Leu DHFR mutant (Andrews *et al.*, 1989, Birdsall *et al.*, 1989a). NMR studies on the W21L-MTX complex revealed that, although there were small changes in the positions of residues at the site of the mutation, MTX bound tightly to W21L DHFR (K_d less than 10nM) and in essentially the same conformation as observed in the wild-type DHFR-MTX complex.

The binding of the inhibitor trimethoprim (TMP) to W21H DHFR was 200-fold weaker than to the wild-type enzyme suggesting an important role for Trp 21 in the binding of this particular inhibitor. This is in contrast to the binding of TMP to W21L DHFR which was virtually unaffected by the mutation (Birdsall *et al.*, 1989a). When TMP is bound to DHFR, its diaminopyrimidine ring interacts in an analogous manner to the corresponding part of MTX (Baker *et al.*, 1981, Matthews *et al.*, 1985a, Matthews *et al.*, 1985b, Champness *et al.*, 1986, Stammers *et al.*, 1987, Groom *et al.*, 1991). In free solution the pyrimidine N1 of TMP has a pK_a value of 7.7 (Roberts *et al.*, 1981), the pK_a of His 21 in the W21H-MTX complex has been measured to be 6.33. It may be feasible that at pH 6.5, the pH at which the binding experiments were performed, the decreased binding of TMP to W21H DHFR may therefore be due to a direct repulsion between protonated inhibitor and the mutant protein. Alternatively, the weaker binding of TMP to W21H DHFR may be attributed to structural changes that accompany the W21H mutation (and not the W21L

substitution), leading it to adopt a different conformation to that observed in the wild-type DHFR-TMP complex.

By far the most dramatic effect of the Trp 21 substitution is upon the affinity of the coenzyme NADPH, which was reduced by a factor of approximately 1000 in both W21H and W21H/D26N mutants when compared to wild-type DHFR. From the ternary *L.casei* DHFR-MTX-NADPH crystal structure it is known that the benzene component of the Trp 21 indole ring is in hydrophobic contact with the nicotinamide ring of NADPH (Filman *et al.*, 1982). This is shown schematically below:

nicotinamide ring

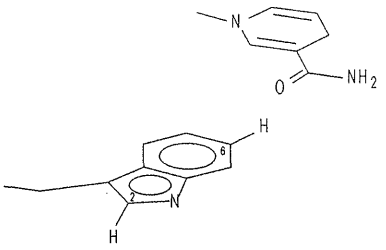

Trp 21 indole ring

It may be feasible that the smaller size of the His imidazole ring leads to a reduction in the hydrophobic contacts made with the nicotinamide ring, resulting in weaker binding of the coenzyme. The results imply that the Trp 21-NADPH nicotinamide ring contact is critical for the binding of NADPH to *L.casei* DHFR which is consistent with the kinetic data of Birdsall *et al.* (1980) who have shown that the nicotinamide ring makes a major contribution to the overall binding energy of NADPH.

The effects of the W21H mutation on the binding of substrates and coenzyme are in line with results obtained on W21L DHFR and also with *L.casei* DHFR in which Trp 21 has

been chemically modified by N-bromosuccinimide to produce oxindole (this introduces a carbonyl group at the C2 position of the indole ring; Thomson *et al.*, 1980, Feeney *et al.*, 1980). In both instances the binding of substrates was virtually unaffected (by less than a factor of 5), but NADPH binding was decreased by a factor of 200 for the chemically modified enzyme and 400 for W21L when compared to wild-type DHFR. However, the reduction in coenzyme affinity to both chemically and genetically modified Trp 21 mutants is thought to originate by different means. Chemical modification of Trp 21 by N-bromosuccinimide occurs at the opposite end of the indole ring (at the C2 position) that makes contact with the coenzyme. The authors suggest that the weaker binding of NADPH was due to a change in the position of the oxindole ring that occurs as a result of unfavourable contacts between the C2 oxygen atom and other protein residues, for example Leu 19 (which also interacts with the nicotinamide ring; Filman *et al.*, 1982). In the W21L mutant, weaker binding of NADPH was attributed to a change in the orientation of the nicotinamide ring in the binding pocket. This was due to a loss of the hydrophobic contact between the C6 proton of Trp 21 and the carboxamide group of NADPH. A similar situation may also exist in the W21H-NADPH complex.

Site-directed mutagenesis has been used to substitute the strictly conserved Trp 21 (*L.casei* DHFR numbering) in various DHFRs for other residues (Andrews *et al.*, 1989, Huang *et al.*, 1989, Warren *et al.*, 1991, Beard *et al.*, 1991). The effects that the replacements have produced on some of the kinetic parameters are shown in Table 4.4. In contrast to the results obtained with the Trp 21 mutants of *L.casei* DHFR, substitution of Trp 21 in *E.coli* and human DHFRs has very little effect on the binding of NADPH, suggesting a much lesser role for this residue in the binding of coenzyme to DHFR from these species.

Table 4.4 The effects of Trp 21 mutations (L.casei numbering) on the kinetic parameters of DHFR from various sources[a]

	L.casei[b] W21L	*E.coli*[c] W22H	*E.coli*[c] W22F	human[d] W24F
FH_2				
k_{off}/k_{on}	5.1	-	6.2	7.3
K_m	0.83	4.4	15	25
NADPH				
k_{off}/k_{on}	420	-	2	2.2
K_m	-	1.9	2.2	0.81
k_{cat}	0.14	0.063	0.87	3.2

[a] Numbers are the ratios of mutant to wild-type parameter for each species
[b] from Andrews *et al.*, 1989
[c] from Warren *et al.*, 1991
[d] from Beard *et al.*, 1991

4.3.2 Steady state kinetic parameters

The Trp 21→His substitution in both single (W21H) and double (W21H/D26N) mutants has a modest effect on the K_m of NADPH (no greater than 10-fold), but results in a large increase in its K_d value (approximately 1000-fold when compared to the wild-type enzyme). With wild-type DHFR the K_m of NADPH reflects the affinity of the coenzyme not to the apoenzyme (as the K_d value does) but to the binary enzyme-FH_4 complex as shown schematically in Figure 4.5 (Fierke *et al.*, 1987, Andrews *et al.*, 1989). After the formation of FH_4 and $NADP^+$, the oxidised coenzyme dissociates quickly from the ternary complex. The other product of the reaction, FH_4, does not dissociate at this stage and instead the enzyme binds another molecule of NADPH (this reflects the K_m value for NADPH). Due to the negative cooperativity between the binding of NADPH and FH_4 (Fierke *et al.*, 1987, Andrews *et al.*, 1989), FH_4 dissociates at a rate 80 times faster from the ternary enzyme-

Figure 4.5 Scheme showing the role of negative cooperativity between FH_4 and NADPH in the preferred kinetic pathway of L.casei DHFR

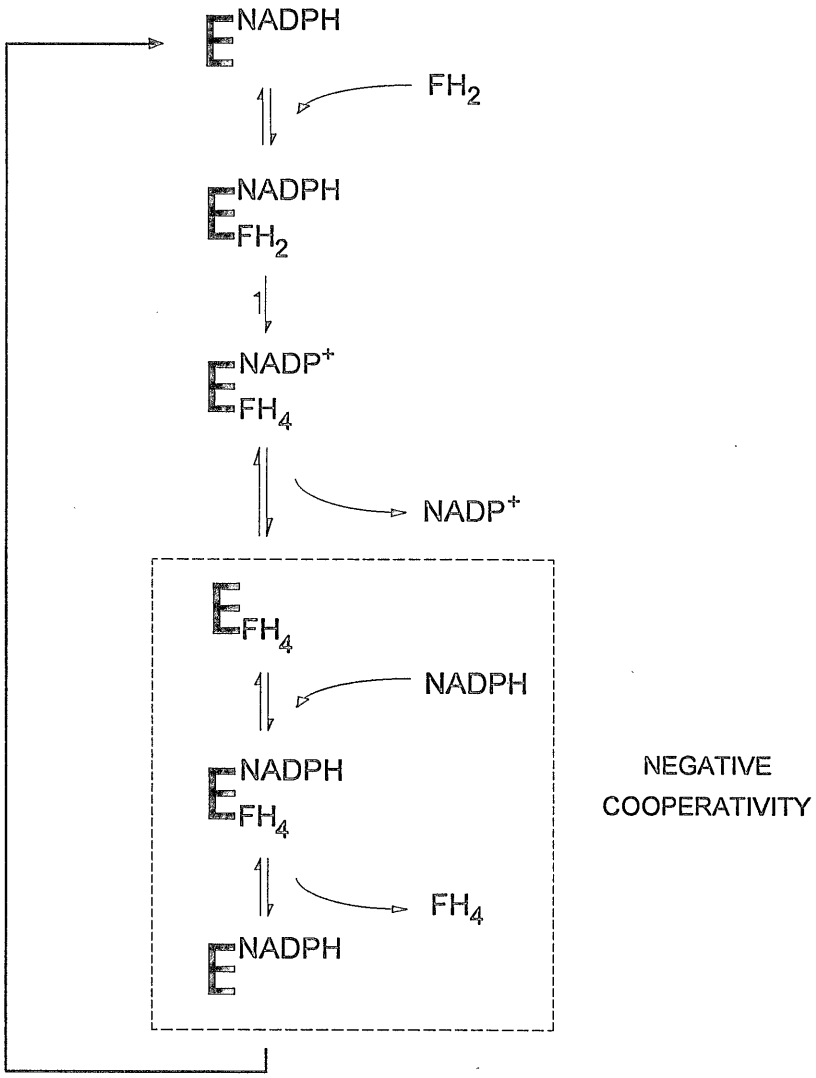

NADPH-FH_4 complex than from the binary enzyme-FH_4 complex. With wild-type DHFR the negative cooperative effect results in the K_m for NADPH being 100-fold greater than its K_d value (1μM compared with 0.01μM; Andrews *et al.*, 1989). The W21H mutation has a greater effect on coenzyme binding in the binary complex than in the ternary enzyme-FH_4-NADPH complex with the result that the K_m/K_d ratio is greatly reduced (to less than a factor of 3) in both W21H and W21H/D26N DHFR. The results imply that Trp 21 is involved in the mechanism of negative cooperativity.

Since the *E.coli* DHFR Trp 22→Phe mutation has not altered either K_m or K_d for NADPH (Table 4.4), the degree of negative cooperativity in this mutant also remains unaffected. In contrast, direct measurement of the dissociation rate constant (k_{off}) for NADPH from the human DHFR-FH_4-NADPH complex is nearly 60-fold greater than from the binary human DHFR-NADPH complex; this ratio is reduced to a factor of only 10 in the human W24F mutant again suggesting that this Trp may play a role in negative cooperativity in human DHFR.

A large deuterium isotope effect with NADPD (approximately 2.6 throughout the pH range) shows that the reaction catalysed by W21H DHFR is limited by the rate of hydride ion transfer from NADPH to FH_2. Thus a comparison of k_{cat} in the W21H mutant (which is equivalent to the rate of hydride ion transfer) with the rate of hydride ion transfer in the wild-type enzyme at the same pH (Andrews *et al.*, 1989) shows that this step has been reduced by a factor of 50. This compares with values of 100 for *L.casei* W21L DHFR and 130 for *E.coli* W22H DHFR (Andrews *et al.*, 1989, Warren *et al.*, 1991). Based on theoretical calculations, Benkovic *et al.* (1988) have suggested that in the transition-state of wild-type DHFR the optimum distance for hydride ion transfer between donor and acceptor is 2.6Å. Any minor variations in this distance can have substantial effects on the rate of hydride ion transfer; for instance, it was calculated that a difference of 0.3Å could lead to a 5000-fold decrease in the rate of hydride ion transfer. Indeed, NMR studies on the *L.casei* W21L mutant have demonstrated that substitution for Leu 21 leads to a change in the

orientation of the nicotinamide ring of bound coenzyme which may account for the 100-fold reduction in the rate of hydride ion transfer seen with this mutant (Andrews *et al.*, 1989, Birdsall *et al.*, 1989a).

4.3.3 The pH dependence of k_{cat} for W21H DHFR

The pH dependence of k_{cat} for W21H DHFR was fitted to a model which describes the cooperative ionisation of two groups:

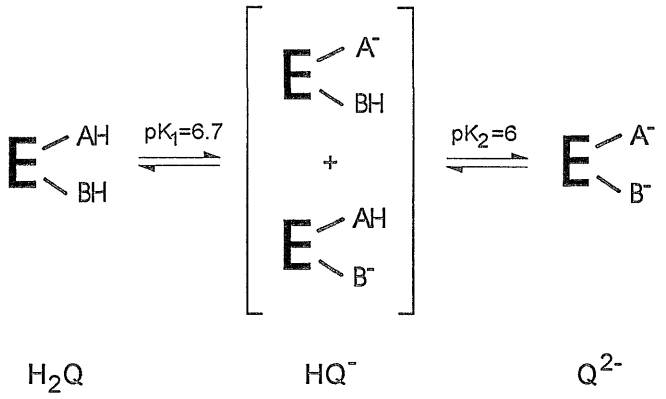

In this scheme, the groups "A" and "B" in the active site of the enzyme are sufficiently close enough to influence one anothers ionisation, possibly through electrostatic or hydrogen bonding interactions (Tipton and Dixon, 1983, Dixon, 1992). As noted in the results section only molecular pK_a values (pK_1 and pK_2 in the above scheme) will be discussed. Usually the value of pK_1 is smaller than that of pK_2; this is a reasonable assumption to make since the extra negative charge on Q^{2-} could give it a higher affinity for a proton compared with HQ^-. However, with W21H DHFR it can be seen that pK_2 is less than pK_1, this is referred to as positive cooperativity of proton binding (Dixon and Tipton, 1973). In this situation, loss of the first proton facilitates loss of the second proton, possibly through a conformational change. Thus, loss of a proton in going from $H_2Q \rightarrow HQ^-$ will facilitate $HQ^- \rightarrow Q^{2-}$ and as a consequence of this, the concentration of HQ^- will always be very low.

It is possible that in this scheme one of the ionisations could be that of His 21. Introduction of His 21 into the active site of DHFR would place it in close proximity to the substrate pteridine ring and the only other ionisable sidechain in the region, namely Asp 26. There is good evidence which supports the fact that one of the groups responsible for the cooperative ionisation observed in W21H DHFR is His 21. The pH dependence of k_{cat} seen in W21H DHFR is not observed in the wild-type enzyme under conditions where hydride ion transfer is rate-limiting (Andrews *et al.*, 1989). The unusual pH dependence of k_{cat} (W21H) is not observed with the *L.casei* Trp 21→Leu mutant (Andrews *et al.*, 1989 and experiments carried out in this study; data not shown). In W21L DHFR, catalysis is also governed by the rate of hydride ion transfer, the pH dependence of k_{cat} having a pK_a value of 5.9. The pK_a of His 21 in the W21H-MTX binary complex has been measured directly by ^1H NMR and found to be 6.33; a value which correlates well with both values obtained from the kinetic studies. Recently, the pK_a of His 21 has also been measured in the W21H DHFR-FH_2 binary complex and shown to have a similar value to that in the W21H-MTX complex (M.G. Casarotto, personal communication).

The identity of the other group responsible for the cooperative ionisation seen with W21H is less clear. It was thought that Asp 26 was a likely candidate; this residue has been postulated to be responsible for the pH dependence of k_{cat} observed with the wild-type enzyme (see Section 1.6 of the Introduction Chapter). In an attempt to resolve this, the double mutant (W21H/D26N DHFR) was made. With W21H/D26N DHFR, the variation of k_{cat} with pH has a more "normal" profile with a pK_a value of 7.4±0.06, i.e. the cooperative ionisation seen with the single W21H mutant has been abolished. At first glance this seems to imply that Asp 26 is indeed the other ionisable group, however the results are not so straight forward. Deuterium isotope effect experiments revealed that, in the double mutant a full isotope effect is only observed at higher pH values, implying that hydride ion transfer is only totally rate-limiting at these pH values. At low pH another step, in addition to hydride ion transfer, must be contributing to catalysis. Therefore, as with the wild-type enzyme, the pK_a value calculated from the variation of k_{cat} with pH for the double mutant

could be an apparent one reflecting a change in rate-limiting step. Another, albeit indirect line of evidence that may argue against the involvement of Asp 26 in the cooperative ionisation observed with W21H DHFR has come from the direct measurement of the pK_a of Asp 26 in *L.casei* DHFR (M.G. Casarotto, personal communication). The ability to incorporate ^{13}C γ-Asp into DHFR (Badii *et al.*, 1994), and the establishment of protocols for the stabilisation of FH_2, has enabled the pK_a of Asp 26 to be measured by NMR in apoDHFR and various DHFR-FH_2 containing complexes. These studies have shown that in all the complexes studied, the pK_a value of Asp 26 is no greater than 4.5. Thus, in ground state complexes of *L.casei* DHFR, Asp 26 is likely to be in its ionised form. Another probable candidate for the second ionisable group may be some group on the substrate, possibly the C4 enol group of FH_2 as it ionises to the enolate form.

4.3.4 pK_a values of His residues in the W21H-MTX binary complex

The pK_a of His 21 in the W21H-MTX binary complex has been measured to be 6.33. The mutation also has an effect on the pK_a of the neighbouring residue, His 22 which has increased by 0.44 units compared to its value in the wild-type DHFR-MTX complex. The ionisation states of His 77 and His 89 have also been affected by the Trp 21→His substitution and may suggest that this mutation is accompanied by quite widespread structural changes. Small (less than 0.2Å) but distant structural changes accompanied the Trp 21→Leu mutation (Birdsall *et al.*, 1989a). A significant change in the pK_a of either His 28 or His 64 (which has decreased by approximately 0.7 units) was observed as a result of the W21H mutation. Both these residues are quite remote from the site of the substitution; His 28 interacts with the γ-carboxylate of substrates and inhibitors whereas His 64 is present at the adenine binding site of NADPH (Filman *et al.*, 1982). It is interesting to note that in the W21L-MTX complex the chemical shift of the C2 proton of His 28 was measured, and found to be the same as that in wild-type DHFR (Birdsall *et al.*, 1989a). It was concluded that the interaction between the γ-carboxylate of MTX and His 28 was the same in both wild-type DHFR- and W21L-MTX complexes. If the ionisation of His 64 has been affected

by the W21H mutation then this may indicate that structural changes have occurred at the adenine binding site. Both the nicotinamide and adenine binding regions of DHFR have been implicated to be involved in negative cooperativity (see the General Discussion chapter). However, His pK_a values quoted here are for the W21H DHFR-MTX complex and not the W21H-NADPH-FH_4 complex. Experiments are underway to unambiguously identify which of these two His residues has the lower pK_a value.

4.4 SUMMARY

The Trp 21→His mutation has no effect on the binding of the substrates folate and FH_2. Unlike the inhibitor MTX, which still binds very tightly to the W21H mutant, the binding of the inhibitor trimethoprim TMP, is reduced by a factor of 200 when compared to the wild-type enzyme. The weaker binding of TMP could be due to a direct repulsion between the protonated His 21 ring and the protonated N1 of the inhibitor but structural data on this complex is required before any firm conclusions can be drawn. The 1000-fold increase in the binding constant of the coenzyme, NADPH to W21H DHFR (and the double mutant W21H/D26N) compared with the wild-type enzyme implies a vital role for the Trp 21-nicotinamide ring contacts in the binding of NADPH.

In contrast to the dramatic effect on K_d (NADPH), the Trp 21→His substitution, in both single and double mutants, has only a minor (less than 10-fold) effect on the K_m for the coenzyme. As a direct consequence of this, the K_m/K_d ratio (which is a measure of the degree of negative cooperativity) is significantly reduced in the Trp 21 mutants when compared to the wild-type enzyme. These results suggest an important role for Trp 21 in negative cooperativity between coenzyme and the product, FH_4 which is a unique (and crucial) feature of the kinetic mechanism of DHFR.

The rate of hydride ion transfer is reduced by a factor of 50 in W21H DHFR (when compared to the wild-type at pH 6) and limits catalytic turnover in this mutant. It may be possible that Trp 21 is necessary in correctly orientating the nicotinamide ring for optimum hydride ion transfer from coenzyme to substrate. The pH dependence of k_{cat} for the W21H mutant is also significantly different from that of the wild-type enzyme and has a form which suggests the cooperative ionisation of two groups. The pK_a of the new His 21 in the binary W21H-MTX complex has been calculated to have a value of 6.33; a similar number has recently been estimated for the same residue in the W21H DHFR-FH_2 complex (M.G. Casarotto, personal communication). His 21 could therefore be one of the groups

responsible for the unusual form of the pH-k_{cat} profile seen with W21H DHFR. Experiments are underway to determine the identity of the other species.

CHAPTER 5 R57K DHFR

5.1 INTRODUCTION

Arg 57 is a strictly conserved residue that forms an ion-pair interaction with the α-carboxylate of the glutamic acid moiety of substrates and the inhibitor MTX (Bolin *et al.*, 1982, Filman *et al.*, 1982, Oefner *et al.*, 1988, Bystroff *et al.*, 1990). In *L.casei* DHFR the γ-carboxylate forms a second ion-pair interaction with His 28:

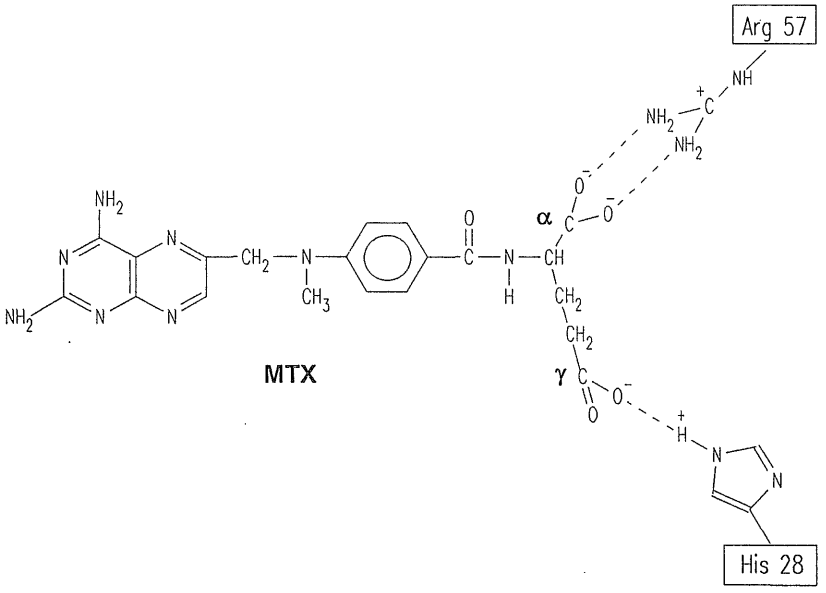

Figure 5.1 Ion-pair interactions between the carboxylates of MTX and L.casei DHFR

The interaction with His 28 is specific to the *L.casei* enzyme. In *E.coli* DHFR, for example, Ala 29 is the equivalent residue and the γ-carboxylate of MTX interacts with the solvent (Bolin *et al.*, 1982). The importance of these ionic interactions to the overall binding of the inhibitor MTX has been probed by the use of MTX analogues which are shown in Figure 5.2 (Antonjuk *et al.*, 1984). Substitution of the carboxylate with an amide group effectively

Figure 5.2 Analogues of methotrexate (MTX)

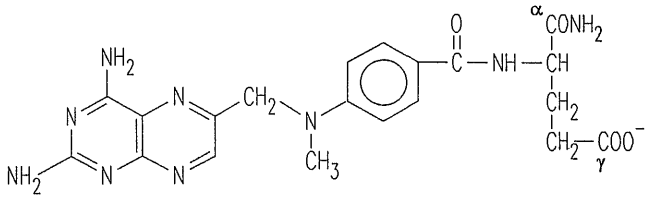

MTX-α-amide

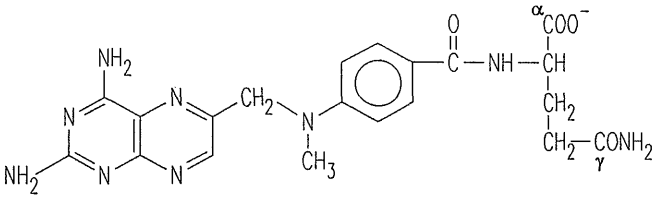

MTX-γ-amide

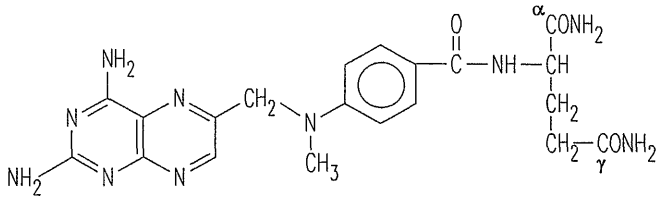

MTX-αγ-diamide

"blocks" the protein sidechain-MTX interaction. MTX-α-amide is an analogue of MTX in which the α-carboxylate has been replaced by an amide group and similarly the γ-amide derivative involves substitution of the γ-carboxylate with an amide group. In the αγ-diamide analogue both carboxylates have been replaced. As long as the substitution(s) result in no gross change in the mode of binding of the analogues, they can be used to assess the contribution the Arg 57 and His 28 ion-pair interactions make to the overall binding energy. Effects of the binding of these MTX analogues to wild-type *L.casei* DHFR have been previously assessed by kinetic and ^{1}H NMR methods by Antonjuk *et al.* (1984) and the results are outlined below.

In wild-type DHFR the interaction between the γ-carboxylate of MTX and the imidazole ring of His 28 is characterised by a one unit increase in the pK_a of this residue from 6.7 (in the enzyme alone) to 7.8 (in the complex with MTX). The binding of MTX-γ-amide to the DHFR-NADPH complex was reduced 9-fold compared to the binding of MTX and there was no increase in the pK_a of His 28 suggesting that this ion-pair interaction has been abolished. NMR studies demonstrated that the overall mode of binding of the γ-amide analogue to wild-type DHFR was similar to that of MTX, and it is therefore reasonable to assume that only the His 28-γ-carboxylate interaction has been affected by the substitution. The 9-fold reduction in binding (change in binding energy; ΔG_{app} of 5.7kJ/mol) is a good assessment of the contribution of the His 28-γ-carboxylate interaction to the overall binding energy of MTX.

MTX-α-amide bound 100-fold weaker to the wild-type DHFR-NADPH complex than did MTX. At first glance these results suggest that the Arg 57-α-carboxylate interaction makes a greater contribution to the binding energy than does the His 28-γ-carboxylate interaction. However, measurement of the pK_a of His 28 in the enzyme-α-amide complex gave a value of 6.7, implying that His 28 is not interacting with the γ-carboxylate of the α-amide analogue. It was concluded that loss of the Arg 57-α-carboxylate interaction also leads to the His 28-γ-carboxylate ion-pair being broken.

Furthermore, NMR studies showed that the α-amide substitution results in the whole of the *p*-aminobenzoyl glutamic acid (PABG) moiety binding differently to the enzyme and hence the α-amide analogue cannot be used to assess the contribution the Arg 57-α-carboxylate interaction makes to the overall binding energy. These conclusions were supported by the similar binding affinities of the αγ-diamide and the α-analogue to wild-type DHFR, since with both of these analogues both ion-pair interactions have been broken.

This work demonstrated the importance of Arg 57 in the binding of MTX, where it appears to be involved in correctly orienting the whole of the PABG moiety. Moreover, loss of the Arg 57-α-carboxylate interaction also results in loss of the His 28-γ-carboxylate interaction. With this background knowledge, similar experiments have been carried out on a DHFR mutant in which Arg 57 has been replaced with a Lys (R57K DHFR). In the Arg 57→Lys mutant, it was postulated that the shorter Lys sidechain (by approximately one C-C bond length) would maintain the charge interaction with the α-carboxylate of MTX, and at the same time have little effect on the structure of the protein. The effects of the R57K mutation on the binding of MTX and its analogues have been probed.

5.2 RESULTS

5.2.1 Equilibrium binding constants

The equilibrium dissociation constants for MTX and its analogues to wild-type and R57K DHFR are given in Table 5.1.

Table 5.1 Equilibrium dissociation constants of MTX and its amide analogues binding to wild-type and R57K DHFR (pH 6.5).

Ligand	K_d (μM)	
	Wild-type DHFR	R57K DHFR
MTX	<0.001	<0.001
MTX-α-amide	0.1±0.004	0.02±0.002
MTX-αγ-diamide	0.16±0.003	0.16±0.002

For wild-type DHFR the dissociation constant of MTX was too low to measure accurately using the fluorescence titration method. The same is true for the R57K mutant and a maximum value of 1nM is quoted for both enzymes. The MTX-α-amide analogue binds 5-fold tighter to the R57K mutant than to the wild-type enzyme suggesting that the mutation has actually increased the binding of this analogue. The binding of the αγ-diamide analogue was the same to both enzymes.

Equilibrium dissociation constants of MTX-γ-amide to R57K and wild-type DHFR were measured at three different pH values and the results are given in Table 5.2. It can be seen that at low pH the γ-derivative binds very tightly to wild-type and mutant DHFRs although K_d values can be calculated, with accuracy, at higher pH values. With the wild-type enzyme there is a slight (at least 14-fold) change in the binding constant of MTX-γ-

amide over the pH range 5.3 to 8. In the case of R57K DHFR the K_d value of the γ derivative appears to increase 180-fold over the same pH range. The results suggest that the binding of γ-amide MTX (and indeed MTX itself; data not shown) to the R57K mutant may be more pH dependent than in the wild-type enzyme.

Table 5.2 Equilibrium dissociation constants of MTX-γ-amide binding to wild-type and R57K DHFR at different pH values.

pH	MTX-γ-amide K_d (μM)	
	Wild-type DHFR	R57K DHFR
5.3	<0.001	0.003±.0007
6.5	0.003±0.001	0.023±0.001
8	0.014±0.001	0.55±0.06

5.2.2 Determination of Histidine pK_a values in enzyme-MTX and enzyme-MTX-α-amide binary complexes

The pH dependence of the His C2-proton chemical shifts were determined for enzyme-MTX and enzyme-MTX-α-amide complexes. Figure 5.3 shows the spectrum of the His region of the wild-type DHFR-MTX complex plotted as a function of pH. As noted in section 4.2.4 of the W21H Chapter, all seven His residues of wild-type *L.casei* DHFR have been assigned (Carr *et al.*, 1991). Titration curves were obtained by plotting the His C2-proton chemical shifts against pH as shown in Figure 5.4. The pK_a value for each His residue was calculated by fitting the titration data to an equation that describes the ionisation of a single group. pK_a values of the His residues obtained in this manner for various enzyme-inhibitor complexes are given in Table 5.3. The His pK_a values for wild-type DHFR complexes agree well with published values; pK_a values for His 153 have not been calculated (see section 4.2.4 of the W21H chapter). From the table it can be seen that

Figure 5.3 Chemical shifts of His C2-protons as a function of pH for the binary wild-type-MTX complex.

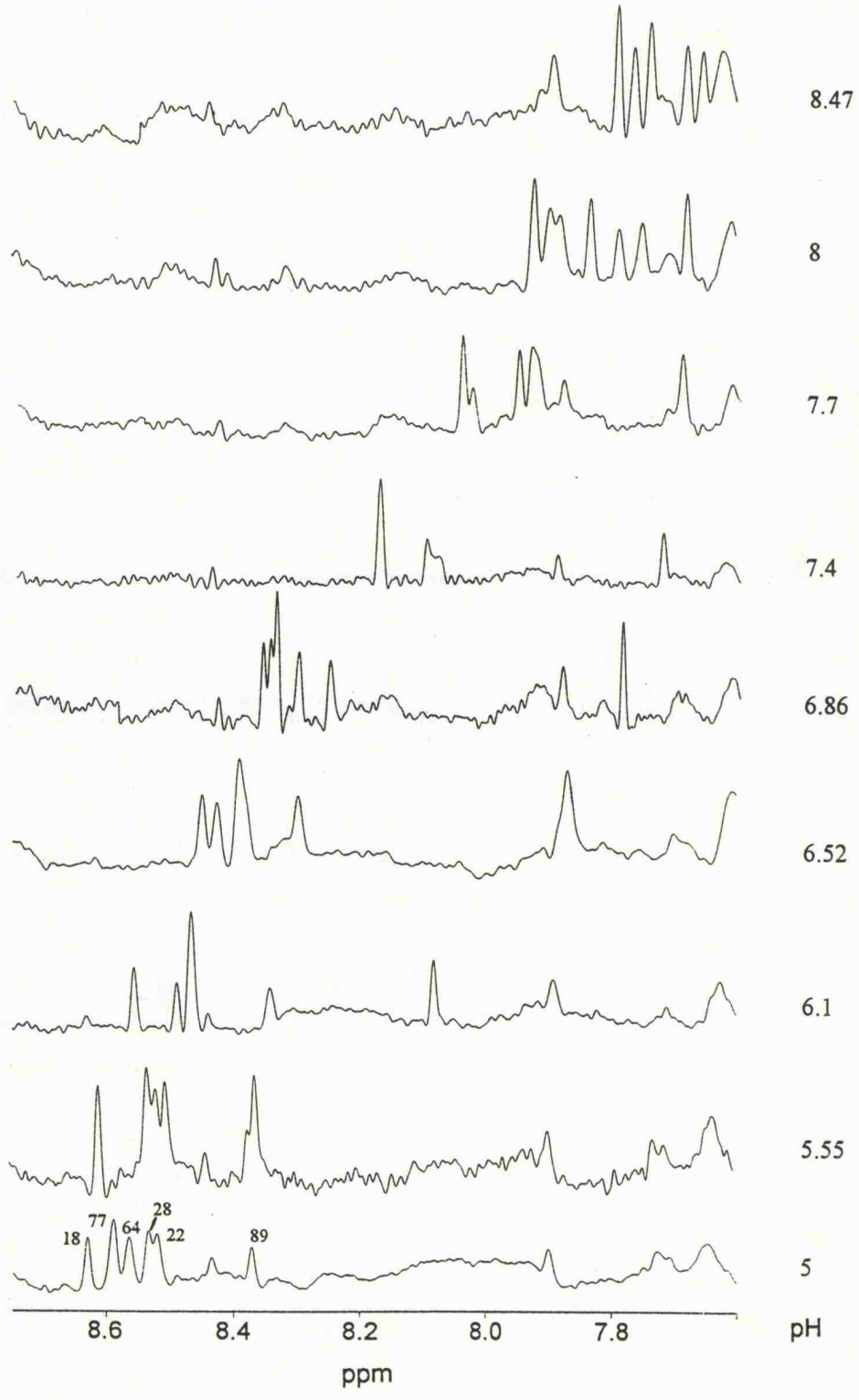

Numbers refer to the particular His C2-proton resonance

Figure 5.4 pH dependence of the C2 proton chemical shifts of His residues in the binary wild-type-MTX complex

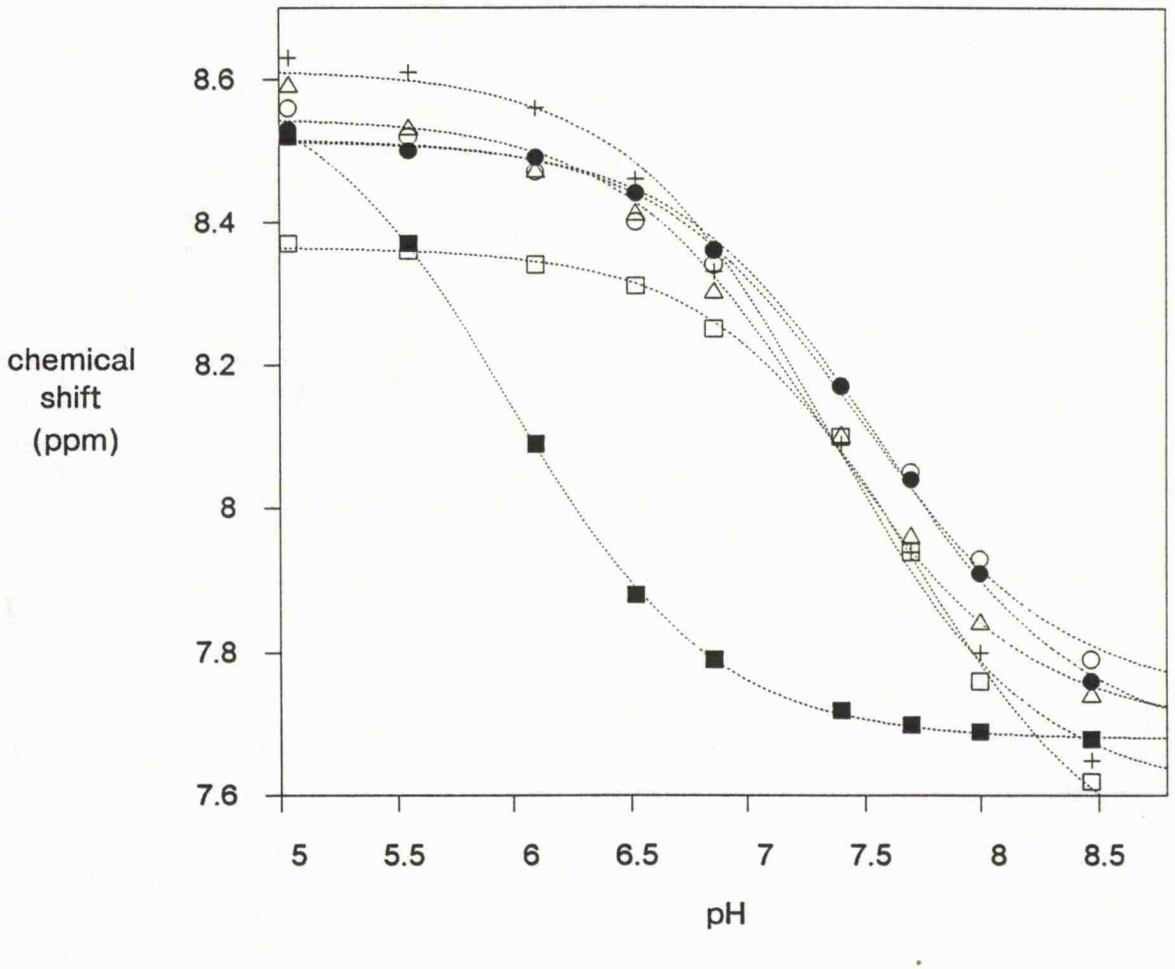

the only significant difference in pK_a values in the various complexes is that of His 28 which has a value of 6.68 in the wild-type DHFR-MTX-α-amide complex and a value of approximately 7.5 in both wild-type-MTX and R57K-MTX complexes. Unfortunately, His residues 28, 64 and 77 could not be unambiguously assigned in the R57K-MTX-α-amide complex. Despite this, His 28 still has a minimum pK_a value of 7.28 in this complex, at least 0.6 units higher than its value in the wild-type DHFR-MTX-α-amide complex. It is known that in the wild-type DHFR-MTX-α-amide complex the lower pK_a value of His 28 is due to an absence of the His 28-γ-carboxylate interaction (see Introduction to this chapter). The higher pK_a value of His 28 in the R57K-MTX-α-amide complex now suggests that as a result of the Arg 57→Lys mutation this interaction has been regained.

Table 5.3 pK_a values of histidine residues in wild-type and R57K DHFR when in complex with either MTX or its α-amide derivative.

Histidine	pK_a of Histidine in complex:			
	wild-type-MTX	wild-type-MTX-α-amide	R57K-MTX	R57K-MTX-α-amide
18	7.34	7.32	7.24	7.25
22	6.0	6.1	6.2	5.94
28	7.56	6.68	7.45	7.48*
64	7.47	7.57	7.77	7.36*
77	7.3	7.37	7.4	7.28*
89	7.73	7.84	7.9	7.72

Standard errors omitted for clarity; all are less than ±0.08.
pK_a values of His 153 not shown (see text).
* tentatively assigned

5.2.3 The pH dependence of k_{cat} for R57K DHFR

k_{cat} values for wild-type DHFR and the R57K mutant were measured over the pH range 5.2-8.6 and the results are shown in Figure 5.5. The Arg 57→Lys substitution has little effect on the rate of catalysis: $22s^{-1}\pm0.4$ in wild-type DHFR compared with $20s^{-1}\pm0.6$ in the R57K mutant. However, the R57K mutation does decrease the apparent pK_a of k_{cat} from 7.3±0.1 (wild-type DHFR) to 6.7±0.06 in the mutant.

Figure 5.5 pH dependence of k_{cat} for wild-type DHFR and the R57K mutant

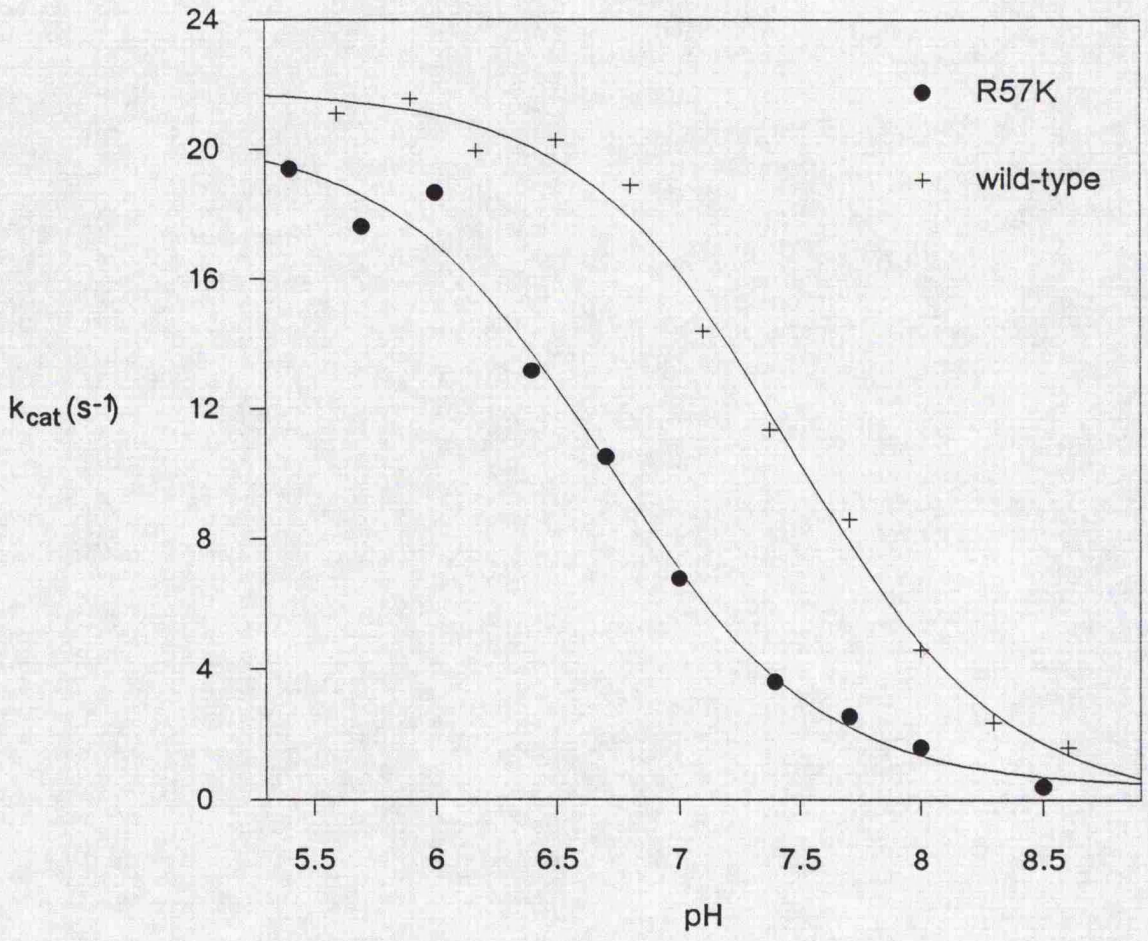

5.3 DISCUSSION

5.3.1 Structural effects of the R57K mutation

Initial studies to characterise the effects of the R57K mutation in *L.casei* DHFR have been carried out (J.A. Thomas and M.G. Casarotto, personal communication). NMR studies on the R57K-MTX binary complex have shown that the structural effects of the conservative Arg 57→Lys mutation are quite widespread, some occurring more than 10Å away from the mutation site (see Figure 5.6; M.G. Casarotto, personal communication). Residues with chemical shift differences greater than 0.2 ppm (when compared to the wild-type enzyme) are marked in red in Figure 5.6 and include Arg 31, Val 35, Glu 56 and Thr 58, with the latter two adjacent to the mutation site. Smaller (between 0.05 and 0.2 ppm) more widespread chemical shift differences (coloured in purple in the figure) belong to residues contained in some of the strands of the β-sheet network and in Helix B. The other predominant effect of the R57K mutation is upon residues that are part of Helix B (23-34). Although Arg 57 is itself not part of this helix, the γ-carboxylate of MTX (and substrates) does form an ion-pair interaction with His 28 in this helix (Filman *et al.*, 1982). The structural changes that have occurred as a result of the R57K substitution are most likely due to the interaction between the new Lys 57 and the α-carboxylate of MTX. In order for the shorter (by approximately one C-C bond length) sidechain of Lys to maintain an ion-pair interaction with MTX, it may be necessary to exert a "pull" on the rest of the inhibitor molecule. Consequently, residues which are involved in binding or in close proximity to the inhibitor may also be affected; this is reflected by a difference in their chemical shift values. However, the structural perturbations of the R57K mutation have been shown to have no effect on the binding of substrates, inhibitors and coenzyme NADPH (J.A. Thomas, personal communication).

Figure 5.6 Residues affected by the R57K mutation in the R57K-MTX binary complex.

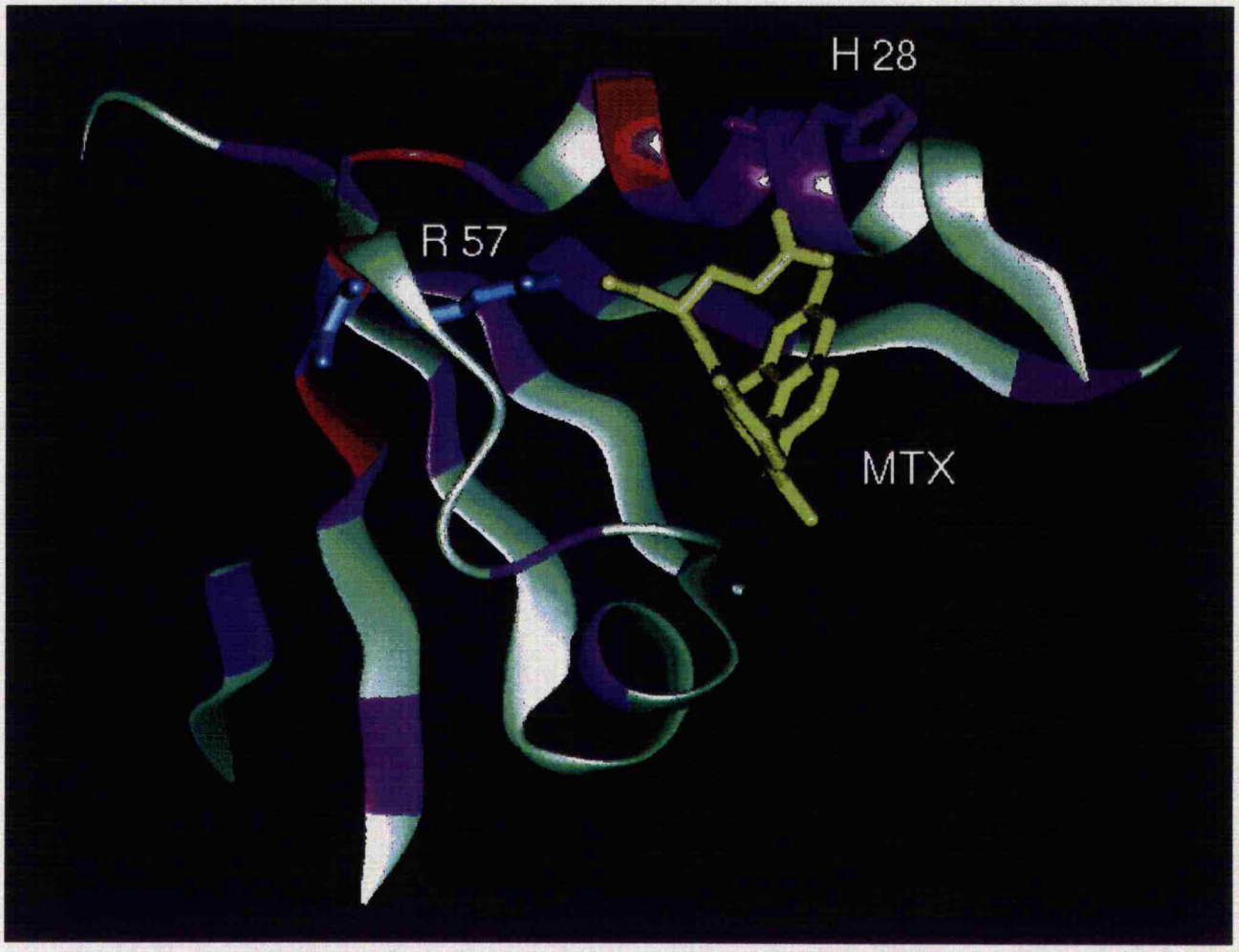

Residues whose chemical shifts differ by greater than 0.2 ppm when compared to the wild-type-MTX complex are coloured in red, those that differ by 0.05-0.2 ppm are marked in purple. The substituted residue is coloured in blue and the inhibitor MTX is coloured in yellow.

5.3.2 Binding of MTX analogues to R57K DHFR

Although the Arg 57→Lys substitution results in structural changes in the R57K-MTX complex, a direct comparison with effects on the binding constant of MTX cannot be made since it still binds very tightly to R57K DHFR (K_d less than 1nM). The interaction between His 28 and the γ-carboxylate of MTX is still maintained in the R57K-MTX binary complex as judged by the characteristic increase in the pK_a of His 28 (see Table 5.4). The results suggest that although there are minor structural changes around this region in the R57K-MTX complex they have not significantly affected the His 28-MTX-γ-carboxylate interaction.

Table 5.4 Interactions and pK_a values of His 28 in enzyme-MTX and enzyme-MTX-α-amide complexes.

Complex	Interaction of γ-carboxylate with His 28	pK_a of His 28
Wild-type alone[a]	N/A	6.67±0.04
Wild-type-MTX	✓	7.56±0.03
R57K-MTX	✓	7.45±0.04
Wild-type-MTX-α-amide	x	6.68±0.03
R57K-MTX-α-amide	✓	7.48±0.04[b]

[a]From Antonjuk *et al.*, 1984

[b] tentatively assigned

The mutation has actually increased the binding of MTX-α-amide to R57K DHFR when compared to the wild-type enzyme (by a factor of 5). In the wild-type DHFR-MTX-

α-amide complex it is known that both Arg 57 and His 28 ion-pair interactions are broken and that the whole of the *p*-aminobenzoyl glutamic acid (PABG) moiety binds differently (Antonjuk *et al.*, 1984). The increase in the pK_a value of His 28 in the R57K-MTX-α-amide complex (compared with the equivalent wild-type complex) suggests that the interaction between His 28 and the γ-carboxylate of MTX is present in the mutant complex. Although it is not possible to unambiguously assign His 28 in this complex, all three possible candidates have pK_a values greater than 7.28. The α-amide analogue binds 8-fold tighter to the R57K mutant than does the αγ-diamide analogue. These results again point to an interaction between inhibitor and His 28 in the R57K-MTX-α-amide complex. This is not the case with the wild-type enzyme where the binding of α-amide and αγ-MTX-diamide is equivalent since in both these complexes the γ-carboxylate interactions have been broken.

In the wild-type DHFR-MTX-α-amide complex it may be unfavourable contacts between the carboxamide of MTX-α-amide and the enzyme that resulted in a change in the mode of binding of this analogue. The shorter sidechain of Lys 57 in R57K DHFR may avoid these unfavourable contacts and hence maintain the interaction with His 28. In order to determine how the PABG moiety binds in the mutant, a more detailed structural analysis of this complex will be required.

It is interesting to note that the binding constants of MTX-α-amide and MTX-γ-amide to the R57K mutant (pH 6.5) are identical. If in both cases only the individual ion-pair interactions have been "blocked" and the rest of the inhibitor molecule binds in the same way, then these results may suggest that the α and γ carboxylate interactions make a comparable contribution to the overall binding energy. A similar conclusion was reached by Antonjuk *et al.* (1984) albeit with some degree of uncertainty because of the difference in the mode of binding of MTX-α-amide to wild-type DHFR.

The binding constant of MTX-γ-amide to R57K DHFR is 40-fold greater than that to wild-type DHFR at high pH. The binding of the γ-amide analogue to the R57K mutant

appears to be more pH dependent than to the wild-type enzyme although the results have to be interpreted cautiously due to the inability of calculating accurate K_d values at low pH. If correct, and because the effect is seen only in the R57K mutant the pH dependence could be due to ionisation of the new Lys 57. When the Lys sidechain is protonated it forms an ionic interaction with the α-carboxylate of MTX-γ-amide. Loss of the positive charge on Lys 57 at high pH results in weaker binding of the analogue to R57K DHFR compared to wild-type DHFR. A similar result has been observed with the equivalent mutant of human DHFR (R70K, Arg 70 due to the different numbering system; Thompson and Freisheim, 1991). The binding of both MTX and the substrate FH_2 to R70K DHFR were reduced approximately 12-fold over the pH range 7 to 8.5; there was no change in the binding constant of these ligands to wild-type human DHFR over the same pH range. From the pH dependence of K_d (MTX or FH_2) to R70K DHFR an approximate pK_a for Lys 70 was calculated to be 8.3. It was suggested that the relatively low pK_a value for the ε-amino group of Lys 70 was due to the hydrophobic nature of the environment this residue is present in. Analogous pH studies on the *L.casei* R57K mutant and direct measurement of the pK_a of Lys 57 by NMR will hopefully allow us to calculate a pK_a value for this residue.

5.3.3 The pH dependence of k_{cat} for R57K DHFR

Work carried out in this thesis and previous experiments (J.A. Thomas, personal communication) have shown that the Arg 57→Lys substitution has no effect on the rate of catalysis but the apparent pK_a that describes k_{cat} is 0.6 pH units lower in the R57K mutant. With wild-type DHFR, the pK_a value obtained from a plot of k_{cat} against pH is an apparent one which arises from a change in rate-limiting step in going from product dissociation at low pH to hydride ion transfer at high pH (Fierke *et al.*, 1987, Andrews *et al.*, 1989 and see section 3.3.3 of the D26N DHFR chapter). Thus, a change in the apparent pK_a value of k_{cat} for R57K DHFR could be due to the mutation having an effect on either of these processes. Since the rate of catalysis and the size of the deuterium isotope effect (J.A. Thomas unpublished work) at low pH (where product dissociation is the major rate-limiting step)

are similar in the wild-type and in the mutant, the results suggest that it is unlikely that the rate of FH_4 dissociation has been affected by the mutation.

It is possible therefore that the shift in pH dependence of k_{cat} for R57K DHFR is due to an effect on the pK_a of the group controlling hydride ion transfer. This group has been postulated to be Asp 26, or taking into account recent work from this laboratory, possibly a group on the substrate. However, what is clear is that the group responsible is at the pteridine ring binding site which is more than 10Å away from the site of the mutation. The Arg 57→Lys substitution may exert its effect on k_{cat} through structural changes or by long-range electrostatic effects. It is plausible for instance that conformational effects of the R57K mutation may be transmitted to the pteridine ring binding pocket principally via Helix B and this may in turn affect the pK_a of the group controlling hydride ion transfer. Theoretical studies have shown that the binding of FH_2 to DHFR is accompanied by a shift in electron density from the pteridine ring to the glutamic acid moiety of the substrate and that this could be important in the reaction mechanism of the enzyme (Bajorath *et al.*, 1991a, 1991b). Arg 57 was postulated to be one of three positively charged residues (localised at the glutamic acid binding site) that is responsible for this effect.

5.4 SUMMARY

The replacement of Arg 57 by Lys in DHFR has no effect on the binding of substrates, inhibitors (MTX and TMP) or the coenzyme NADPH. The binding of MTX-α-amide to wild-type DHFR is accompanied by the loss of both the Arg 57-α-carboxylate and His 28-γ-carboxylate interactions. This is not the case with R57K DHFR where the tighter binding of the MTX-α-amide analogue is a result of regaining the His 28-γ-carboxylate interaction. At pH 8 the binding constant of MTX and its analogues to the R57K mutant is 40-fold greater than that to the wild-type enzyme. This weaker binding may be due to the difference in binding energy between the interaction of the α-carboxylate of MTX and a charged Lys 57 sidechain in the R57K mutant and that to a charged Arg 57 guanidinium group in the wild-type.

The rate of catalysis of R57K DHFR is similar to that of the wild-type enzyme but the pK_a describing the pH dependence of k_{cat} is lower by 0.6 units compared to wild-type DHFR. The mutation has thus had an effect on the group responsible for the pH dependence of catalysis. This may arise from an electrostatic effect of the Arg 57→Lys substitution which could affect the electron distribution around the pteridine ring. Alternatively, the effect may arise from structural changes at the pteridine ring binding site which have been transmitted via Helix B from the site of the mutation; there is some NMR evidence for this.

CHAPTER 6 GENERAL DISCUSSION

Before the technique of site-directed mutagenesis became available to the enzymologist, the functional role of an amino acid in a protein was deduced mainly from chemical modification of the protein. For example, studies on the chemical modification of tryptophans (Liu and Dunlap, 1974; Freisheim *et al.*, 1977; Reddy *et al.*, 1978; Thomson *et al.*, 1980), arginines (Vehar and Freisheim, 1976) and histidines (Greenfield, 1974) amongst others have been reported on DHFR from a variety of different species. Such studies were particularly informative if the structure of the protein was available to help identify which particular modified residue(s) were responsible for the change in ligand binding and/or catalysis. Additionally, groups on the substrate important in interacting with the enzyme have been defined by the use of substrate analogues. However, there were major drawbacks with these approaches: experiments were limited to modifying aminoacids for which chemical reactions were available. Modification was generally not specific, and where possible, it was often difficult to stop side reactions occurring and to separate the modified enzyme from the native enzyme. Particular caution had to be used when interpreting the results obtained with such "mutant" enzymes since chemical modification almost inevitably led to an increase in the bulk of a residue often distorting the local structure of the protein. In the case of substrate modification, it is necessary to ensure that the analogue binds to the protein in a similar manner to the parent molecule, if the data are to be meaningfully interpreted. With DHFR for example, MTX a close structural analogue of FH_2 binds with its pteridine ring in an inverse orientation to that of the substrate (see Section 1.2 of the Introduction chapter).

The more traditional methods for the elucidation of the structure-function relationship of a protein have acted as a basis for, and been extended by, the technique of site-directed mutagenesis which overcomes many of the inherent problems associated with the chemical modification approach. The advent of this technique meant that for the first

time any desired mutation could be introduced into a protein at a specific location. Structural and kinetic characterisation of the resulting mutant provides a unique opportunity to answer questions regarding the basis of substrate specificity and to rigorously test hypothetical mechanisms that have been put forward for the manner by which an enzyme catalyses a particular reaction.

Most site-directed mutagenesis work has focused on enzyme systems for which a detailed knowledge of structural, biochemical and kinetic data is available. Examples include the serine proteases subtilisin and trypsin, tyrosine tRNA synthetase, triosephosphate isomerase and lactate dehydrogenase (for reviews see Shaw, 1987; Knowles, 1987; Knowles, 1991; Leatherbarrow and Fersht, 1986; Fersht and Leatherbarrow, 1987; Rutter *et al.*, 1987; Wells and Estell, 1988, Clarke *et al.*, 1989). It is not surprising therefore, that DHFR was also one of the first enzymes targeted for site-directed mutagenesis (Villafranca *et al.*, 1983), the *E.coli* D27N and D27S DHFRs amongst the first mutants to have their structures determined (Howell *et al.*, 1986). Examination of these mutant structures helped to reinforce the idea that conservative substitutions could be tolerated in proteins and usually only resulted in local minor structural perturbations. However, this should not be taken for granted and the need to confirm the overall structural integrity of a mutant is critical if meaningful deductions are to be made.

Obtaining structural information by X-ray crystallography can sometimes be a rate-limiting step (for instance due to the inability of obtaining good quality crystals) when characterising a mutant. NMR is the other major technique for structure determination. We are in a very fortunate position working on DHFR from *L.casei* since many of the assignments on this reductase have been made (Hammond *et al.*, 1986, Birdsall *et al.*, 1990, Carr *et al.*, 1991 and Soteriou *et al.*, 1993). This means that a direct comparison of wild-type and mutant spectra enables the structural effects of a substitution to be conveniently and quickly assessed. In conjunction with this, elucidation of the complete kinetic scheme for DHFR allows us to determine the effects of the mutation on individual rate constants,

such as the rate of hydride ion transfer and association and dissociation rate constants for ligand binding. This is critical if the functional effects of a mutation are to be correctly defined and the role of a particular residue in a protein to be accurately assessed (see the example of the *L.casei* T63A mutant discussed below). With DHFR, for example, a number of mutations have resulted in a change in the rate-limiting step that governs catalysis (see Section 1.7 of Introduction chapter). Such a change can be readily identified by carrying out steady state isotope effect experiments, and if necessary, followed by direct measurement of appropriate rate constants using pre-steady state kinetic methods.

In wild-type DHFR from *L.casei* the sidechain of Thr 63 forms a hydrogen bond to the 2'-phosphate of NADPH (Filman *et al.*, 1982); the importance of this interaction was probed by replacing the Thr with an Ala (T63A; Thomas *et al.*, 1994). The T63A mutant bound NADPH 600-fold more weakly than the wild-type enzyme, a contribution of some 3.8 kcal/mol to the overall binding energy. However, closer analysis by pre-steady state measurements revealed that the reduced binding of NADPH was due, in part, to a 90-fold decrease in the association rate constant. The mutation causes some sort of conformational change in the apoenzyme (as yet undefined) that "hinders" and therefore slows down the binding of NADPH. This example demonstrates that a lack of detailed analysis on the T63A mutant could have led to a misinterpretation of the effects of the substitution.

The distinct advantage of having at our disposal both NMR and kinetic methods for characterising mutants of *L.casei* DHFR is clear, and has been seen with various mutants. For example, the effects of the Asp 26→Asn mutation on catalysis can be attributed specifically to the substitution, and not to any widespread structural perturbations. Direct measurement of the pK_a of Asp 26 and identification of the tautomeric forms of the substrate in the relevant enzyme complexes will hopefully provide further insight into the catalytic mechanism of DHFR. The advantage of using both NMR and kinetic data to determine pK_a values of particular species has been seen with both W21H and D26N mutants. With W21H DHFR for example, both methods have indicated that His 21 could be

one of the groups responsible for the unusual form of the pH dependence of activity observed with this mutant. NMR has demonstrated that in the W21L DHFR-NADPH complex, the nicotinamide ring adopts a slightly different orientation to that in the wild-type complex (Birdsall *et al.*, 1989a). This may offer an explanation for the reduction in the rate of hydride ion transfer observed in this mutant (Andrews *et al.*, 1989). In binding studies the tighter binding of a MTX analogue to R57K DHFR when compared to the wild-type enzyme suggested, and was confirmed by NMR, to be due to a regain of the His 28-γ-carboxylate interaction. These examples illustrate the benefits of using both techniques in mutant characterisation.

Over the past decade site-directed mutagenesis has advanced our knowledge of DHFR both in terms of residues important in catalysis and substrate specificity, as well as identifying regions of the protein that may be involved in cooperativity. In terms of gaining further insight into the catalytic mechanism of DHFR, results obtained on the active site Asp 26 mutant of the *E.coli* enzyme (Howell *et al.*, 1986) and now of the *L.casei* enzyme seriously question the unique role of this Asp as the proton donor in the reaction catalysed by these bacterial enzymes. As yet no mutants of the analogous Glu residue found at this position in mammalian DHFRs have been reported. In the light of these results some of the postulated mechanisms for catalysis need to be reassessed. The possibility of direct protonation from solvent, the importance of the orientation of active site water molecules and/or enolisation of the substrate molecule will have to be examined further.

A mutant of *E.coli* glutathione reductase has given similar results to those obtained with Dihydrofolate reductase. His 439 is present in the glutathione binding site of *E.coli* glutathione reductase and has been suggested to act as the proton donor/acceptor in the catalytic mechanism (Deonarain *et al.*, 1989, Berry *et al.*, 1989). Substitution of His 439 by a Gln (H439Q) resulted in a mutant that had 1% of the activity of the wild-type enzyme and suggests that a protonatable sidechain at this position is not absolutely essential for activity. The His 439→Ala mutant had comparable activity to H439Q and thus it was concluded that

the residual activity of H439Q was not due to the ability of the Gln residue to hydrogen bond to a water molecule which could then protonate the substrate. It was concluded that the imidazole sidechain of His 439 probably acts a proton donor/acceptor in the wild-type enzyme, and this accounts for the 100-fold increase in catalytic rate compared with the mutants. In the mutants however, protonation was probably directly from solvent (this part of the active site has a relatively open structure), or they recruit an alternative proton donor (identity unknown) for activity, albeit inefficiently.

Results obtained on the *L.casei* Trp 21 DHFR mutants (W21L and W21H) and the equivalent Trp→His mutant from the *E.coli* enzyme suggest that this residue may be critical in the correct alignment of the NADPH nicotinamide ring for efficient hydride ion transfer to the substrate (Andrews *et al.*, 1989, Birdsall *et al.*, 1989a, Warren *et al.*, 1991). Reduction in the rate of hydride ion transfer has also been observed in an *E.coli* DHFR deletion mutant of a mobile loop ("teen" loop; residues 13-21 in *L.casei* DHFR and 9-24 in *E.coli* DHFR) which this Trp residue is a part of (Li *et al.*, 1992, Falzone *et al.*, 1994). Residues 16-19 of this loop are disordered in crystal structures of apoDHFR and when the enzyme is bound to $NADP^+$ (Bystroff *et al.*, 1990, Bystroff and Kraut 1991). However, they form a hairpin turn which folds over the nicotinamide and pteridine rings of $NADP^+$ and folate in the ternary complex (Bystroff *et al.*, 1990). Residues 16-19 have been deleted in *E.coli* DHFR and replaced with a Gly (DL1; Li *et al.*, 1992, Falzone *et al.*, 1994). In the DL1 mutant the K_m values for the substrates, the rate of FH_4 dissociation and pK_a of the pH dependence of hydride ion transfer (value of 6.2) are all similar to the wild-type enzyme. However, the substitution results in a dramatic decrease in the rate of hydride ion transfer from $950s^{-1}$ (wild-type) to $1.7s^{-1}$ (mutant) so that it is the major rate-limiting step in catalytic turnover. The authors suggest that the function of the mobile loop is in a form of transition state stabilisation whereby hydrophobic residues (possibly Ile 14 (conserved) and Met 20; conserved as either a Met or Leu in all DHFRs) are recruited into the active site for the correct alignment of substrate and coenzyme rings for optimal hydride ion transfer. Met

20 has also been implicated in transition state stabilisation in the catalytic mechanism proposed by the Kraut group (see Section 1.6 of the Introduction chapter).

Mobile loops close to the active site of enzymes have been reported to be important in the catalytic mechanisms of lactate dehydrogenase (Clarke *et al.*, 1986, Clarke *et al.*, 1989) and triosephosphate isomerase (Pompliano *et al.*, 1990, Knowles, 1991, Sampson and Knowles 1992a, 1992b). In lactate dehydrogenase (LDH) from *B.stearothermophilus*, binding of substrates causes a 13 residue (98-110) "loop" to close over the active site. Loop closure brings the conserved Arg 109 into the active site (a movement of some 8Å) so that it is within hydrogen bonding distance of the substrate carbonyl and the catalytic His 195. The role of this Arg was probed by substituting it with a Gln (Clarke *et al.*, 1986). The mutation increased the K_m for the substrate pyruvate by 30-fold and decreased k_{cat} by a factor of 420 when compared to the wild-type enzyme. There was also a change in rate-limiting step from a structural rearrangement of the enzyme-NADH-substrate complex (in the wild-type enzyme) to hydride ion transfer in the mutant. It was concluded that the role of Arg 109 was to polarise the carbonyl bond of the substrate and stabilise the transition state for pyruvate reduction.

Triosephosphate isomerase catalyses the interconversion of glyceraldehyde-3-phosphate and dihydroxyacetone phosphate via an enediol intermediate (Knowles, 1991). As with LDH, binding of substrate to Triosephosphate isomerase induces closure of a loop (residues 166-176) which forms a "lid" over the active site. The function of the loop was investigated by deleting four residues (170-173) that, when in the "closed" form interact with the substrate (Pompliano *et al.*, 1990). The deletion mutation causes a 10^5-fold drop in the rate of catalysis with very little effect on substrate binding. However, the binding of a reaction intermediate analogue, did decrease by some 200-fold when compared to the wild-type. The mutant appears to have lost its "grip" on the intermediate as demonstrated by the detection of decomposition products of the intermediate with the mutant (this is not

observed with the wild-type enzyme). From the results it was concluded that the function of loop closure is to stabilise and prevent loss of the intermediate in the isomerisation reaction.

Appropriate DHFR mutants have enabled us to start to identify regions of the protein that may provide the structural basis for negative cooperativity, a crucial feature of the kinetic mechanism of this enzyme. In wild-type DHFR the magnitude of the K_m/K_d (NADPH) ratio can be used as a measure of the degree of negative cooperativity (see the W21H DHFR chapter). It appears that substitutions at the NADPH nicotinamide and adenine ring binding sites of DHFR affect the K_m/K_d ratio i.e. the degree of negative cooperativity between NADPH and the product FH_4. The *L.casei* Trp 21 DHFR mutants and the *E.coli* DHFR loop deletion mutant have large effects on K_d but only minor effects on K_m (Andrews *et al.*, 1989, Li *et al.*, 1992). However, the converse is true for mutations at the adenine ring binding pocket. Arg 44 in *E.coli* DHFR (corresponds to Arg 43 in *L.casei* DHFR) and Thr 63 in *L.casei* DHFR both interact with the 2'-phosphate of NADPH at this site (Bolin *et al.*, 1982, Filman *et al.*, 1982). Substitution of Arg 44 for a Leu (R44L) in *E.coli* DHFR (Adams *et al.*, 1989) and Thr 63 for an Ala (T63A) in *L.casei* DHFR (Thomas *et al.*, 1994) have greater effects on the binding of the coenzyme in the ternary enzyme-NADPH-FH_4 complex than in the binary enzyme-NADPH complex (i.e. a larger effect on K_m than K_d for NADPH). These results have substantiated earlier NMR work on the *L.casei* DHFR-NADPH-folinic acid (analogue of FH_4) which provided some evidence for the involvement of these regions in negative cooperativity (Birdsall *et al.*, 1981a).

Evidence is accumulating that conserved residues in DHFR, quite distant from the pteridine ring binding site, contribute to catalysis. The R57K mutation in *L.casei* DHFR results in a 0.6 pK_a unit shift in the pH dependence of k_{cat}, although it is some 15Å away from the site of the substitution. NMR results have suggested that the effects may be transmitted via Helix B (M.G. Casarotto, personal communication and see the R57K DHFR chapter). Mutations of the conserved residues Leu 54 and Arg 44 (conserved as either an Arg or a Lys in all DHFRs) in *E.coli* DHFR, similar to the *L.casei* Arg 57→Lys

substitution, have shifted the pH dependence of k_{cat}; they also lead to a reduction in the rate of hydride ion transfer (Mayer *et al.*, 1986, Murphy and Benkovic 1989, Adams *et al.*, 1989). In all these instances it is postulated that there must be a structural change which alters the environment of the group responsible for the pH dependence of catalysis, although the site of the mutation is some 20Å away. A shift in the pH dependence of catalysis has also been observed in a mutant of subtilisin from *B.amyloliquefaciens* (Thomas *et al.*, 1985). When the surface residue Asp99 was substituted for a Ser, the mutation lowers the pK_a of the active site His (His 64) by 0.3 units, despite being 15Å away from the active site. In this case the change was due to electrostatic factors. The activity and K_m for the substrate were unaffected by the D99S mutation.

Site-directed mutagenesis of DHFR has started to give us an insight into the manner by which this small reductase relates its structure to function. Knowledge gained from this, and other enzyme systems will hopefully contribute significantly to our further understanding of protein molecules in general.

APPENDIX A

Sterilisation of all culture media and necessary solutions was carried out by autoclaving at 121°C for 20 minutes.

A.1 GROWTH AND MAINTENANCE OF STRAINS

All cultures were grown in Luria Bertini (LB) broth at 37°C in a shaking incubator unless stated otherwise. Overnight cultures were grown by inoculating 5ml of LB broth with the required bacterial strain.

Bacterial strains were stored in glycerol and prepared by adding 250µl of a 3 hour culture to 50µl of 80% glycerol, mixed and then rapidly frozen by using an ethanol/dry-ice bath. Glycerol stocks were stored at -70°C.

Bacterial strains:	**BL21(DE3)**	F^{-}*ompT*($r_B^{-}m_B^{-}$)
	TG1	*sup*E*hsd*Δ5*thi*Δ(*lac-proAB*) F'[*traD*36*proAB*$^{+}$*lacI*^{q}*lacZ*ΔM15]
Culture media:	**LB broth**	10g tryptone, 5g yeast extract, 10g NaCl Dissolved in 1 litre of distilled water and autoclaved.
	2YT broth	16g tryptone, 10g yeast extract, 5g NaCl Dissolved in 1 litre of distilled water and autoclaved.

A2. PLASMID DNA PREPARATION AND PURIFICATION

A2.1 Purification of DNA using the Promega Magic™ DNA Purification System

For large scale plasmid DNA preparation, an overnight culture of *E.coli* BL21(DE3) harbouring the pET11a/DHFR plasmid was grown and used to inoculate 500ml of 2YT

media. The culture was grown in the presence of 100μg/ml ampicillin at 37°C for 5 hours. The cells were harvested by spinning at 10,000 rpm for 10 minutes and plasmid DNA purified from the pellet using the Promega Magic™ Maxipreps DNA purification system according to the manufacturer's protocol.

For smaller scale DNA preparations (plasmid and replicative form (RF) M13 DNA) a 3ml overnight culture of bacterial cells was spun down in a microcentrifuge and the DNA purified using the Promega Magic™ Minipreps DNA purification system. In both cases the purified DNA was stored at -20°C until required. The concentration and purity of the DNA was determined by absorbance spectroscopy as outlined below.

A2.2 Determination of DNA concentration and purity by absorbance spectroscopy

The concentration of DNA was determined by measuring the absorbance at λ=260nm (A_{260}):

Concentration of double stranded DNA = A_{260} x 50μg/ml
Concentration of single stranded DNA = A_{260} x 40μg/ml

DNA purity was assessed by calculating the A_{260}:A_{280} ratio; DNA with a ratio of greater than 1.8 was deemed pure.

A2.3 Purification of DNA by phenol/chloroform extraction

Contaminating proteins can be removed from DNA preparations by performing a phenol/chloroform extraction. Organic solvents such as phenol and chloroform will precipitate proteins (which form a coagulated mass at the organic solvent-aqueous solution interface) but leave nucleic acids in solution.

An equal volume of phenol/TE (Tris-EDTA) buffer was added to the DNA solution, mixed by vortexing for 20 seconds and then spun for 5 minutes in a microcentrifuge. The

aqueous phase (top layer) containing nucleic acids was removed and transferred to a new microcentrifuge tube. Remaining traces of phenol were removed by the addition of an equal volume of chloroform/isoamyl alcohol (24:1). The solution was mixed by vortexing, spun for 5 minutes and the aqueous phase (top layer) transferred to a fresh tube. Any final traces of chloroform/isoamyl alcohol were removed by drying the sample under vacuum. The DNA in solution was then concentrated by ethanol precipitation.

A2.4 Concentration of DNA by ethanol precipitation

The volume of the DNA solution to be concentrated was measured and 0.1 volumes of 3M sodium acetate pH 5.2 added and mixed by vortexing. Two volumes of ice cold ethanol were added, mixed by vortexing and the sample incubated at -20°C for 15 minutes during which time the DNA would be precipitated. The DNA was recovered by spinning the sample for 15 minutes in a microcentrifuge. The supernatant was carefully discarded and any final traces of ethanol were removed by drying the pellet under vacuum. The DNA pellet was dissolved in the desired volume of water and stored at -20°C.

A2.5 Purification of DNA using the GeneClean™ kit

The GeneClean™ protocol has been developed for the isolation and purification of DNA. The procedure involves the use of a silica matrix (GLASSMILK™) which, in the presence of salt binds DNA. Proteins and most RNA molecules do not bind to the matrix and are removed during the wash stages of the protocol. DNA is then eluted from the matrix with water. The GeneClean™ kit was used to purify DNA during sequential restriction digests (for removal of proteins and to allow a change of buffer), and whenever it was necessary to isolate and purify DNA from agarose gels. The kit was used according to the manufacturer's protocol.

A3. RESTRICTION DIGESTION REACTIONS

All reagents were kept on ice with the exception of the restriction enzymes which, due to their instability were kept at -20°C until just before use.

2-6 μg of DNA, 3μl 10x restriction buffer and water to give a final reaction mix volume of 30μl were transferred to a microcentrifuge tube. 15 units of restriction enzyme (10 units/μl) were added, the solution mixed gently and then incubated for 3 hours at 37°C to enable the digestion to proceed.

Whenever sequential restriction digests were carried out, the DNA was cut with the first restriction enzyme (as outlined above), purified using the GeneClean™ protocol (section A2.5) and then digested with the second restriction enzyme. Double digests (the addition of both restriction enzymes together) were carried out using 4μl of 10x "Buffer H" as the restriction buffer, 15 units of each enzyme and the final volume of the reaction mixture was kept at 40μl.

When the digestion reaction was complete, the products of the digest were analysed by agarose gel electrophoresis.

Buffers:	**10x BamHI buffer**	200mM Tris-HCl pH 8.5, 100mM $MgCl_2$, 10mM dithiothreitol, 1M KCl
	10x XbaI buffer	100mM Tris-HCl pH 7.5, 100mM $MgCl_2$, 10mM dithiothreitol, 500mM NaCl, 0.1% BSA
	10x Buffer H	500mM Tris-HCl pH 7.5, 100mM $MgCl_2$, 10mM dithiothreitol, 1M NaCl

A4 PREPARATION AND RUNNING OF AGAROSE GELS

In order to analyse the products of restriction digests, and subsequently purify the required DNA, the restriction digest mixture was run out on a 1.5% agarose gel.

0.75g of Miles agarose was added to 50ml of TAE (Tris/Acetate/EDTA) buffer and the solution heated in a microwave oven until all the agarose had dissolved. The agarose solution was allowed to cool slightly before the addition of 5µl of a 10mg/ml solution of ethidium bromide (final concentration of 1µg/ml). The agarose was then poured into a gel casting tray that had been sealed with autoclave tape and fitted with a 10 well comb. The gel was left to set (usually for 20 minutes) after which time the comb and the autoclave tape were removed. The cast gel was placed into an electrophoresis tank and enough TAE buffer added to submerge the gel.

2µl of agarose dye mix (40% sucrose, 100mM Tris-HCl pH 7.5, 1mM EDTA, 0.05% bromophenol blue, 0.05% xylene cyanol FF) was added to 20µl of the DNA sample, mixed and loaded into a well of the gel. 1µg of λ DNA that had been cut with the restriction enzyme HindIII was also loaded onto each gel. The products of the digested λ DNA produce a series of DNA fragments that can be used as standard molecular weight markers. The smallest fragment produced by the λ DNA/HindIII digest is 564 bp in size and hence acts as a good marker for the DHFR gene which is 558 bp in size. The gel was run at 100V for 45 minutes or until the faster dye front had migrated two-thirds the length of the gel. The gel was removed from the tank and the DNA visualised under ultraviolet light.

Buffer:	**50x TAE buffer**	2M Tris base, 50mM EDTA (Na salt), 1M Acetic acid

A5 LIGATION OF THE DHFR GENE INTO VECTOR DNA

For the ligation reaction a 1:3 molar ratio of vector DNA (RF M13 or plasmid) to DHFR insert was used.

1ng of vector DNA, 30-40ng of insert and 4µl of 5x DNA ligase buffer were placed into a microcentrifuge tube. 1µl of T4 DNA ligase (10 units/µl) was added, and the solution mixed gently (final reaction volume was kept at 20µl). The reaction mixture was incubated at 16°C for 16 hours and then either used immediately to transform competent *E.coli* TG1 cells or stored at -20°C until required.

Buffer:	**5x T4 DNA ligase buffer**	250mM Tris-HCl pH 7.5, 5mM ATP, 50mM $MgCl_2$, 50mM dithiothreitol, 2.5% BSA

A6 PREPARATION AND TRANSFORMATION OF COMPETENT *E.coli* CELLS

In order for cells to be transformed with DNA (plasmid or phage) the cells must be made competent. One method for achieving this is by treating cells with ice-cold $CaCl_2$ followed by brief heating which induces a transient state of "competence". During this period bacteria can take up foreign DNA. The procedure is outlined below.

A6.1 Preparation of competent *E.coli* TG1 cells using calcium chloride ($CaCl_2$)

50µl of a fresh overnight culture of *E.coli* TG1 cells was used to inoculate 50ml of LB broth. The culture was grown at 37°C until OD_{595} was 0.5 (approximately 2 hours). The cells were transferred aseptically to a sterile, ice-cold 50ml polypropylene (Falcon™) tube. 3ml of the culture was removed and kept at 4°C (to be used as a source of host cells for plating out later). The cells were harvested by centrifuging at 3000 rpm for 10 minutes. All the supernatant was carefully discarded and the pellet gently resuspended in 5ml ice-cold

0.1M sterile $CaCl_2$ solution. The cells were kept on ice for 40 minutes and then harvested as above. The supernatant was removed and the pellet resuspended in 1ml of ice-cold 0.1M $CaCl_2$ solution.

A6.2 Transformation of competent *E.coli* TG1 cells

20µl of the DNA ligation reaction mix (i.e. the DNA to be transfected) was added to 300µl of competent cells, mixed by gentle swirling and stored on ice for 30 minutes. The cells were "heat-shocked" by incubating them at 42°C for 45 seconds and then returned to ice for 5 minutes.

Duplicate sets of tubes containing 1µl, 10µl, 50µl and 100µl of the transformed competent cells were set up. To each tube the following solutions were added:

4µl	20% IPTG (final concentration of 1mM)
200µl	*E.coli* host TG1 cells
4ml	top agar
16µl	X-gal (50mg/ml)

Each solution was mixed by gentle swirling and then poured onto an LB-agar plate. The plates were incubated overnight at 37°C to allow for the formation of plaques (usually 24 hours). Plates were stored at 4°C until the phage DNA (double and single stranded) was to be isolated.

A6.3 Preparation and transformation of competent *E.coli* BL21(DE3) cells

The preparation and transformation of *E.coli* BL21(DE3) cells was as for TG1 cells with the following modifications:

i) 50µl of an overnight culture of *E.coli* BL21(DE3) cells was used to inoculate 25ml

of 2YT media instead of LB broth.

ii) After the cells had been transformed with DNA (i.e. left on ice for 30 minutes and then heat shocked at 42°C for 45 seconds), 700µl of 2YT media (prewarmed to 37°C) was added, mixed by gentle swirling and then incubated at 37°C for 40 minutes. Cells were then plated out on LB/ampicillin agar plates in 50µl, 100µl and 150µl aliquots and incubated at 37°C overnight.

Reagents:	**Top agar**	10g tryptone, 8g NaCl, 8g Agar Dissolved in 1 litre of distilled water and autoclaved.
	LB-agar plates	LB broth + 1.5% agar (for LB/ampicillin agar plates add 100µg/ml ampicillin)
	IPTG	20% solution, filter sterilised
	X-gal	2% solution made up in dimethylformamide, stored at -20°C wrapped in foil

A7 PREPARATION OF BACTERIOPHAGE M13 DNA

Bacteria infected with bacteriophage M13 will contain the double stranded replicative form (RF) of M13 DNA and will produce virus particles that contain single stranded DNA. Both forms of M13 DNA can be isolated from small scale cultures of infected bacteria.

50µl of a fresh overnight culture of *E.coli* TG1 cells was used to inoculate 5ml of 2YT media and grown for 3 hours at 37°C. 50µl of this culture and a single plaque (picked from a fresh plate) were used to inoculate a further 5ml of 2YT media. The infected culture was grown at 37°C for 5 hours and then spun down for 5 minutes at 13,000 rpm and the supernatant transferred to a new tube. The infected bacteria which carry the RF M13 DNA will form a pellet at the bottom of the tube, whereas the supernatant will contain M13 phage

particles (single stranded M13 DNA). Single and double stranded DNA was then prepared as outlined below.

A7.1 Preparation of RF M13 DNA

Double stranded (RF) M13 DNA was isolated and purified from infected bacterial cells using the Promega Magic™ Minipreps DNA purification system. The DNA was further purified by phenol/chloroform extraction and then ethanol precipitated.

A7.2 Preparation of single stranded M13 DNA

The supernatant containing M13 phage was transferred to a new microcentrifuge tube and the phage particles precipitated by the addition of 200µl of 20% PEG 6000 in 2.5M NaCl, mixed by vortexing and left at room temperature for 15 minutes. The precipitated phage were pelleted by centrifuging at 13,000 rpm for 5 minutes and the supernatant discarded. Any remaining traces of PEG/NaCl were removed by spinning for a further 2 minutes and blotting the pellet with tissue paper.

The pellet was resuspended in 100µl of TE buffer pH 8 by vortexing for 30 seconds. RNA was removed by the addition of RNase A to a final concentration of 50µg/ml and incubated at 37°C for 30 minutes. Contaminating proteins were removed by the addition of 50µl of phenol/TE, mixed by vortexing and then incubated at room temperature for 15 minutes. The tube was vortexed again and then centrifuged for 3 minutes in a microcentrifuge. The aqueous solution (top layer) containing the DNA was transferred to a new microcentrifuge tube and 10µl of sodium acetate (3M, pH 5.2) added and mixed by vortexing. 250µl of ice-cold ethanol was added and the sample incubated at -20°C for 30 minutes. The DNA was precipitated by centrifuging (15 minutes at 13,000 rpm) and most of the supernatant discarded. The pellet was washed with 500µl of 70% ethanol and then vacuum dried.

The pellet was resuspended in 100µl of water, centrifuged for 5 minutes and the supernatant transferred to a new tube. The amount of purified single stranded M13 DNA present was determined by measuring the A_{260} (see A2.2). The DNA was stored at -20°C until required.

Buffer: **TE (Tris/EDTA) buffer** 10mM Tris-HCl pH 8, 1mM EDTA

A8 MUTAGENESIS OF DHFR

Mutagenesis of the DHFR gene was carried out using the Amersham Oligonucleotide-directed *in vitro* Mutagenesis system (version 2.1)™.

1. Purification and 5' phosphorylation of mutant oligonucleotides

Mutant oligonucleotides were purified by ethanol precipitation and their concentrations determined by absorbance spectroscopy.

3µl of 10x kinase buffer, 2.5µl (0.05 nmoles) of mutant oligonucleotide and 2 units of T4 polynucleotide kinase were mixed in a microcentrifuge tube and the volume made up to 30µl with water. The reaction mixture was incubated at 37°C for 15 minutes and then heated at 70°C for 10 minutes to inactivate the enzyme. The reaction mix was then either used in the annealing reaction (see below) or stored at -20°C until required.

2. Annealing the mutant oligonucleotide to single stranded M13 DNA template

For the annealing reaction a 1:1 molar ratio of template DNA to oligonucleotide primer was used:

3.5µl of Buffer 1, 5µg of recombinant single stranded M13 template DNA and 4 pmoles of phosphorylated mutant oligonucleotide were pipetted into a microcentrifuge tube,

mixed and the volume made up to 17µl with water. The annealing mixture was incubated at 70°C for 3 minutes (to denature any regions of secondary structure), and then incubated at 37°C for 30 minutes to allow annealing to occur. The sample was placed on ice until the next stage of the protocol.

3. Synthesis and ligation of mutant DNA strand

5µl of $MgCl_2$, 19µl of Nucleotide mix 1 and 6µl of water were added to the annealing reaction mix. 6 units each of Klenow DNA polymerase and T4 DNA ligase were added and the solution mixed. The reaction mixture was incubated at 16°C overnight.

4. Removal of single stranded (non-mutant) DNA

Single stranded non-mutant (template) DNA was removed by the use of disposable nitro-cellulose filter units supplied with the kit. Only single stranded DNA binds to the nitrocellulose membranes and centrifugation of the filter unit allows the separation of single stranded and double stranded DNA molecules.

170µl of water and 30µl of 5M NaCl were added to the polymerisation reaction and mixed. The sample was transferred to a filter unit and the double stranded DNA collected by centrifugation at 1500 rpm for 10 minutes. Any remaining double stranded DNA was washed through by adding 100µl of 0.5M NaCl and respinning for a further 10 minutes. The double stranded DNA was ethanol precipitated, the pellet dried under vacuum and then resuspended in 25µl of Buffer 2.

5. Nicking of the non-mutant DNA strand using NciI

10µl of the filtered DNA sample was added to 65µl of Buffer 3 and 5 units of NciI. The solution was mixed and then incubated at 37°C for 90 minutes.

6. Digestion of non-mutant DNA strand using exonuclease III

12µl of 500mM NaCl, 10µl of Buffer 4 and 50 units of exonuclease III were added to the reaction mix from (5) above, mixed and incubated at 37°C for 30 minutes. The reaction mixture was heated at 70°C for 15 minutes to inactivate the enzymes.

7. Repolymerisation, ligation and transformation of DNA

13µl of Nucleotide mix 2, 5µl of $MgCl_2$, 3 units of DNA Polymerase I and 2 units of T4 DNA ligase were added to the reaction mix from step 6. The solution was mixed and incubated at 16°C for 3 hours. 20µl of this DNA was then used to transform competent *E.coli* TG1 cells and recombinant plaques identified by α-complementation blue/white selection.

A9 SEQUENCING OF MUTANT DHFR GENES

DNA sequencing was carried out using the Sequenase® Version 2.0 kit and protocols.

A9.1 Primers

Two primers were used in the sequencing reactions:

1. ***Oligonucleotide 68***

Oligonucleotide 68 is a primer that anneals to the DHFR coding sequence in the region of bases 332-349. This oligonucleotide was used to read the first 260 bases of the DHFR gene which incorporates both mutation sites.

2. ***Oligonucleotide -40***

This is a "universal" primer used for the sequencing of bacteriophage M13 recombinant clones. It anneals to the polycloning region of M13mp19 DNA that flanks the insert and was used to read the DNA sequence from base 250 to the end of the DHFR gene.

A9.2 Sequencing reactions

All reagents were kept on ice with the exception of the enzyme Sequenase® Version 2.0 which, due to its instability, was kept at -20°C until just prior to use. A single annealing and labelling reaction was carried out, the reaction mixture was then divided into four and each reaction terminated by the appropriate ddNTP.

A9.2.1 Annealing template and primer DNA

A 1:1 molar ratio of primer to template DNA was used in the annealing reaction:

2µl of 5x Sequenase® buffer, 1µl of oligonucleotide primer (2.5ng) and 7µl of recombinant M13 DNA (1.2µg) were transferred to a microcentrifuge tube and mixed. The sample was heated at 65°C for two minutes and then allowed to cool to room temperature, during which time the annealing reaction takes place. Once the temperature was below 30°C the annealing reaction was complete and the sample stored on ice (for no longer than 4 hours) until the labelling reaction was carried out.

Buffer:	**5x Sequenase® buffer**	200mM Tris-HCl pH 7.5, 100mM $MgCl_2$, 250mM NaCl

A9.2.2 Labelling reactions

Labelling mix was diluted 5-fold with water (2µl of this mix is required for each labelling reaction). Sequenase® enzyme was diluted 1:8 in ice-cold Enzyme Dilution buffer.

1µl of dithiothreitol (0.1M), 2µl of the diluted Labelling mix and 0.5µl [α-^{35}S dATP] were added to the annealed template DNA/primer mix. For reading sequences close to the primer, 1µl of Mn buffer was added to the reaction mixture at this stage. 2µl of diluted Sequenase® enzyme was added, mixed gently and the solution incubated at room temperature for 5 minutes.

Four microcentrifuge tubes were labelled "G", "T", "A" and "C". 2.5µl of ddGTP Termination mix (80µM dGTP, 80µM dATP, 80µM dCTP, 80µM dTTP, 8µM ddGTP, 50mM NaCl) was transferred into the tube labelled "G". This was repeated with the ddTTP, ddCTP and ddATP Termination mixes. The tubes were pre-warmed at 37°C for at least one minute before proceeding immediately with the termination reactions.

Buffers:	**Labelling mix**	7.5µM dGTP, 7.5µM dCTP, 7.5µM dTTP
	Enzyme dilution buffer	10mM Tris-HCl pH 7.5, 5mM dithiothreitol, 0.5mg/ml BSA
	Mn buffer	0.15M sodium isocitrate, 0.1M $CaCl_2$

A9.2.3 Termination reactions

3.5µl of the labelling reaction mix was added to each tube containing the termination reaction mix and incubated at 37°C for 5 minutes. 4µl of Stop solution (95% formamide, 20mM EDTA, 0.05% bromophenol blue, 0.05% xylene cyanol FF) was added to each tube and mixed thoroughly. The samples were either placed on ice until ready to load onto the sequencing gel, or stored at -20°C for up to one week.

Before loading, the samples were heated at 75-80°C for 2 minutes and then 3µl immediately loaded onto the gel.

A10 DENATURATING GEL ELECTROPHORESIS

A10.1 Siliconisation and preparation of sequencing gel plates

Glass gel plates were siliconised before use to prevent the gel sticking to them which could cause it to tear on removal. The plates were washed with hot water and detergent, dried and then cleaned with ethanol. The plates were placed "face up" (i.e. surfaces that would be in contact with the gel) and a small quantity (2ml) of siliconising fluid poured onto them. The fluid was wiped over the surface of the plates and then left to dry for 5 minutes.

The plates, spacers and a sharkstooth comb were all washed thoroughly with hot water and detergent and finally rinsed with distilled water. The plates were placed on the bench (siliconised face up) and cleaned with ethanol. The plastic spacers (0.44mm thick) were placed along the sides of one of the plates and the other plate placed on top. The sides and bottom of both plates were sealed with gel-sealing tape and the plates held in place by bulldog clips.

A10.2 Preparation and pouring of polyacrylamide gels

21g of urea, 2.5ml of 10x TBE (Tris/Borate/EDTA) buffer and 26.1ml of water were placed in a Falcon tube and the solution warmed in a microwave oven for just long enough to dissolve the urea (typically 4x 5 second bursts). 6.4ml of 40% acrylamide was added and the solution filtered and degassed twice. To polymerise the gel 50µl of TEMED and 50µl 40% APS were added to the degassed monomer solution and mixed by swirling.

The acrylamide solution was carefully pipetted between the gel plates using a 50ml disposable plastic syringe. A sharkstooth comb was inserted into the top of the gel (with the straight edge 0.5cm into the gel) and clamped with bulldog clips. The gel was left to polymerise at an angle to prevent leaks and bowing of the plates for at least 2 hours. If the

gel was not to be loaded and run on the same day, the exposed (top) edge of the gel was covered with Saran™ wrap to prevent it from dehydrating and shrinking.

Buffers:	**10x TBE buffer**	0.89M Tris-base, 0.89M boric acid, 20mM EDTA
	40% Acrylamide	380g acrylamide, 20g N,N'-Methylene-bis Acrylamide Made up to one litre with distilled water, filtered and stored in the dark at 4°C

A10.3 Loading and running of gradient sequencing gels

The sharkstooth comb, bulldog clips and the tape along the bottom of the plates were all removed. A metal plate was clamped to the back of the glass plates to prevent the gel from heating up during electrophoresis. The gel set-up was attached to the electrophoresis apparatus. The top reservoir was filled with 0.5x TBE buffer and the bottom reservoir with 0.5x TBE/1M sodium acetate. The top of the gel was rinsed with TBE buffer to remove any unpolymerised acrylamide and the sharkstooth comb was reinserted with its teeth 0.5cm into the gel.

The denatured sequencing reactions (section A9.2.3) were loaded in sets of four (TCGA) onto the gel. The gel was run at 2000V (60W) until the dye front was one inch from the bottom of the gel.

A10.4 Autoradiography of sequencing gels

Once the gel had run, the plates were removed from the electrophoresis apparatus and carefully separated, leaving the gel attached to one plate. The gel and glass plate were transferred to a solution of 10% methanol/10% acetic acid for 15 minutes. The gel and plate were removed from the fixing solution, the excess fluid allowed to drain away and the gel/plate placed on the bench. A piece of Whatman™ 3MM paper was placed on top of the

gel and pressure applied gently so that it became firmly attached to the paper. The gel/paper was covered in Saran™ wrap and dried on a vacuum dryer at 80°C for 45 minutes. The dried gel was exposed to X-ray film (Fugi medical X-ray film RX) in a metal cassette for 16-24 hours. The film was developed using an automatic developing machine and the DNA sequence read off it.

A11 SMALL SCALE EXPRESSION OF W21H DHFR AND W21H/D26N DHFR

10ml of 2YT media supplemented with ampicillin (concentration of 100μg/ml) was inoculated with a single mutant colony from a fresh plate and grown at 37°C until an OD_{595} of 0.6 was reached. At this stage 1ml of culture was aseptically removed and the following two steps carried out:

i) 250μl was used to prepare glycerol stocks of pET11a/W21H DHFR and pET11a/W21H-D26N DHFR.

ii) The remaining 750μl of cells were harvested by spinning for 5 minutes in a microcentrifuge. The pellet was resuspended in 500μl of Tris-HCl pH 7.4 buffer and was then used as a "non-induced" control sample when checking for protein expression by SDS-PAGE (see below).

The remaining 9ml of culture was divided into two Sterilins. One culture was left to grow for a further 3 hours. These cells were then harvested by centrifuging at 3000 rpm for 10 minutes. Plasmid DNA was isolated from these cells using the Promega Magic™ Minipreps purification system and further purified by phenol/chloroform extraction. The plasmid was cut with restriction enzymes BamHI and XbaI to ensure that it contained the DHFR gene insert of correct size.

IPTG (final concentration 1mM) was added to the other 4.5ml of culture to induce protein expression. The culture was grown for a further 3 hours, the cells harvested and the

pellet resuspended in 500µl of Tris-HCl pH 7.4 buffer. Cell lysate ("induced" and "non-induced") were run on a 12% SDS polyacrylamide gel to check for expression of mutant proteins.

APPENDIX B

Figure B1. Active site of L.casei DHFR showing the positions of key residues (The inhibitor MTX is shown in yellow)

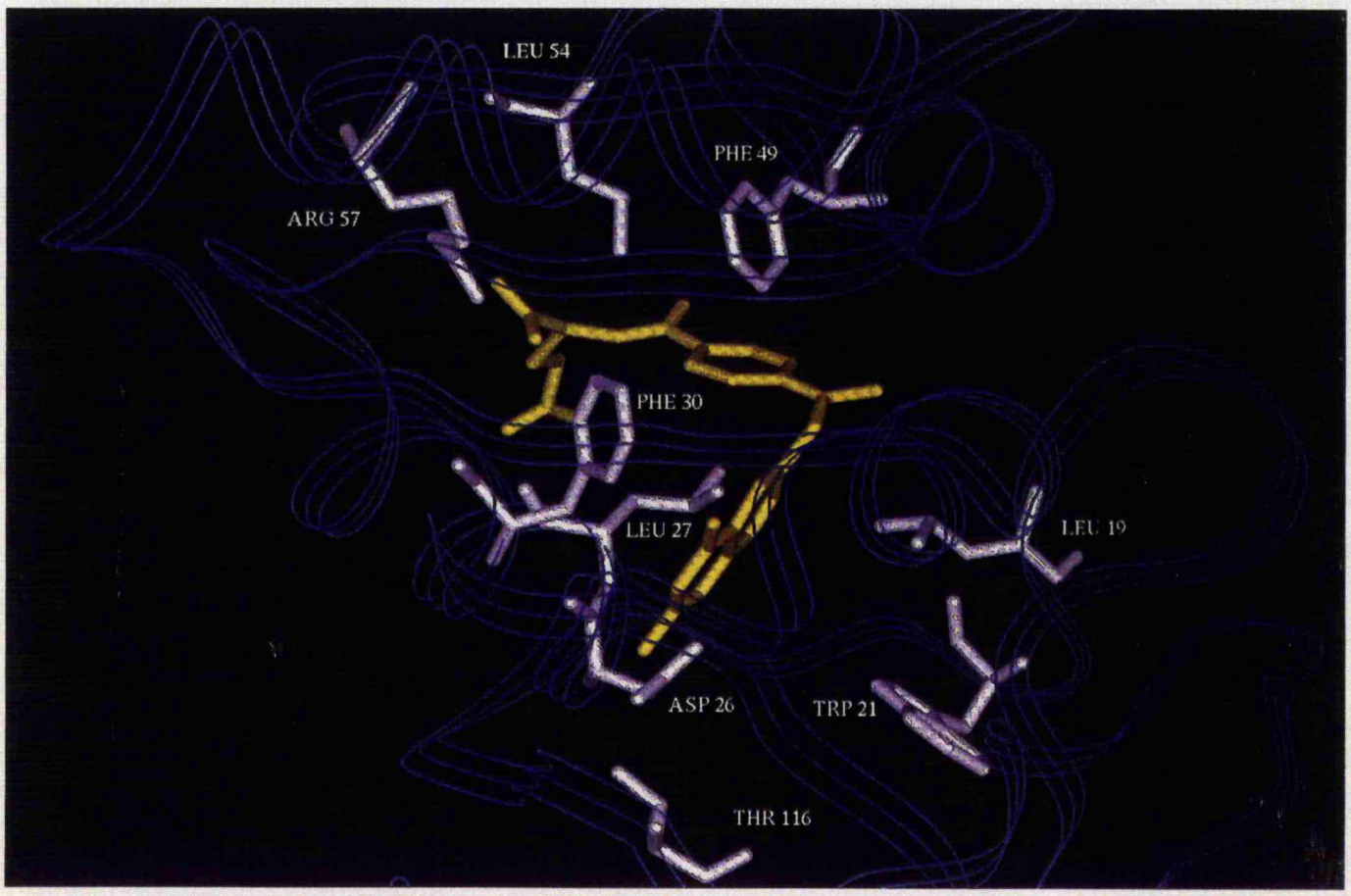

Figure B2. Interactions between L.casei DHFR and the pteridine ring of
(a) FH_2 (hypothetical)
(b) MTX (from crystal structure)
From Bolin et al., 1982.

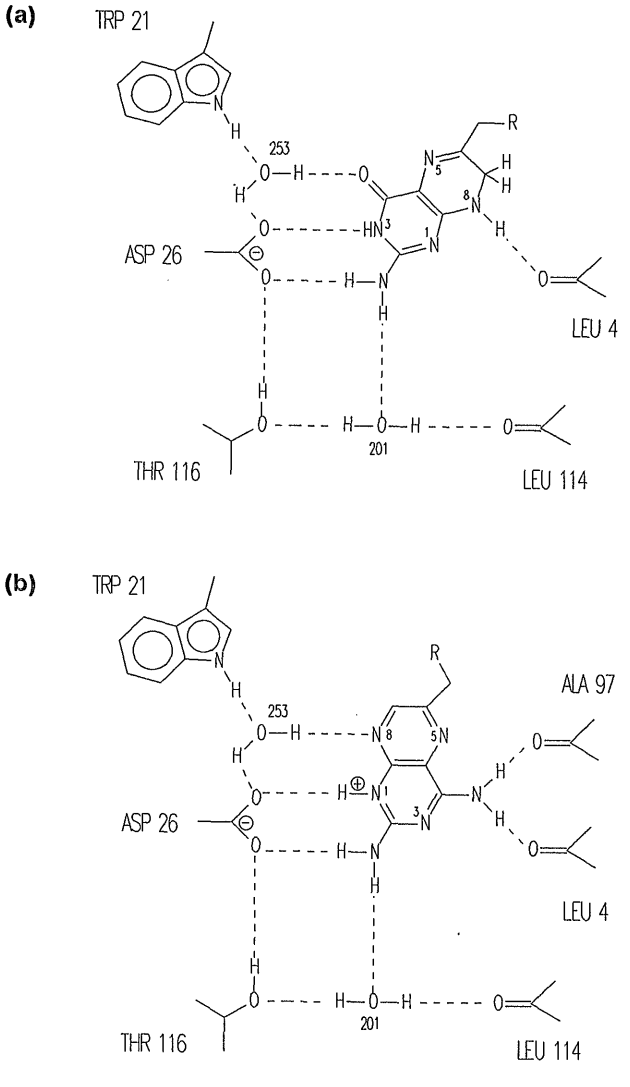

REFERENCES

Adams, J., Johnson, K., Matthews, R., and Benkovic, S.J. (1989). Effects of distal point-site mutations on the binding and catalysis of Dihydrofolate reductase from *Escherichia coli*. Biochemistry, **28**, 6611-6618.

Andrews, J., Fierke, C.A., Birdsall, B., Ostler, G., Feeney, J., Roberts, G.C.K., and Benkovic, S.J. (1989). A kinetic study of wild-type and mutant Dihydrofolate reductases from *Lactobacillus casei*. Biochemistry, **28**, 5743-5750.

Andrews, J., Minter, S.J., and Davies, R.W. (1991). Production of mutant Dihydrofolate reductases of *Lactobacillus casei* for nuclear magnetic resonance spectroscopy. Gene, **100**, 219-224.

Antonjuk, D.J., Birdsall, B., Cheung, H.T.A., Clore, G.M., Feeney, J., Gronenborn, A., Roberts, G.C.K., and Tran, T.Q. (1984). A ^{1}H n.m.r. study of the role of the glutamate moiety in the binding of methotrexate to *Lactobacillus casei* Dihydrofolate reductase. Br. J. Pharm., **81**, 309-315.

Appleman, J.R., Howell, E.E., Kraut, J., Kuhl, M., and Blakley, R.L. (1988a). The role of Aspartate 27 in the binding of methotrexate to Dihydrofolate reductase from *Escherichia coli*. J. Biol. Chem., **263**, 9187-9198.

Appleman, J.R., Prendergast, N., Delcamp, T.J., Freisheim, J.H., and Blakley, R.L. (1988b). Kinetics of the formation and isomerisation of methotrexate complexes of recombinant human Dihydrofolate reductase. J. Biol. Chem., **263**, 10304-10313.

Appleman, J.R., Beard, W.A., Delcamp, T.J., Prendergast, N.J., Freisheim, J.H., and Blakley, R.L. (1990a). Unusual transient- and steady-state kinetic behaviour is predicted by the kinetic scheme operational for recombinant human DHFR. J. Biol. Chem., **265**, 2740-2748.

Appleman, J.R., Howell, E.E., Kraut, J., and Blakley, R.L. (1990b). Role of Aspartate 27 of Dihydrofolate reductase from *Escherichia coli* in interconversion of active and inactive enzyme conformers and binding of NADPH. J. Biol. Chem., **265**, 5579-5584.

Baccanari, D.P., Daluge, S., and King, R.W. (1982). Inhibition of Dihydrofolate reductase: effect of reduced nicotinamide adenine dinucleotide phosphate on the selectivity and affinity of diaminobenzyl pyrimidines. Biochemistry, **21**, 5068-5075.

Baccanari, D.P., Phillips, A., Smith, S., Sinski, D., and Burchall, J. (1975). Purification and properties of *Escherichia coli* Dihydrofolate reductase. Biochemistry, **14**, 5267-5273.

Badii, R., Basran, J., Casarotto, M.G., and Roberts, G.C.K. (1994). High level expression and isotopic labelling of *Lactobacillus casei* Dihydrofolate reductase for Nuclear Magnetic Resonance spectroscopy. Prot. Exp. Purif., submitted for publication.

Bagshaw, C.R., and Harris, D.A. (1987). Measurement of ligand binding to proteins. In Spectrophotometry and spectrofluorimetry: a practical approach (pp. 91-113). Rickwood, D., and Hames, B.D. (Eds.), IRL Press Ltd., Oxford, England.

Bajorath, J., Kraut, J., Li, Z., Kitson, D.H., and Hagler, A.T. (1991a). Theoretical studies on the dihydrofolate reductase mechanism: electronic polarisation of bound substrates. Proc. Natl. Acad. Sci. USA, **88**, 6423-6426.

Bajorath, J., Li, Z., Fitzgerald, G., Kitson, D.H., Farnum, M., Fine, R.M., Kraut, J., and Hagler, A.T. (1991b). Changes in the electron density of the cofactor NADPH on the binding to *Escherichia coli* Dihydrofolate reductase. Proteins: structure, function and genetics, **11**, 263-270.

Baker, D.J., Beddell, C.R., Champness, J.N., Goodford, P.J., Norrington, F.E.A., Smith, D.R., and Stammers, D.K. (1981). The binding of TMP to bacterial dihydrofolate reductase. FEBS Lett., **216**, 49-52.

Beard, W.A., Appleman, J.R., Huang, S.M., Delcamp, T.J., Freisheim, J.H., and Blakley, R.L. (1991). Role of the conserved active site residue tryptophan-24 of human dihydrofolate reductase as revealed by mutagenesis. Biochemistry, **30**, 1188-1192.

Benkovic, S.J., Fierke, C.A., and Naylor, A.M. (1988). Insights into enzyme function from studies on mutants of Dihydrofolate reductase. Science, **239**, 1105-1110.

Bennet, C.D. (1974). Similarity in the sequence of *Escherichia coli* Dihydrofolate reductase with other pyridine nucleotide-requiring enzymes. Nature, **248**, 67-68.

Bennet, C.D., Rodney, J.A., Sondey, J.M., and Hirschman, R. (1978). Dihydrofolate reductase: the amino acid sequence of the enzyme from a methotrexate-resistant mutant of *Escherichia coli*. Biochemistry, **17**, 1328-1337.

Berry, A., Scrutton, N.S., and Perham, R.N. (1989). Switching kinetic mechanism and putative proton donor by directed mutagenesis of Glutathione reductase. Biochemistry, **28**, 1264-1269.

Birdsall, B., Arnold, J.R.P., Jimenez-Barbero, J., Frenkiel, T.A., Bauer, C.J., Tendler, S.J.B., Carr, M.D., Thomas, J.A., Roberts, G.C.K., and Feeney, J. (1990). The ^{1}H-NMR assignments of the aromatic resonances in complexes of *Lactobacillus casei* dihydrofolate reductase and the origins of their chemical shifts. Eur. J. Biochem., **191**, 659-668.

Birdsall, B., Andrews, J., Ostler, G., Tendler, S.J.B., Feeney, J., Roberts, G.C.K., Davies, R.W., and Cheung, H.T.A. (1989a). NMR studies of differences in the conformations and

dynamics of ligand complexes formed with mutant dihydrofolate reductases. Biochemistry, **28**, 1353-1362.

Birdsall, B., Feeney, J., Tendler, S.J.B., Hammond, S.J., and Roberts, G.C.K. (1989b). Dihydrofolate reductase: Multiple conformations and alternative modes of substrate binding. Biochemistry, **28**, 2297-2305.

Birdsall, B., De Graw, J., Feeney, J., Hammond, S., Searle, M.S., Roberts, G.C.K., Colwell, W.T., and Crase, J. (1987). ^{15}N and ^{1}H NMR evidence for multiple conformations of the complex of Dihydrofolate reductase with its substrate, folate. FEBS Lett., **217**, 106-110.

Birdsall, B., Bevan, A.W., Pascual, C., Roberts, G.C.K., Feeney, J., Gronenborn, A., and Clore, G.M. (1984). Multinuclear NMR characterization of two coexisting conformational states of the *Lactobacillus casei* DHFR-TMP-$NADP^+$ complex. Biochemistry, **23**, 4733-4742.

Birdsall, B., King, R.W., Wheeler, M.R., Lewis, C.A., Goode, S.R., Dunlap, R.B., and Roberts, G.C.K. (1983). Correction for light absorption in fluorescence studies of protein-ligand interactions. Anal. Biochem., **132**, 353-361.

Birdsall, B., Gronenborn, A., Hyde, E.I., Clore, G.M., Roberts, G.C.K., Feeney, J., and Burgen, A.S.V. (1982). Hydrogen-1, carbon-13, and phosphorus-31 nuclear magnetic resonance studies of the dihydrofolate reductase-nicotinamide adenine dinucleotide phosphate-folate complex: characterization of three coexisting conformational states. Biochemistry, **21**, 5831-5838.

Birdsall, B., Burgen, A.S.V., Hyde, E.I., Roberts, G.C.K., and Feeney, J. (1981a). Negative cooperativity between folinic acid and coenzyme in their binding to *Lactobacillus casei* Dihydrofolate reductase. Biochemistry, **20**, 7186-7195.

Birdsall, B., Gronenborn, A., Clore, G.M., Roberts, G.C.K., Feeney, J., and Burgen, A.S.V. (1981b). ^{13}C NMR evidence for three slowly interconverting conformations of the dihydrofolate reductase-$NADP^+$-folate complex. Biochem. Biophys. Res. Commun., **101**, 1139-1144.

Birdsall, B., Burgen, A.S.V., and Roberts, G.C.K. (1980). Binding of coenzyme analogues to *Lactobacillus casei* dihydrofolate reductase: binary and ternary complexes. Biochemistry, **19**, 3723-3731.

Birdsall, B., Burgen, A.S.V., Rodrigues de Miranda, J., and Roberts, G.C.K. (1978). Cooperativity in ligand binding to dihydrofolate reductase. Biochemistry, **17**, 2102-2110.

Bitar, K.G., Blankenship, D.T., Walsh, K.A., Dunlap, R.B., Reddy, A.V., and Freisheim, J.H. (1977). Amino acid sequence of dihydrofolate reductase from an amethopterin-resistant strain of *Lactobacillus casei*. FEBS Lett., **80**, 119-122.

Blakley, R.L. (1969). The biochemistry of folic acid and related pteridines. North-Holland Publishing company, Amsterdam.

Blakley, R.L. (1984). Dihydrofolate Reductase. In Folates and Pterins (pp. 191-253). Blakley, R.L., and Benkovic S.J. (Eds.), John Wiley and Sons, New York.

Blakley, R.L., and Cocco, L. (1985). Role of isomerization of initial complexes in the binding of inhibitors to dihydrofolate reductase. Biochemistry, **24**, 4772-4777.

Blakley, R.L., Ramasatri, B.V., and McDougall, M. (1963). The biosynthesis of thymidylic acid. J. Biol. Chem., **238**, 3075-3079.

Blakley, R.L., Cocco, L., London, R.E., Walker, T.E., and Matwiyoff, N.A. (1978). Nuclear magnetic resonance studies on bacterial Dihydrofolate reductase containing [*methyl*-^{13}C] methionine. Biochemistry, **17**, 2284-2293.

Bolin, J.T., Filman, D.J., Matthews, D.A., Hamlin, R.C., and Kraut, J. (1982). Crystal structures of *Escherichia coli* and *Lactobacillus casei* Dihydrofolate reductase refined at 1.7Å resolution. I. General features and binding of methotrexate. J. Biol. Chem., **257**, 13650-13662.

Brown, K.A., and Kraut, J. (1992). Exploring the molecular mechanism of Dihydrofolate reductase. Faraday Discuss., **93**, 217-224.

Bystroff, C., and Kraut, J. (1991). Crystal structure of unliganded *Escherichia coli* dihydrofolate reductase. Ligand-induced conformational changes and cooperativity in binding. Biochemistry, **30**, 2227-2239.

Bystroff, C., Oatley, S.J., and Kraut, J. (1990). Crystal structures of *Escherichia coli* Dihydrofolate reductase: The $NADP^+$ holoenzyme and the folate-$NADP^+$ ternary complex. Substrate binding and a model for the transition state. Biochemistry, **29**, 3263-3277.

Carr, M.D., Birdsall, B., Frenkiel, T.A., Bauer, C.J., Jimenez-Barbero, J., Polshakov, V.I., McCormick, J.E., Roberts, G.C.K., and Feeney, J. (1991). Dihydrofolate reductase: sequential resonance assignments and secondary structure in solution. Biochemistry, **30**, 6330-6341.

Cayley, P.J., Dunn, S.M.J., and King, R.W. (1981). Kinetics of substrate, coenzyme, and inhibitor binding to *Escherichia coli* dihydrofolate reductase. Biochemistry, **20**, 874-879.

Champness, J.N., Stammers, D.K., and Beddell, C.R. (1986). Crystallographic investigation of the cooperative interaction between TMP, reduced cofactor and DHFR. FEBS Lett., **199**, 61-67.

Charlton, P.A., Young, D.W., Birdsall, B., Feeney, J., and Roberts, G.C.K. (1979). Stereochemistry of reduction of folic acid using dihydrofolate reductase. J. Chem. Soc. Chem. Commun., **734**, 922-924.

Chen, J.-T., Taira, K., Tu, C.-P.D., and Benkovic, S.J. (1987). Probing the functional role of Phe-31 of *Escherichia coli* DHFR by site-directed mutagenesis. Biochemistry, **26**, 4093-4100.

Chen, Y.-Q., Kraut, J., Blakley, R.L., and Callender, R. (1994). Determination by Raman spectroscopy of the pK_a of N5 of dihydrofolate bound to Dihydrofolate reductase: mechanistic implications. Biochemistry, **33**, 7021-7026.

Cheung, H.T.A., Birdsall, B., Frenkiel, T.A., Chau, D.D., and Feeney, J. (1993). ^{13}C NMR determination of the tautomeric and ionisation states of folate in its complexes with *Lactobacillus casei* Dihydrofolate reductase. Biochemistry, **32**, 6846-6854.

Cheung, H.T.A., Searle, M.S., Feeney, J., Birdsall, B., Roberts, G.C.K., Kompis, I., and Hammond, S.J. (1986). Trimethoprim binding to *Lactobacillus casei* dihydrofolate reductase: A ^{13}C NMR study using selectively ^{13}C-enriched trimethoprim. Biochemistry, **25**, 1925-1931.

Chunduru, S.K., Cody, V., Luft, J.R., Pangborn, W., Appleman, J.R., and Blakley, R.L. (1994). Methotrexate-resistant variants of Human dihydrofolate reductase: effects of Phe 31 substitutions. J. Biol. Chem., **269**, 9547-9555.

Clarke, A.R., Atkinson, T., and Holbrook, J.J. (1989). From analysis to synthesis: new ligand binding sites on the lactate dehydrogenase framework. Trends Biochem. Sci., **14**, 101-105.

Clarke, A.R., Wigley, D.B., Chia, W.N., Barstow, D., Atkinson, T., and Holbrook, J.J. (1986). Site-directed mutagenesis reveals role of mobile arginine residue in Lactate dehydrogenase catalysis. Nature, **324**, 699-702.

Cocco, L., Roth, B., Temple, Jr.,C., Montgomery, J.A., London, R.E., and Blakley, R.L. (1983). Protonated state of methotrexate, trimethoprim, and pyrimethamine bound to dihydrofolate reductase. Arch. Biochem. Biophys., **226**, 567-577.

Cocco, L., Groff, J.P., Temple, C., Montgomery, J.A., London, R.E., Matwiyoff, N.A., and Blakley, R.L. (1981a). Carbon-13 nuclear magnetic resonance study of protonation of methotrexate and aminopterin bound to dihydrofolate reductase. Biochemistry, **20**, 3972-3978.

Cocco, L., Temple, Jr.,C., Montgomery, J.A., London, R.E., and Blakley, R.L. (1981b). Protonation state of methotrexate bound to the catalytic site of Dihydrofolate reductase from *Lactobacillus casei*. Biochem. Biophys. Res. Commun., **100**, 413-419.

Dann, J.G. (1975). Enzymological studies on Dihydrofolate reductase. Ph.D. thesis, University of Cambridge.

Dann, J.G., Ostler, G., Bjur, R.A., King, R.W., Scudder, P., Turner, P.C., Roberts, G.C.K., and Burgen, A.S.V. (1976). Large-scale purification and characterisation of dihydrofolate reductase from a methotrexate-resistant strain of *Lactobacillus casei*. Biochem. J., **157**, 559-571.

David, C.L., Howell, E.E., Farnum, M.F., Villafranca, J.E., Oatley, S.J., and Kraut, J. (1992). Structure and function of alternative proton-relay mutants of DHFR. Biochemistry, **31**, 9813-9822.

Davies, J.F., Delcamp, T.J., Prendergast, N.J., Ashford, V.A., Freisheim, J.H., and Kraut, J. (1990). Crystal structures of recombinant human dihydrofolate reductase complexed with folate and 5-deazafolate. Biochemistry, **29**, 9467-9479.

Dawson, R.M.C., Elliot, D.C., Elliot, W.H., and Jones, K.M. (1986). Data for Biochemical Research. 3rd Edition, Oxford University Press, Oxford, U.K.

Deonarain, M.P., Berry, A., Scrutton, N.S., and Perham, R.N. (1989). Alternative proton donors/acceptors in the catalytic mechanism of the Glutathione reductase of *E.coli*: the role of Histidine 439 and Tyrosine 99. Biochemistry, **28**, 9602-9607.

Dixon, H.B.F. (1992). How groups of proteins titrate: a new approach. In Essays in Biochemistry (Vol. 27, pp. 161-175). Tipton, K.F. (Ed.), Portland Press, London.

Dixon, H.B.F. (1976). The unreliability of estimates of group dissociation constants. Biochem. J., **153**, 627-629.

Dixon, H.B.F., and Tipton, K.F. (1973). Negatively co-operative ligand binding. Biochem. J., **133**, 837-842.

Dunn, S.M.J., Batchelor, J.G., and King, R.W. (1978). Kinetics of ligand binding to Dihydrofolate reductase: binary complex formation with NADPH and coenzyme analogues. Biochemistry, **17**, 2356-2364.

Dunn, S.M.J., and King, R.W. (1980). Kinetics of ternary complex formation between Dihydrofolate reductase, coenzyme and inhibitors. Biochemistry, **19**, 766-773.

Ellis, K.J., and Morrison, J.F. (1982). Buffers of constant ionic strength for studying pH-dependent processes. Methods Enzymol., **87**, 405-426.

Erickson, J.S., and Mathews, C.K. (1972). Spectral changes associated with binding of folate compounds to bacteriophage T4 Dihydrofolate reductase. J. Biol. Chem., **247**, 5661-5667.

Falzone, C.J., Benkovic, S.J., and Wright, P.E. (1990). Partial ^{1}H NMR assignments of the *Escherichia coli* dihydrofolate reductase complex with folate: evidence for a unique conformation of bound folate. Biochemistry, **29**, 9667-9677.

Falzone, C.J., Wright, P.E., and Benkovic, S.J. (1994). Dynamics of a flexible loop in dihydrofolate reductase from *Escherichia coli* and its implication for catalysis. Biochemistry, **33**, 439-442.

Fawcett, C.P., Ciotti, M.M., and Kaplan, N.O. (1961). Inhibition of dehydrogenase reactions by a substance formed from reduced diphosphopyridine nucleotide. Biochim. Biophys. Acta, **54**, 210-212.

Feeney, J., Roberts, G.C.K., Thomson, J.W., King, R.W., Griffiths, D.V., and Burgen, A.S.V. (1980). Proton nuclear magnetic resonance studies of the effects of ligand binding on tryptophan residues of selectively deuterated Dihydrofolate reductase from *Lactobacillus casei*. Biochemistry, **19**, 2316-2321.

Feeney, J., Roberts, G.C.K., Birdsall, B., Griffiths, D.V., King, R.W., Scudder, P., and Burgen, A.S.V. (1977). ^{1}H nuclear magnetic resonance studies of the tyrosine residues of selectively deuterated *Lactobacillus casei* dihydrofolate reductase. Proc. R. Soc. Lond. B., **196**, 267-290.

Fersht, A.R. (1985). Enzyme structure and mechanism. (2nd Edition), W.H. Freeman and Company, New York.

Fersht, A.R., and Leatherbarrow, R.J. (1987). Structure and activity of the tyrosyl-tRNA Synthetase. In Protein Engineering (pp. 269-278). Oxender D.L., and Fox, C.F. (Eds.), Alan R. Liss, Inc., New York.

Fierke, C.A., and Benkovic, S.J. (1989). Probing the functional role of Thr-113 of *Escherichia coli* DHFR for its effect on turnover efficiency, catalysis and binding. Biochemistry, **28**, 478-486.

Fierke, C.A., Johnson, K.A., and Benkovic, S.J. (1987). Construction and evaluation of the kinetic scheme associated with dihydrofolate reductase from *Escherichia coli*. Biochemistry, **26**, 4085-4092.

Filman, D.J., Bolin, J.T., Matthews, D.A., and Kraut, J. (1982). Crystal structures of *Escherichia coli* and *Lactobacillus casei* Dihydrofolate reductase refined at 1.7Å resolution. II. Environment of bound NADPH and implications for catalysis. J. Biol. Chem., **257**, 13663-13672.

Freisheim, J.H., and Matthews, D.A. (1984). The comparative biochemistry of Dihydrofolate reductase. In Folate Antagonists as Therapeutic Agents (pp. 69-131). Sirotnak, F.M., Burchill, J.J., Esminger, W.B., and Montgomery J.A. (Eds.), Academic Press Inc., New York.

Freisheim, J.H., Bitar, K.G., Reddy, A.V., and Blankenship, D.T. (1978). Dihydrofolate reductase from amethopterin-resistant *Lactobacillus casei*: sequences of the cyanogen bromide peptides and complete sequence of the enzyme. J. Biol. Chem., **253**, 6437-6444.

Freisheim, J.H., Ericsson, L.H., Bitar, K.G., Dunlap, R.B., and Reddy, A.V. (1977). An active site tryptophan residue in Dihydrofolate reductase: chemical modification, sequence surrounding the critical residue, and structural homology considerations. Arch. Biochem. Biophys., **180**, 310-317.

Gready, J.E. (1980). Dihydrofolate reductase: binding of substrates and inhibitors and catalytic mechanism. Adv. Pharm. Chemother., **17**, 37-102.

Gready, J.E. (1985). Theoretical studies on the activation of the pterin cofactor in the catalytic mechanism of Dihydrofolate reductase. Biochemistry, **24**, 4761-4766.

Greenfield, N.J. (1974). The effect of histidine modification on the activity of Dihydrofolate reductase from a methotrexate-resistant strain of *E.coli* B. Biochemistry, **13**, 4494-4500.

Gronenborn, A., Birdsall, B., Hyde, E.I., Roberts, G.C.K., Feeney, J., and Burgen, A.S.V. (1981a). Direct observation by NMR of two coexisting conformations of an enzyme-ligand complex in solution. Nature, **290**, 273-274.

Gronenborn, A., Birdsall, B., Hyde, E.I., Roberts, G.C.K., Feeney, J., and Burgen, A.S.V. (1981b). Effects of coenzyme binding on Histidine residues of *Lactobacillus casei* Dihydrofolate reductase. Biochemistry, **20**, 1717-1722.

Groom, C.R., Thillet, J., North, A.C.T., Pictet, R., and Geddes, A.J. (1991). Trimethoprim binds in a bacterial mode to the wild-type and E30D mutant of mouse Dihydrofolate reductase. J. Biol. Chem., **266**, 19890-19893.

Gupta, S.V., Greenfield, N.J., Poe, M., Makulu, D.R., Williams, M.N., Moroson, B.A., and Bertino, J.R. (1977). Dihydrofolate reductase from a resistant subline of the L1210 lymphoma. Purification by affinity chromatography and UV difference spectrophotometric and CD studies. Biochemistry, **16**, 3073-3079.

Hammond, S.J., Birdsall, B., Searle, M.S., Roberts, G.C.K., and Feeney, J. (1986). Dihydrofolate Reductase: ^{1}H resonance assignments and coenzyme-induced conformational changes. J. Mol. Biol., **188**, 81-97.

Hood, K., and Roberts, G.C.K. (1978). Ultraviolet difference-spectroscopic studies of substrate and inhibitor binding to *Lactobacillus casei* Dihydrofolate reductase. Biochem. J., **171**, 357-366.

Howell, E.E., Booth, C., Farnum, M., Kraut, J., and Warren, M.S. (1990). A second-site mutation at phenylalanine-137 that increases catalytic efficiency in the mutant aspartate 27→serine *Escherichia coli* dihyrofolate reductase. Biochemistry, **29**, 8561-8569.

Howell, E.E., Villafranca, J.E., Warren, M.S., Oatley, S.J., and Kraut, J. (1986). Functional role of Aspartic acid-27 in Dihydrofolate reductase revealed by mutagenesis. Science, **231**, 1123-231.

Huang, F., Yang, Q.-X., Huang, T., Gelbaum, L., and Kuyper, L.F. (1991). The conformations of TMP-*Escherichia coli* DHFR complexes. FEBS Lett., **283**, 44-46.

Huang, S., Delcamp, T.J., Tan, X., Smith, P.L., Prendergast, N.J., and Freisheim, J.H. (1989). Effects of conversion of an invariant tryptophan residue to phenylalanine on the function of human dihydrofolate reductase. Biochemistry, **28**, 471-478.

Huennekens, F.M., and Scrimgeour, K.G. (1964). Tetrahydrofolic acid: the coenzyme of one-carbon metabolism. In Pteridine Chemistry (pp. 355-376). Pfleiderer W., and Taylor E.C. (Eds.), Pergammon, Oxford.

Jimenez, M.A., Arnold, J.P.R., Andrews, J., Thomas, J.A., Roberts, G.C.K., Birdsall, B., and Feeney, J. (1989). Dihydrofolate reductase: control of the mode of substrate binding by aspartate 26. Prot. Eng., **2**, 627-631.

Kimber, B.J., Griffiths, D.V., Birdsall, B., King, R.W., Scudder, P., Feeney, J., Roberts, G.C.K., and Burgen, A.S.V. (1977). ^{19}F Nuclear magnetic resonance studies of ligand binding to 3-fluorotyrosine- and 6-fluorotryptophan-containing Dihydrofolate reductase from *Lactobacillus casei*. Biochemistry, **16**, 3492-3500.

Knowles, J.R. (1987). Tinkering with enzymes: what are we learning? Science, **236**, 1252-1258.

Knowles, J.R. (1991). Enzyme catalysis: not different, just better. Nature, **350**, 121-124.

Kraut, J., and Matthews, D.A. (1987). Dihydrofolate reductase. In Biological macromolecules and assemblies (Vol. 3, pp. 1-72). Jurnak, F.A., and McPherson, A. (Eds.), John Wiley and Sons, New York.

Kumar, A.A., Blankenship, D.T., Kaufman, B.T., and Freisheim, J.H. (1980). Primary structure of chicken liver Dihydrofolate reductase. Biochemistry, **19**, 667-678.

Lai, P.-H., Pan, Y.-C.E., Gleisner, J.M., Peterson, D.L., Williams, K.R., and Blakley, R.L. (1982). Structure of Dihydrofolate reductase: primary sequence of the bovine liver enzyme. Biochemistry, **21**, 3284-3294.

Leatherbarrow, R.J. (1990). Grafit Version 2.0, Erithacus Software Ltd., Staines, U.K.

Leatherbarrow, R.J. (1987). Enzfitter, Elsevier Science Publishers BV., Amsterdam.

Leatherbarrow, R.J., and Fersht, A.R. (1986). Protein Engineering. Prot. Eng., **1**, 7-16.

Li, L., Falzone, J., Wright, P.E., and Benkovic, S.J. (1992). Functional role of a mobile loop of *Escherichia coli* Dihydrofolate reductase in transition-state stabilization. Biochemistry, **31**, 7826-7833.

Liu, J.K., and Dunlap, R.B. (1974). Implication of a tryptophyl residue in the active site of dihydrofolate reductase. Biochemistry, **13**, 1807-1814.

London, R.E., Groff, J.P., Cocco, L., and Blakley, R.L. (1982). Nuclear magnetic resonance study of interaction of ligands with *Streptococcus faecium* Dihydrofolate reductase labelled with [γ-^{13}C] tryptophan. Biochemistry, **21**, 4450-4458.

London, R.E., Howell, E.E., Warren, M.S., Kraut, J., and Blakley, R.L. (1986). Nuclear magnetic resonance study of the state of protonation of inhibitors bound to mutant dihydrofolate reductase lacking the active-site carboxyl. Biochemistry, **25**, 7229-7235.

Lund, H. (1976). Electrochemistry of pteridines. In Chemistry and Biology of Pteridines (pp. 645-670). Pfleiderer, W. (Ed.), de Gruyter, Berlin.

Maharaj, G., Selinsky, B.S., Appleman, J.R., Perlman, M.E., London, R.E., and Blakley, R.L. (1990). Dissociation constants for dihydrofolic acid and dihydrobiopterin and implications for mechanistic models for DHFR. Biochemistry, **29**, 4554-4560.

Masters, J.N., and Arttardi, G. (1983). The nucleotide sequence of the cDNA coding for human dihydrofolate reductase. Gene, **21**, 59-63.

Matthews, C.K., and Huennekens, F.M. (1963). Further studies on DHFR. J. Biol. Chem., **238**, 3436-3442.

Matthews, D.A., Bolin, J.T., Burridge, J.M., Filman, D.J., Volz, K.W., Kaufman, B.T., Beddell, C.R., Champness, J.N., Stammers, D.K., and Kraut, J. (1985a). Refined crystal structures of *Escherichia coli* and Chicken liver DHFR containing bound TMP. J. Biol. Chem., **260**, 381-391.

Matthews, D.A., Bolin, J.T., Burridge, J.M., Filman, D.J., Volz, K.W., and Kraut, J. (1985b). Dihydrofolate Reductase: The stereochemistry of inhibitor selectivity. J. Biol. Chem., **260**, 392-399.

Matthews, D.A., Alden, R.A., Freer, S.T., Xuong, N., and Kraut, J. (1979). Dihydrofolate reductase from *Lactobacillus casei*: stereochemistry of NADPH binding. J. Biol. Chem., **254**, 4144-4151.

Matthews, D.A., Alden, R.A., Bolin, J.T., Filman, D.J., Freer, S.T., Hamlin, R., Hol, W.G.J., Kisliuk, R.L., Pastore, E.J., Plante, L.T., Xuong, N., and Kraut, J. (1978). Dihydrofolate reductase from *Lactobacillus casei*: X-ray structure of the enzyme-methotrexate-NADPH complex. J. Biol. Chem., **253**, 6946-6954.

Matthews, D.A., Alden, R.A., Bolin, J.T., Freer, S.T., Hamlin, R., Xuong, N., Kraut, J., Poe, M., Williams, M., and Hoogsteen, K. (1977). Dihydrofolate reductase: X-ray structure of the binary complex with methotrexate. Science, **197**, 452-455.

Mayer, R.J., Chen, J.T., Taira, K., Fierke, C.A., and Benkovic, S.J. (1986). Importance of a hydrophobic residue in binding and catalysis by dihydrofolate reductase. Proc. Natl. Acad. Sci. USA, **83**, 7718-7720.

McTigue, M.A., Davies, J.F., Kaufman, B.T., and Kraut, J. (1992). Crystal structure of chicken liver dihydrofolate reductase complexed with $NADP^+$ and biopterin. Biochemistry, **31**, 7264-7273.

McTigue, M.A., Davies, J.F., Kaufman, B.T., and Kraut, J. (1993). Crystal structures of chicken liver Dihydrofolate reductase: Binary $thioNADP^+$ and ternary $thioNADP^+$-biopterin complexes. Biochemistry, **32**, 6855-6862.

Morrison, J.F., and Stone, S.R. (1988). Mechanism of the reaction catalysed by Dihydrofolate Reductase from *Escherichia coli*: pH and deuterium isotope effects with NADPH as the variable substrate. Biochemistry, **27**, 5499-5506.

Murphy, D.J., and Benkovic, S.J. (1989). Hydrophobic interactions via mutants of *Escherichia coli* DHFR: separation of binding and catalysis. Biochemistry, **28**, 3025-3131.

Oefner, O., D'Arcy, A., and Winkler, F.K. (1988). Crystal structure of human dihydrofolate reductase complexed with folate. Eur. J. Biochem., **174**, 377-385.

Pastore, E.J., and Friedkin, M. (1962). The enzymatic synthesis of thymidylate. J. Biol. Chem., **237**, 3802-3810.

Pastore, E.J., and Williamson, K.L. (1968). An NMR study of 5-formyl-FH_4 (CF) specifically labelled with deuterium (D): novel characteristics of the molecule and site of action of Dihydrofolate reductases from different species. Fed. Proc. Fed. Am. Soc. Exp. Biol., 27, 764.

Poe, M. (1977). Acidic dissociation constants of folate acid, dihydrofolic acid and methotrexate. J. Biol. Chem., **252**, 3724-3728.

Poe, M., and Hoogsteen, K. (1974). Stereochemistry of dihydrofolate reduction to tetrahydrofolate: direct hydrogen transfer to C6 by *Escherichia coli* MB 1428 Dihydrofolate Reductase. Fed. Proc. Fed. Am. Soc. Exp. Biol., **33**, 1382.

Poe, M., Greenfield, N.J., Hirshfield, J.M., and Hoogsteen, K. (1974). Dihydrofolate Reductase from a methotrexate-resistant strain of *Escherichia coli*: binding of several folates and pteridines as monitored by ultraviolet difference spectroscopy. Cancer Biochem. Biophys., **1**, 7-11.

Pompliano, D.L., Peyman. A., and Knowles, J.R. (1990). Stabilisation of a reaction intermediate as a catalytic device: definition of the functional role of the flexible loop in Triosephosphate isomerase. Biochemistry, **29**, 3186-3194.

Prendergast, N.J., Appleman, J.R., Delcamp, T.J., Blakley, R.L., and Freisheim, J.H. (1989). Effects of conversion of Phe-31 to Leu on the function of human DHFR. Biochemistry, **28**, 4645-4650.

Reddy, A.V., Belinke, W.D., and Freisheim, J.H. (1978). Binary and ternary complexes of Dihydrofolate reductase with substrates, coenzymes and inhibitors: circular dichroic and magnetic circular dichroic studies. Biochim. Biophys. Acta, **533**, 415-427.

Roberts, G.C.K., Feeney, J., Burgen, A.S.V., and Daluge, S. (1981). The charge state of trimethoprim bound to *Lactobacillus casei* dihydrofolate reductase. FEBS Lett., **131**, 85-88.

Roth, B., and Strelitz, J.Z. (1969). The protonation of 2,4-diaminopyrimidines I. Dissociation constants and substituent effects. J. Org. Chem., **34**, 821-836.

Rutter, W.J., Gardell, S.J., Roczniak, S., Hilvert, D., Sprang, S., Fletterick, R.J., and Craik, C.S. (1987). Redesigning proteins via genetic engineering. In Protein Engineering (pp. 257-267). Oxender D.L., and Fox, C.F. (Eds.), Alan R. Liss, Inc., New York.

Sampson, N.S., and Knowles, J.R. (1992a). Segmental movement: definition of the structural requirements for loop closure in catalysis by Triosephosphate isomerase. Biochemistry, **31**, 8482-8487.

Sampson, N.S., and Knowles, J.R. (1992b). Segmental motion in catalysis: investigation of a hydrogen bond critical for loop closure in the reaction of triosephosphate isomerase. Biochemistry, **31**, 8488-8494.

Schweitzer, B.I., Srimatkandada, S., Gritsman, H., Sheridan, R., Venkataraghavan, R., and Bertino, J.R. (1989). Probing the role of two hydrophobic active site residues in human DHFR by site-directed mutagenesis. J. Biol. Chem., **264**, 20786-20795.

Searle, M.S., Forster, M.J., Birdsall, B., Roberts, G.C.K., Feeney, J., Cheung, H.T.A., Kompis, I., and Geddes, A.J. (1988). Dynamics of trimethoprim bound to dihydrofolate reductase. Proc. Natl. Acad. Sci. USA, **85**, 3787-3791.

Seegar, D.R., Cosulich, D.B., Smith, J.M., and Hultquist, M.E. (1949). Analogues of pteroylglutamic acid III. 4-amino derivatives. J. Am. Chem. Soc., **71**, 1753-1758.

Shaw, W.V. (1987). Protein engineering: the design, synthesis and characterization of factitious proteins. Biochem. J., **246**, 1-17.

Soteriou, A., Carr, M.D., Frenkiel, T.A., McCormick, J.E., Bauer, C.J., Sali, D., Birdsall, B., and Feeney, J. (1993). 3D $^{13}C/^{1}H$ NMR-based assignments for side-chain resonances of *Lactobacillus casei* Dihydrofolate reductase. Evidence for similarities between solution and crystal structures of the enzyme. J. Biomol. NMR, **3**, 535-546.

Stammers, D.K., Champness, J.N., Beddell, C.R., Dann, J.G., Eliopoulos, E., Geddes, A.J., Ogg, D., and North, A.C.T. (1987). The structure of mouse L1210 dihydrofolate reductase-drug complexes and the construction of a model of human enzyme. FEBS Lett., **218**, 178-184.

Stone, S.R., and Morrison, J.F. (1982). Kinetic mechanism of the reaction catalysed by dihydrofolate reductase from *Escherichia coli*. Biochemistry, **21**, 3757-3765.

Stone, S.R., and Morrison, J.F. (1983). The pH dependence of the binding of dihydrofolate and substrate analogues to DHFR from *E. coli*. Biochim. Biophys. Acta, **745**, 247-258.

Stone, S.R., and Morrison, J.F. (1984). Catalytic mechanism of the Dihydrofolate reductase reaction as determined by pH studies. Biochemistry, **23**, 2753-2758.

Stone, S.R., and Morrison, J.F. (1988). Dihydrofolate Reductase from *Escherichia coli*: The kinetic mechanism with NADPH and reduced acetylpyridine adenine dinucleotide phosphate as substrates. Biochemistry, **27**, 5493-5499.

Subramanian, S., and Kaufman, B.T. (1978). Interaction of MTX, folates and pyridine nucleotides with dihydrofolate reductase: calorimetric and spectroscopic binding studies. Proc. Natl. Acad. Sci. USA, **75**, 3201-3205.

Taira, K., Fierke, C.A., Chen, J., Johnson, K.A., and Benkovic, S.J. (1987). On interpreting the inhibition of and catalysis by Dihydrofolate reductase. Trends Biochem. Sci., **12**, 275-278.

Thillet, J., Adams, J.A., and Benkovic, S.J. (1990). The kinetic mechanism of wild-type and mutant mouse dihydrofolate reductases. Biochemistry, **29**, 5195-5202.

Thomas, J.A. (1990). Structure and activity studies on mutants of the enzyme Dihydrofolate reductase. Ph.D. thesis, University of Leicester.

Thomas, J.A., Arnold, J.R.P., Basran, J., Andrews, J., Roberts, G.C.K., Birdsall, B., and Feeney, J. (1994). Effects of substitution of Thr63 by Alanine on the structure and function of *Lactobacillus casei* Dihydrofolate reductase. Prot. Eng. 7, 783-792.

Thomas, P.G., Russell, A.J., and Fersht, A.R. (1985). Tailoring the pH dependence of enzyme catalysis using protein engineering. Nature, **318**, 375-376.

Thompson, P.D., and Freisheim, J.H. (1991). Conversion of Arg to Lys at position 70 of Human DHFR: generation of a MTX-insensitive mutant enzyme. Biochemistry, **30**, 8124-8130.

Thomson, J.W., Roberts, G.C.K., and Burgen, A.S.V. (1980). The effects of modification with *N*-Bromosuccinimide on the binding of ligands to Dihydrofolate reductase. Biochem. J., **187**, 501-506.

Tipton, K.F., and Dixon, H.B.F. (1983). Effect of pH on enzymes. In Contemporary enzyme kinetics and mechanism (pp. 97-148). Purich, D.L. (Ed.), Academic Press Inc., London.

Tsay, J.-T., Appleman, J.R., Beard, W.A., Prendergast, N.J., Delcamp, T.J., Freisheim, J.H., and Blackley, R.L. (1990). Kinetic investigation of the functional role of phenylalanine-31 of recombinant human dihydrofolate reductase. Biochemistry, **29**, 6428-6436.

Uchimaru, T., Tsuzuki, S., Tanabe, K., Benkovic, S.J., Furukawa, K., and Taira, K. (1989). Computational studies on pterins and speculations on the mechanism of Dihydrofolate reductase. Biochem. Biophys. Res. Commun., **161**, 64-68.

Vehar, G.A., and Freisheim, J.H. (1976). Functional arginine residues involved in coenzyme binding by Dihydrofolate reductase. Biochem. Biophys. Res. Commun., **68**, 937-940.

Villafranca, J.E., Howell, E.E., Voet, D.H., Strobel, M.S., Ogden, R.C., Abelson, J.N., and Kraut, J. (1983). Directed mutagenesis of Dihydrofolate reductase. Science, **222**, 782-788.

Volz, K.W., Matthews, D.A., Alden, R.A., Freer, S.T., Hansch, C., Kaufman, B.T., and Kraut, J. (1982). Crystal structure of avian DHFR containing phenyltriazine and NADPH. J. Biol. Chem., **257**, 2528-2536.

Wagner, C.R., Thillet, J., and Benkovic, S.J. (1992). Complementary perturbation of the kinetic mechanism and catalytic effectiveness of Dihydrofolate reductase by sidechain interchange. Biochemistry, **31**, 7834-7840.

Warren, M.S., Brown, K.A., Farnum, M.F., Howell, E.E., and Kraut, J. (1991). Investigation of the functional role of Tryptophan-22 in *Escherichia coli* Dihydrofolate reductase by site-directed mutagenesis. Biochemistry, **30**, 11092-11103.

Wells, J.A., and Estell, D.A. (1988). Subtilisin: an enzyme designed to be engineered. Trends Biochem. Sci., **13**, 291-297.

Williams, J.W., Duggleby, R.G., Cutler, R., and Morrison, J.F. (1980). The inhibition of Dihydrofolate Reductase by folate analogues: structural requirements for slow- and tight-binding inhibition. Biochem. Pharm., **29**, 589-595.

Wyeth, P., Gronenborn, A., Birdsall, B., Roberts, G.C.K., Feeney, J., and Burgen, A.S.V. (1980). Histidine residues of *Lactobacillus casei* Dihydrofolate reductase: paramagnetic relaxation and deuterium-exchange studies and partial assignments. Biochemistry, **19**, 2608-2615.

Zakrzewski, S.F. (1963). The mechanism of binding of folate analogues by folate reductase. J. Biol. Chem., **238**, 1485-1490.